**University of Alberta**

# Quality of Distillates from Coking of Recycled Residue

by

Mohamed Shakir Japanwala

A thesis submitted to the Faculty of Graduate Studies and Research in partial fulfilment of the requirements for the degree of Master of Science

in

Chemical Engineering

Department of Chemical and Materials Engineering

Edmonton, Alberta

Spring 2001

National Library of Canada
Acquisitions and Bibliographic Services
395 Wellington Street
Ottawa ON K1A 0N4
Canada

Bibliothèque nationale du Canada
Acquisitions et services bibliographiques
395, rue Wellington
Ottawa ON K1A 0N4
Canada

Your file Votre référence

Our file Notre référence

The author has granted a non-exclusive licence allowing the National Library of Canada to reproduce, loan, distribute or sell copies of this thesis in microform, paper or electronic formats.

L'auteur a accordé une licence non exclusive permettant à la Bibliothèque nationale du Canada de reproduire, prêter, distribuer ou vendre des copies de cette thèse sous la forme de microfiche/film, de reproduction sur papier ou sur format électronique.

The author retains ownership of the copyright in this thesis. Neither the thesis nor substantial extracts from it may be printed or otherwise reproduced without the author's permission.

L'auteur conserve la propriété du droit d'auteur qui protège cette thèse. Ni la thèse ni des extraits substantiels de celle-ci ne doivent être imprimés ou autrement reproduits sans son autorisation.

0-612-60441-1

Canada

**University of Alberta**

**Library Release Form**

**Name of Author:** Mohamed Shakir Japanwala

**Title of Thesis:** Quality of Distillates from Coking of Recycled Residue

**Degree:** Master of Science

**Year this Degree Granted:** 2001

Permission is hereby granted to the University of Alberta Library to reproduce single copies of this thesis and to lend or sell such copies for private, scholarly or scientific research purposes only.

The author reserves all other publication and other rights in association with the copyright in the thesis, and except as herein before provided, neither the thesis nor any substantial portion thereof may be printed or otherwise reproduced in any material form whatever without the author's prior written permission.

Mohamed Shakir Japanwala
# 01A, 9109, 112th Street
Edmonton, Alberta
Canada, T6G 2C5

March 26, 2001
Date

**University of Alberta**

**Faculty of Graduate Studies and Research**

The undersigned certify that they have read, and recommend to the Faculty of Graduate Studies and Research for acceptance, a thesis entitled Quality of Distillates from Coking of Recycled Residue submitted by Mohamed Shakir Japanwala in partial fulfilment of the requirements for the degree of Master of Science in Chemical Engineering.

Murray Gray

Heather Dettman

William McCaffrey

Jeffrey Stryker

March 26, 2001

Date

# Abstract

The yields of gas, liquid and coke from the coking of Athabasca vacuum residue were determined as a function of conversion of the residue. High conversion was achieved by subjecting the unconverted residue to repeated coking steps. The distillate and the residue material obtained at each coking step were characterised using various analytical techniques.

There was a 12% increase in the cumulative yield of liquid from stage 1 of coking where 82% residue conversion was obtained, to stage 3 where 99% cumulative residue conversion was obtained. The quality of the distillates obtained at each stage deteriorated based on the amount of nitrogen and polynuclear aromatics. It was also observed that although coking reactions resulted in a decrease in the number of aliphatic chains, the average chain length remained constant. A mass balance showed that the aromatic carbon increased in the first coking step, then remained constant.

# Acknowledgements

I would like to thank my supervisor Dr. Murray Gray for his guidance, understanding and support. I would also like to thank Dr. Heather Dettman for her tremendous patience while explaining all the concepts of NMR spectroscopy and Dr. William McCaffrey for his helpful suggestions. The valuable suggestions from Keng Chung and Dr. Jeff Stryker are also gratefully acknowledged.

I would also like to thank the support staff here in the department who helped out at various stages of my project. The assistance of the staff at Syncrude research is also acknowledged.

I would like to thank all my colleagues who helped with their invaluable suggestions. I would like to thank Tuyet Le for all her help especially with the enormous asphaltene molecule. I also thank Samina, Liming, Srini, Andrée and Richard for their support. To all my friends, I thank them for making this a liveable few years. Lastly, I would like to thank my parents and my family for always being there.

TABLE OF CONTENTS


| | | |
|---|---|---|
| **1 INTRODUCTION** | | **1** |
| 1.1 Oil Sands of Alberta | | 1 |
| 1.2 Research Objectives | | 2 |
| 1.3 Experimental Plan | | 3 |
| 1.4 Outline of thesis | | 5 |
| **2 LITERATURE SURVEY** | | **6** |
| 2.1 Introduction | | 6 |
| 2.2 Significance of heavy oil and bitumen | | 6 |
| 2.3 Composition of petroleum | | 8 |
| 2.3.1 | Elemental analysis | 8 |
| 2.3.2 | Chemical structures in bitumen | 8 |
| | 2.3.2.1 Hydrocarbon groups | 9 |
| | 2.3.2.2 Heteroatomic groups | 12 |
| 2.3.3 | Class fractionation | 14 |
| | 2.3.3.1 Distillation | 14 |
| | 2.3.3.2 Separations based on solubility | 16 |
| | 2.3.3.3 Other separation methods | 16 |
| 2.3.4 | Asphaltenes | 18 |
| | 2.3.4.1 Molecular Structure | 18 |
| | 2.3.4.2 Molecular Weight | 23 |

2.4 Thermal Cracking 25

2.5 Mechanism of Coke Formation 30

2.5.1 MCR as indicator of coke formation in reactor 31

2.5.2 Pendant Core Model 32

2.5.3 Other factors influencing coke formation 33

2.5.3.1 Phase separation 33

2.5.3.2 Fine solids 34

2.6 Upgrading Processes 35

2.6.1 Coking Processes 36

2.6.1.1 Delayed Coking 36

2.6.1.2 Fluid Coking 38

2.6.1.3 Recycle Stream 40

2.7 Hydrotreating of cracked products 42

2.7.1 Feed and product properties 42

2.7.2 Process flow description 42

2.7.3 Catalyst deactivation 46

**3 MATERIALS AND METHODS 47**

3.1 Materials 47

3.2 Quartz Tube Reactor 49

3.2.1 Introduction 49

3.2.2 Apparatus 49

3.2.3 Procedure 49

3.3 Micro scale distillation at reduced pressure 53

3.3.1 Introduction 53

3.3.2 Apparatus 54

3.3.3 Procedure 56

3.4 Analytical Techniques 56

3.4.1 Nuclear Magnetic Resonance Spectroscopy (NMR) 56

3.4.2 Simulated distillation by gas chromatography (SIMDIST) 63

3.4.3 High performance liquid chromatography (HPLC) 63

3.4.4 Refinery gas analysis 63

3.4.5 Molecular weight 64

3.4.6 Elemental analysis 64

3.4.7 Ash Content 64

**4 RESULTS 65**

4.1 Yield of product fractions 65

4.1.1 Cumulative yields 65

4.1.2 Stagewise yields 67

4.2 Analytical Data 69

4.2.1 Simulated distillation by gas chromatography (SIMDIST) 69

4.2.2 Elemental analysis and ash content 69

4.2.3 Molecular Weight 74

4.2.4 Refinery Gas Analysis 76

4.2.5 Nuclear Magnetic Resonance Spectroscopy (NMR) 77

4.2.5.1 Spectra from $^{1}H$ NMR Spectroscopy 77

4.2.5.2 Spectra from $^{13}C$ NMR Spectroscopy 80

4.2.5.3 Advanced NMR spectroscopic techniques 85

4.2.5.4 Quantitative data analysis 90

4.2.5.5 Other estimated parameters 93

4.2.5.6 Mass balance on aromatic carbon 94

4.2.6 Micro Carbon Residue (MCR) 97

4.2.7 High performance liquid chromatography (HPLC) 102

**5 DISCUSSION 106**

5.1 Feed transformations during thermal cracking 106

5.1.1 Yields on cracking 107

5.1.2 Major reactions and structural changes 111

5.2 Quality of the distillates 113

5.3 A building block model for bitumen 116

5.3.1 Identification and cracking of the building blocks 116

5.3.2 Phase Separation 121

5.4 Process Implications 122

**6 CONCLUSIONS AND RECOMMENDATIONS 125**

6.1 Directions for future work 126

**BIBLIOGRAPHY 127**

## APPENDICES


APPENDIX 1 DEFINITIONS OF REFINING AND UPGRADING TERMS 136

APPENDIX 2 $CS_2$ INSOLUBLE VS TOLUENE INSOLUBLE COKE 137

APPENDIX 3 MICRO SCALE DISTILLATION AT REDUCED PRESSURE 138

APPENDIX 4 SIMULATED DISTILLATION BY GAS CHROMATOGRAPHY 141

APPENDIX 5 HIGH PERFORMANCE LIQUID CHROMATOGRAPHY 143

APPENDIX 6 MASS BALANCE FOR THE QUARTZ TUBE REACTOR 145

APPENDIX 7 THERMAL CRACKING EXPERIMENTS ON THE 3"REACTOR PRODUCTS 146

APPENDIX 8 ROTAMETER CALIBRATION 148

## LIST OF TABLES


| | | |
|---|---|---|
| TABLE 2.1 | ELEMENTAL COMPOSITION OF A VARIETY OF CRUDE OILS | 8 |
| TABLE 2.2 | BOND DISSOCIATION ENERGIES | 25 |
| TABLE 2.3 | PROPERTIES OF OIL BEFORE AND AFTER UPGRADING (WANG, 2000) | 35 |
| TABLE 2.4 | DIFFERENT KINDS OF COKING PROCESSES (LE PAGE *ET AL.*, 1992) | 36 |
| TABLE 2.5 | PROPERTIES OF SYNTHETIC CRUDE OIL (GRAY, 1990) | 43 |
| TABLE 2.6 | PROPERTIES OF PRODUCTS FROM PRIMARY UPGRADING (GRAY, 1990) | 44 |
| TABLE 3.1 | PROPERTIES OF ATHABASCA VACUUM RESIDUE | 47 |
| TABLE 3.2 | CHEMICAL SHIFTS OF PROTON SPECTRAL REGIONS | 60 |
| TABLE 3.3 | CHEMICAL SHIFTS OF CARBON SPECTRAL REGIONS | 61 |
| TABLE 3.4 | GROUP CLASSIFICATIONS OF CHEMICAL SPECIES | 62 |
| TABLE 4.1 | ELEMENTAL ANALYSIS AND ASH CONTENT | 72 |
| TABLE 4.2 | CUMULATIVE DISTILLATE PROPERTIES ON RECYCLE COKING | 73 |
| TABLE 4.3 | MOLECULAR WEIGHT AND AVERAGE MOLECULAR FORMULA | 75 |
| TABLE 5.1 | SELECTED DISTILLATE PROPERTIES ON RECYCLE COKING | 114 |
| TABLE A 1 | COKE YIELDS | 137 |
| TABLE A 2 | AMOUNT DISTILLED FOR VARYING FLASK SIZES | 138 |
| TABLE A 3 | ELSD DATA FOR THE DISTILLATE FRACTIONS | 143 |
| TABLE A 4 | SOLVENTS USED AND THEIR RESPECTIVE FLOWRATES | 144 |

## LIST OF FIGURES


FIGURE 1.1 FLOWSHEET OF THE EXPERIMENTAL PLAN 4

FIGURE 2.1 US REFINERY CRUDE OIL QUALITY (SWAIN, 2000) 7

FIGURE 2.2 REPRESENTATIVE COMPOUND TYPES 11

FIGURE 2.3 HETEROATOMIC GROUPS PRESENT IN PETROLEUM 13

FIGURE 2.4 VARIATION OF BOILING POINT WITH MOLECULAR WEIGHT AND STRUCTURE 15

FIGURE 2.5 PROPERTIES OF THE VARIOUS FRACTIONS WITH MOLECULAR WEIGHT 17

FIGURE 2.6 ASPHALTENE MODEL PROPOSED BY YEN *ET AL.* (1961). 19

FIGURE 2.7 ASPHALTENE MOLECULE AS PROPOSED BY STRAUSZ *ET AL.* (1992) 22

FIGURE 2.8 MOLECULAR WEIGHT OF ARABIAN HEAVY OIL ASPHALTENE 24

FIGURE 2.9 REACTIONS OF HYDROAROMATICS WITH TETRALIN AS MODEL COMPOUND 27

FIGURE 2.10 MAJOR REACTION PRODUCTS FROM DODECYL PYRENE PYROLYSIS 29

FIGURE 2.11 DELAYED COKER FLOWSHEET 37

FIGURE 2.12 FLUID COKER FLOWSHEET 39

FIGURE 2.13 AROMATICITY AND CONCENTRATION OF PARAFFINIC GROUPS IN FEED AND RECYCLE RESIDUE SAMPLES (GRAY *ET AL.*, 1989). 41

FIGURE 2.14 HYDROTREATER FLOWSHEET 45

FIGURE 3.1 SIMULATED DISTILLATION CURVE FOR ATHABASCA VACUUM RESIDUE 48

FIGURE 3.2 QUARTZ TUBE REACTOR 50

FIGURE 3.3 SALT BATH HEAT UP PROFILE 51

FIGURE 3.4 VACUUM DISTILLATION APPARATUS 55

FIGURE 3.5 HYPOTHETICAL MOLECULE TO REPRESENT DIFFERENT CARBON FUNCTIONALITIES 58

FIGURE 4.1 CUMULATIVE PRODUCT YIELDS 65

FIGURE 4.2 CUMULATIVE RESIDUE CONVERSION 66

FIGURE 4.3 PRODUCT YIELDS FOR THE THREE STAGES OF COKING 67

FIGURE 4.4 FEED VAPORISATION AT EACH STAGE OF COKING 68

FIGURE 4.5 SIMULATED DISTILLATION CURVE FOR RESIDUE FRACTIONS 70

FIGURE 4.6 SIMULATED DISTILLATION CURVES FOR DISTILLATE FRACTION 71

FIGURE 4.7 GAS COMPOSITION FOR ALL THREE STAGES 76

FIGURE 4.8 $^{1}H$ NMR SPECTRA FOR RESIDUE FRACTIONS 78

FIGURE 4.9 $^{1}H$ NMR SPECTRA FOR DISTILLATE FRACTIONS 79

FIGURE 4.10 $^{13}C$ NMR SPECTRA FOR RESIDUE FRACTIONS – AROMATIC REGION 81

FIGURE 4.11 $^{13}C$ NMR SPECTRA FOR DISTILLATE FRACTIONS - AROMATIC REGION 82

FIGURE 4.12 $^{13}C$ NMR SPECTRA FOR RESIDUE FRACTIONS - PARAFFINIC REGION 83

FIGURE 4.13 $^{13}C$ NMR SPECTRA FOR DISTILLATE FRACTIONS - PARAFFINIC REGION 84

FIGURE 4.14 DEPT SPECTRA FOR STAGE 3 RESIDUE FRACTIONS – AROMATIC REGION 86

FIGURE 4.15 DEPT SPECTRA FOR STAGE 3 RESIDUE FRACTIONS - PARAFFINIC REGION 87

FIGURE 4.16 COSY SPECTRA FOR STAGE 3 RESIDUE FRACTION 88

FIGURE 4.17 PARAFFINIC REGION OF THE HETCOR SPECTRA FOR STAGE 3 RESIDUE FRACTION 89

FIGURE 4.18 $^{13}C$ NMR DATA FOR RESIDUE FRACTION - AROMATIC REGION 91

FIGURE 4.19 $^{13}C$ NMR DATA FOR RESIDUE FRACTION - PARAFFINIC REGION 91

FIGURE 4.20 $^{13}C$ NMR DATA FOR DISTILLATE FRACTION - AROMATIC REGION 92

FIGURE 4.21 $^{13}C$ NMR DATA FOR DISTILLATE FRACTION - PARAFFINIC REGION 92

FIGURE 4.22 CHAIN LENGTH AND CLUSTER SIZE 93

FIGURE 4.23 MASS BALANCE FOR AROMATIC CARBON ON ALL THREE COKING STAGES 96

FIGURE 4.24 MCR FOR DISTILLATE FRACTIONS 97

FIGURE 4.25 MCR FOR RESIDUE FRACTIONS 99

FIGURE 4.26 MCR CONTENT OF RESIDUE FRACTIONS VS. COKE YIELD 99

FIGURE 4.27 MCR VS. AROMATICITY FOR RESIDUE FRACTIONS 100

FIGURE 4.28 MCR VS. H/C FOR RESIDUE FRACTIONS 100

FIGURE 4.29 AROMATICITY VS. H/C RATIO FOR RESIDUE AND DISTILLATE FRACTIONS 101

FIGURE 4.30 HPLC DATA FOR THE DISTILLATE FRACTIONS (ELSD) 103

FIGURE 4.31 DISTILLATE FRACTION UV ABSORPTION SPECTRA - 282 NM 104

FIGURE 4.32 DISTILLATE FRACTION UV ABSORPTION SPECTRA – 210 NM 105

FIGURE 5.1 FEED TRANSFORMATIONS 106

FIGURE 5.2 FEED CONVERSION AT VARIOUS STAGES 107

FIGURE 5.3 VARIATION OF MW AND AROMATICITY FOR FEED AND PRODUCT RESIDUES 109

FIGURE 5.4 COKE YIELD VS AROMATICITY 110

FIGURE 5.5 TRICYCLIC TERPANE 112

FIGURE 5.6 TRIAROMATIC STEROID 112

FIGURE 5.7 INCREMENTAL DISTILLATE YIELD VS. DISTILLATE QUALITY 115

FIGURE 5.8 BUILDING BLOCK SCHEMATICS FOR BITUMEN MACROMOLECULES 117

FIGURE 5.9 STRAUSZ'S ASPHALTENE MOLECULE (MURGICH *ET AL.*, 1999) 120

FIGURE 5.10 SCHEMATIC DIAGRAM REPRESENTING PHASE SEPARATION 121

FIGURE 5.11 TWO COKERS IN SERIES 123

FIGURE A 1 SIMDIST CURVES FOR VARYING FLASK SIZES 139

FIGURE A 2 RESIDUE REMAINING ON REPEAT EXPERIMENTS (320°C) 140

FIGURE A 3 ORIGINAL SIMDIST CURVES FOR THE LIQUID FRACTIONS 142

FIGURE A 4 NORMALISED SIMDIST CURVES FOR THE LIQUID FRACTIONS 142

FIGURE A 5 MASS BALANCE FOR QUARTZ TUBE REACTOR 145

FIGURE A 6 MCR AND COKE YIELDS FOR 3" REACTOR PRODUCTS 147

FIGURE A 7 CALIBRATION CHART FOR FLOWMETER 148

## LIST OF ABBREVIATIONS

| | |
|---|---|
| AEBP: | Atmospheric Equivalent Boiling Points |
| BPD: | Barrels per Day |
| CCR: | Conradson Carbon Residue |
| COSY: | Correlation Spectroscopy |
| CP/MAS | Cross Polarisation / Magic Angle Spinning |
| DAD: | Diode Array Detector |
| DEPT: | Distortionless Enhancement by Polarisation Transfer |
| ELSD: | Evaporative Light Scattering Detector |
| HETCOR: | Heteronuclear Chemical Shift Correlation |
| HPLC: | High Performance Liquid Chromatography |
| MCR: | Micro Carbon Residue |
| MW: | Molecular Weight |
| NMR: | Nuclear Magnetic Resonance |
| PAH: | Polyaromatic Hydrocarbons |
| RICO: | Ruthenium Ion Catalysed Oxidation |
| SIMDIST: | Simulated Distillation by Gas Chromatography |
| TCD: | Thermal Conductivity Detector |

# 1 Introduction

## 1.1 Oil Sands of Alberta

The production potential of Alberta's three oil sand deposits - Athabasca, Cold Lake, and Peace River could be as high as 1.7 trillion barrels of bitumen of which about 300 billion barrels are recoverable by current technology (Precht and Rokosh, 1998). Currently the production of the two largest synthetic crude oil producers Suncor and Syncrude constitutes more than 18% of Canadian crude oil production.

Bitumen obtained from extraction of these oil sands needs to be upgraded to synthetic crude before it can be utilised or sold to refineries which process conventional crude. Typically Athabasca bitumen is an 8°API crude with 5 wt.% sulphur and more than 50% residue fraction. The synthetic crude sold by Syncrude known as the Syncrude Sweet Blend is a 32°API crude with no residue and low sulphur contents of 0.1-0.2 wt.%. Thus the bitumen has to be significantly processed or upgraded before being sold as synthetic crude. Furthermore, there has also been an increased focus on residue upgrading due to tightening environmental regulations, increasingly heavier crude slates and a rapidly disappearing fuel oil market.

The commercial upgrading scheme may be divided into two areas, namely primary and secondary upgrading. Primary upgrading is focussed on conversion of residue material into lighter products, removal of impurities such as metals as well as the removal of heteroatoms. The product from primary upgrading is still high in sulphur and nitrogen and may have appreciable amounts of olefinic components. Secondary upgrading takes the product from primary upgrading, removes sulphur

and nitrogen and stabilises the reactive olefinic components to form the light, sweet crude oil.

## 1.2 Research Objectives

Coking technologies like fluid coking and delayed coking process approximately 80% of the oil sands bitumen produced in Canada. A characteristic feature of these processes is a recycle stream where the unconverted residue fraction (524°C+) is returned to the reactor. The recycle stream makes it possible to eventually achieve 100% conversion of residue, but limited research has been done to determine the varying characteristics of this stream with increasing conversion.

The literature on repeated thermal cracking (Syndor and Patterson, 1930; Martin and Wills, 1959) showed that recycling resulted in an increase in liquid product yields but the changing quality of the lighter liquid product fraction thus produced has not been comprehensively quantified. This research aims to achieve a better understanding of how exactly the incremental yield will affect the product quality.

The major research objectives are listed below:

1. To determine the yields of gas, liquid and coke (i.e. the yield structure) as a function of conversion of the residue fraction of bitumen. The recycle stream in the coker eventually gives 100% conversion of residue, but the incremental yields are not known.

2. To ascertain the characteristics of the distillate products obtained from coking of residue components at high conversion. These products are produced from the

recycle stream, but their composition and hydrotreating characteristics are unknown.

3. To infer or determine the chemical structure of the MCR causing species.

## 1.3 Experimental Plan

The main target was to subject the residue fraction to repeated coking steps and track the conversion and composition of the distillate and unconverted residue at each step. The flowsheet of Figure 1.1 summarises the experimental framework of the study. The product material obtained from the first pass in the quartz tube reactor was vacuum distilled into a distillate and residue fraction. The residue fraction was then fed into the reactor as second pass feed material and the sequence of steps repeated until approximately 100% residue conversion was achieved. The products at each of the stages were then subjected to a thorough chemical analysis to determine the concentration of the different carbon functionalities, the boiling point distribution, the heteroatom content and the molecular weight. The following chemical characterisation techniques were used to evaluate the quality of the liquid product:

- NMR functional group analysis
- Simulated Distillation Gas Chromatography
- Micro Carbon Residue Analysis
- Elemental Analysis
- Molecular Weight by Vapour Pressure Osmometry
- High Performance Liquid Chromatography for the Distillate fraction

**Figure 1.1 Flowsheet of the experimental plan**

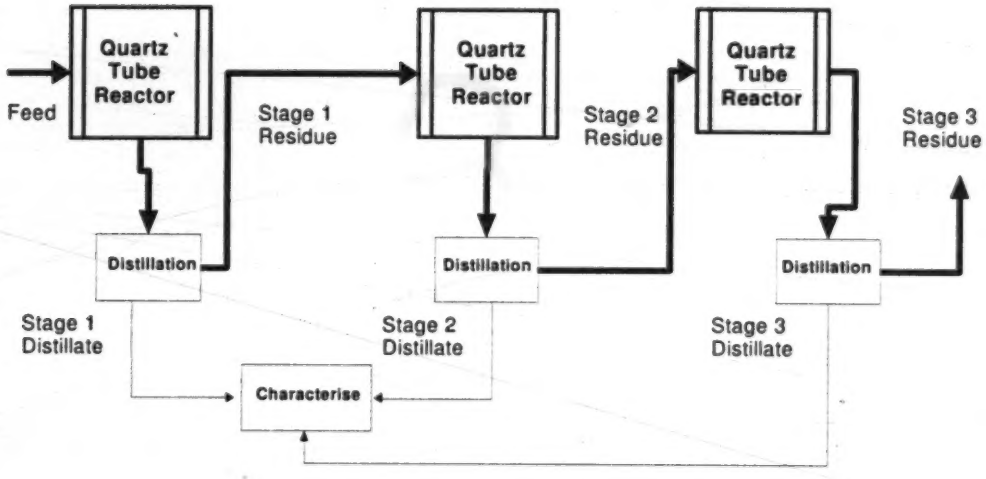

## 1.4 Outline of thesis

Chapter 1 explains the significance of this project to the oil sands industry and briefly summarises the objectives of this thesis. The extensive literature on the composition of bitumen as well as the mechanism and factors influencing coke formation are reviewed in Chapter 2. It also discusses the technology available to upgrade bitumen and heavy oils to marketable products. In Chapter 3 the experimental set-up and the analytical techniques used to characterise the samples are described. Chapter 4 illustrates the results obtained from the experiments and their analysis. Chapter 5 discusses the results and their implications. The conclusions and recommendations for further study can be found in Chapter 6. Appendix 1 contains a glossary of refining and upgrading terms often used in the industry.

# 2 Literature Survey

## 2.1 Introduction

Petroleum or crude oil is defined as a complex mixture of hydrocarbons, oily and inflammable in character (Williams and Meyers, 1964). The mixture contains largely hydrogen and carbon atoms but they often form complex mixtures with non-hydrocarbon substituents like nitrogen, sulphur, oxygen and trace metals.

Based on their physical properties petroleum may be classified into different types. On the basis of API gravity, petroleum can be divided into conventional, heavy and extra heavy oil. Conventional oil is lighter than 20°API. Heavy oil has an API gravity of between 10-20°API and extra heavy oils have an API gravity of less than 10°API. Extra heavy oil with a viscosity of more than 10,000 cP is called bitumen (Meyer and deWitt, 1990).

## 2.2 Significance of heavy oil and bitumen

At current rates of world consumption, the proven reserves of conventional oil are sufficient for only 30 years (Speight, 1991). Although new discoveries continue to be made, most people agree that the era of cheap conventional oil will soon come to an end (Campbell and Laherrere, 1998; Brown, 2000). The trend towards the utilisation of heavier crude oil can be seen from the increasingly heavier crude oils being processed today (Figure 2.1). The large reserves of heavy oil and bitumen are expected to be the major energy source for this century. Significant deposits of

heavy oil and bitumen are found in Canada, Venezuela, Russia and USA. By some estimates the world wide resource base of heavy oil and bitumen may exceed 6 trillion barrels. In the near future Canada's heavy oil sands production alone will exceed 1.2 million BPD (Lanier, 1998). Oilsands contribute towards approximately 26% of Canadian crude oil production today and have the potential to be constitute around 50% of the production by 2005 (Lachambre, 1998).

**Figure 2.1 US refinery crude oil quality (Swain, 2000)**

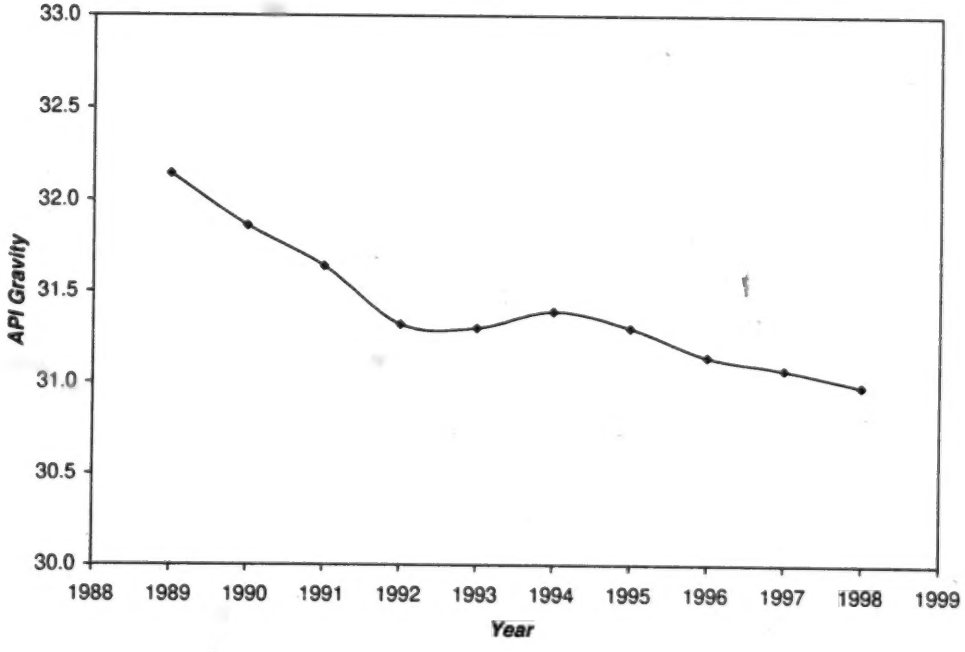

## 2.3 Composition of petroleum

The composition of petroleum varies markedly from reservoir to reservoir. Nevertheless some of the salient features common to all known petroleum types are discussed below:

### 2.3.1 Elemental analysis

Petroleum consists mainly of carbon and hydrogen along with heteroatoms like sulphur, nitrogen and oxygen. Surprisingly, as shown in Table 2.1, the elemental composition of petroleum varies only in a very narrow range for a wide variety of crude oils (Speight, 1991).

**Table 2.1 Elemental composition of a variety of crude oils**

| Element | Weight % |
|---|---|
| Carbon | 83-87 |
| Hydrogen | 10-14 |
| Sulphur | 0.05-6.00 |
| Nitrogen | 0.1-2.0 |
| Oxygen | 0.05-1.50 |

### 2.3.2 Chemical structures in bitumen

The enormous complexity of petroleum makes it difficult and often impossible to identify every compound. Heavy oil contains anywhere from 100,000 to 1,000,000 different molecules (Wiehe and Liang, 1996). Structurally, the hydrocarbon fraction is made up of a few well-defined hydrocarbon homologous series. These

series are identified as paraffins, naphthenes, aromatics and olefins. Depending on the origin and thermal history of the crude varying proportions of these various homologous series are present in the crude. A few representative compound types are shown in Figure 2.2 and Figure 2.3.

#### *2.3.2.1 Hydrocarbon groups*

1) Paraffins: The paraffinic series of hydrocarbon compounds have the general formula $C_nH_{2n+2}$ and can contain either a straight chain or a branched chain carbon backbone. The relative proportion of these types will affect the property of the final refinery product. For example, the branched-chain paraffins give higher octane numbers than normal paraffins. Typically, for the case of Athabasca bitumen, paraffinic structures are found only as side chains on aromatic or cycloparaffinic rings.

2) Aromatics: These are unsaturated ring-type compounds with the general formula $C_nH_{2n+Z}$ where Z = -2(R+DB-1) and R is the number of rings and DB the number of double bonds. The number of rings can vary from a single benzene ring to ten or more rings (Groenzin and Mullins, 2000). Larger polynuclear aromatics are found in heavier fractions of crude oil and processed petroleum fractions. Most of these exist in petroleum as compounds with normal or branched chain alkanes or naphthenics attached. They are an important class of compounds and can be directly correlated with the yield of coke.

3) Naphthenes: These are saturated hydrocarbons arranged in the form of closed rings with the general formula $C_nH_{2n+Z}$ where Z = -2(R-1) and R is the number of rings. Naphthenic compounds contain anywhere from one to six condensed rings. These compounds can dehydrogenate easily under thermal cracking conditions to give aromatics.

4) Alkenes: Olefins have the general formula $C_nH_{2n}$ and contain only one carbon-carbon double bond in the chain. Diolefins have two carbon-carbon double bonds. These series of hydrocarbons have the general formula $C_nH_{2n-2}$. Alkenes are usually formed by thermal and catalytic cracking and rarely occur naturally in unprocessed crude oil. These compounds are more reactive than paraffins or naphthenes and are usually undesirable components as they can easily polymerise forming gummy residues.

**Figure 2.2 Representative compound types**

**Bi-phenyl**
**(polycyclic aromatic)**

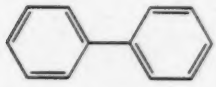

**Pyrene**
**(polycyclic aromatic)**

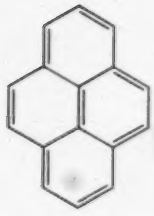

**Tricyclic terpane**
**(Three ring naphthene with alkane side chain)**

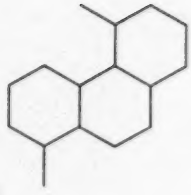

**Diolefin**

#### *2.3.2.2 Heteroatomic groups*

Heteroatoms are undesirable constituents in the refinery product stream and must be removed by catalytic or thermal processes.

1) Sulphur Compounds: Sulphur may be present in crude oil as hydrogen sulphide ($H_2S$) or as compounds like mercaptans, sulphides, disulphides, thiophenes, etc. or even as elemental sulphur. Both the proportion and complexity of the compounds present increase as the crude gets heavier.

2) Nitrogen Compounds: Nitrogen is found in two forms: basic compounds, and nonbasic compounds. Basic nitrogen is present in the form of pyridine, quinoline and acridine rings while pyrrole, indole and carbazole types are the nonbasic ring types. These compounds are generally difficult to remove and cause severe catalyst deactivation in downstream refinery processes.

3) Oxygen Compounds: Oxygen compounds such as phenols, ketones, and carboxylic acids occur in crude oils in small amounts.

4) Trace Metals: Almost every element in the periodic table has been identified in petroleum but the most abundant metals include nickel, iron, and vanadium. Metals maybe present as porphyrin metal complexes or may be associated with the polar groups in asphaltene (Gray, 1994). A simple porphyrin structure is shown in Figure 2.3. It is desirable to remove these metals prior to processing as they have been identified as catalyst poisons.

**Figure 2.3 Heteroatomic groups present in petroleum**

**Benzothiophene**

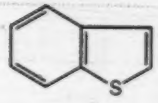


**Sulphide or Thioether**

**Alkyl indole**

**(Non basic Nitrogen)**

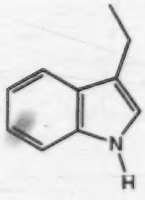


**Alkyl acridine**

**(Basic Nitrogen)**

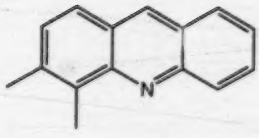


**Vanadyl Porphyrin**

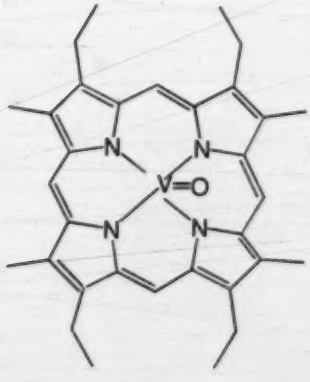

### 2.3.3 Class fractionation

The enormous complexity of petroleum makes component by component analysis extremely difficult. One way to reduce the complexity and thus to obtain a better insight into the processability is to divide the petroleum into various well-defined fractions. There are a number of ways to achieve the fractionation of petroleum based on their molecular size and type (Speight, 1991). Two of the most frequently employed methods are based on molecular size (distillation) and solubility classes (asphaltene precipitation).

#### *2.3.3.1 Distillation*

Distillation is a key separation technique that divides petroleum into various fractions based on boiling point. It is especially significant since most refinery products are classified based on their boiling point ranges. Distillation limits the enormous diversity of petroleum in terms of its molecular weight range as well as the structural diversity of petroleum compounds (Figure 2.4).

It is important to remember that any narrow boiling point range will still include a variety of different molecular types since boiling points are dependent not only on molecular weight, but also on molecular interactions brought about by functional groups involved in hydrogen bonding. For example any narrow boiling cut can consist of lower molecular weight heteroatomic polar molecules and relatively higher molecular weight non-polar hydrocarbons.

Fractionation by distillation is limited due to the thermal instability of crude above 320°C. Even vacuum distillation techniques are limited to cut points of around

550°C (atmospheric equivalent boiling points) or less. Some researchers claim to have developed short path distillation techniques that can achieve cut points up to 660°C without substantial alteration of the molecular structure (Domansky, 1986). Even this high temperature is still a major limitation especially for heavy oil and bitumen that may have more than 25% non-volatile residue fraction with boiling points greater than 660°C. Separation of still higher boiling material requires other fractionation techniques; for example, those based on solubility.

**Figure 2.4 Variation of boiling point with molecular weight and structure (Speight, 1991; Altgelt and Boduszynski, 1994)**

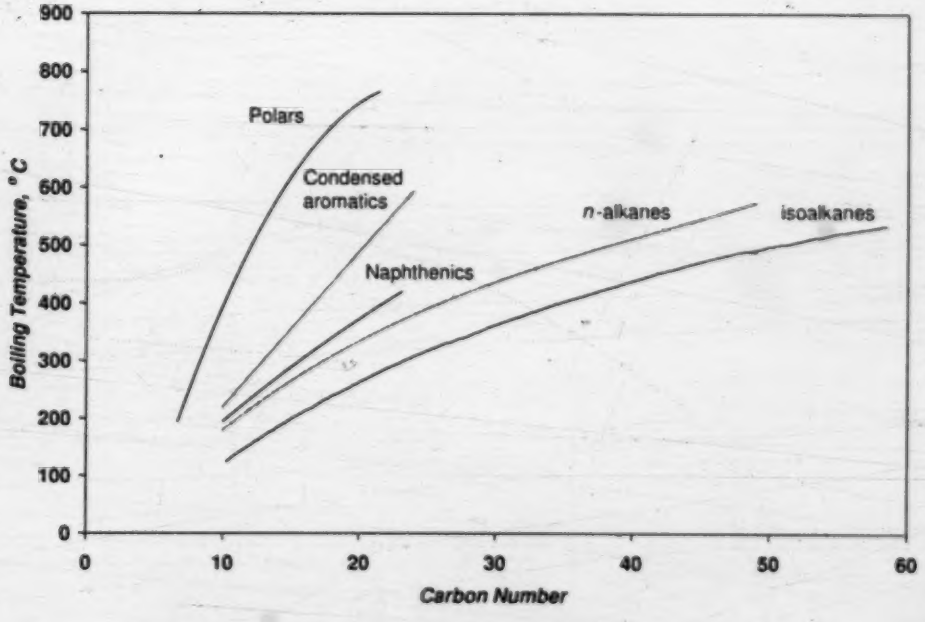

#### 2.3.3.2 *Separations based on solubility*

There are various fractionation techniques applied to petroleum fractions based on differences in solubility in a given solvent. Based on their solubility in low molecular weight *n*-alkanes, petroleum is divided into two fractions, asphaltenes and maltenes. Asphaltenes are defined as the toluene-soluble fraction that precipitates from petroleum when an excess (25 to 40 times) of *n*-heptane (or *n*-pentane) is mixed with petroleum. The *n*-heptane (or *n*-pentane) soluble portions are called maltenes.

SARA is another method of separation by which petroleum is separated into four fractions: saturates, aromatics, resins and asphaltenes. Asphaltenes are first precipitated using *n*-pentane followed by resin separation that is done with the help of a single column containing ion-exchange resins and a clay-$FeCl_3$ packing. This is followed by a silica-gel column for separation of saturates and aromatics (Jewell *et al.*, 1974).

#### 2.3.3.3 *Other separation methods*

A separation technique developed by Boduszynski (1987) involves the use of short path distillation and sequential elution fractionation. He fractionated various petroleum samples into cuts having progressively higher atmospheric equivalent boiling points (AEBP). The distillation was done using short path distillation followed by separation of four fractions based on solubility classes. Boduszynski studied the variation of molecular weights, hydrogen deficiency, heteroatom concentration etc. as a function of AEBP. It was found that although the heteroatom

content and hydrogen deficiency follow monotonically increasing trends, vanadium and nickel display a bimodal distribution.

Supercritical fluid extraction is another technique that has been used to separate petroleum residue into several fractions based on molecular weight (Chung *et al.*, 1997). Athabasca vacuum residue was separated into ten different fractions by supercritical extraction using *n*-pentane as the solvent with the pressure being varied from 3.5 MPa to 12 MPa. The variation of the various properties with molecular weight is shown in Figure 2.5.

**Figure 2.5 Properties of the various fractions with molecular weight**

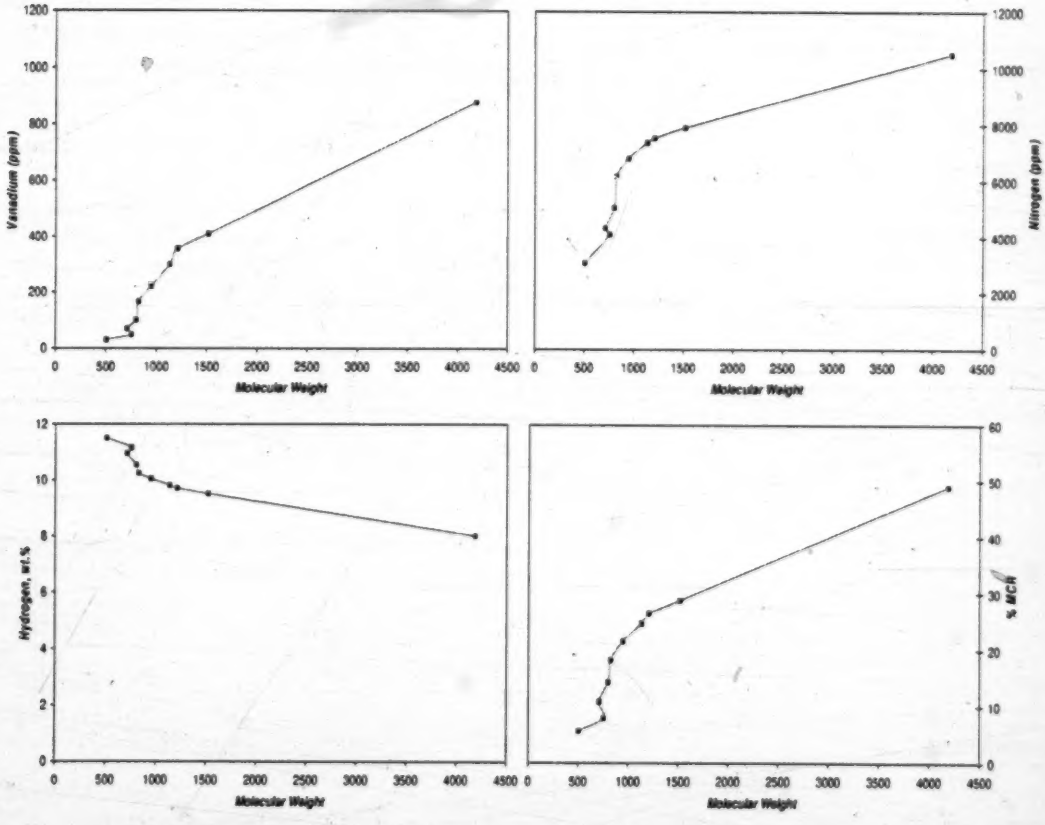

### 2.3.4 Asphaltenes

One of the most intractable portions of petroleum is the asphaltene fraction. Although the most reactive, they contribute some of the most refractory components in petroleum. They are generally thought to be highly complex mixtures containing not only the highest molecular weight components but also some of the most aromatic and most polar components. Disproportionate quantities of coke precursors exist in the asphaltene fraction and thus the interest in trying to understand the asphaltene molecular structure. However, it is difficult to isolate and identify individual asphaltenic components due to their high degree of complexity. Little wonder then that the exact chemical structure of asphaltene remains an area of ongoing research and speculation.

#### *2.3.4.1 Molecular Structure*

The structure of asphaltenes is one of the most contentious issues among researchers. Yen *et al.* (1961) examined the structure of petroleum asphaltenes by using X-ray diffraction (XRD). They resolved the peak obtained by XRD into two, a peak due to condensed aromatic systems and another due to saturated structures. Reproducing the obtained peak from known chemical structures they were able to calculate the aromaticity that ranged from 0.26 to 0.53. The characteristic crystallite parameters of the asphaltene were also obtained. The asphaltene model thus developed is shown in Figure 2.6 with the characteristic parameters. The model consisted of stacked condensed aromatic sheets with alkyl substituents.

**Figure 2.6 Asphaltene model proposed by Yen *et al.* (1961).**

**$d_m$ = interlayer distance, $L_c$ = Diameter of aromatic sheet perpendicular to plane of sheet, $L_a$ = Diameter of aromatic sheet**

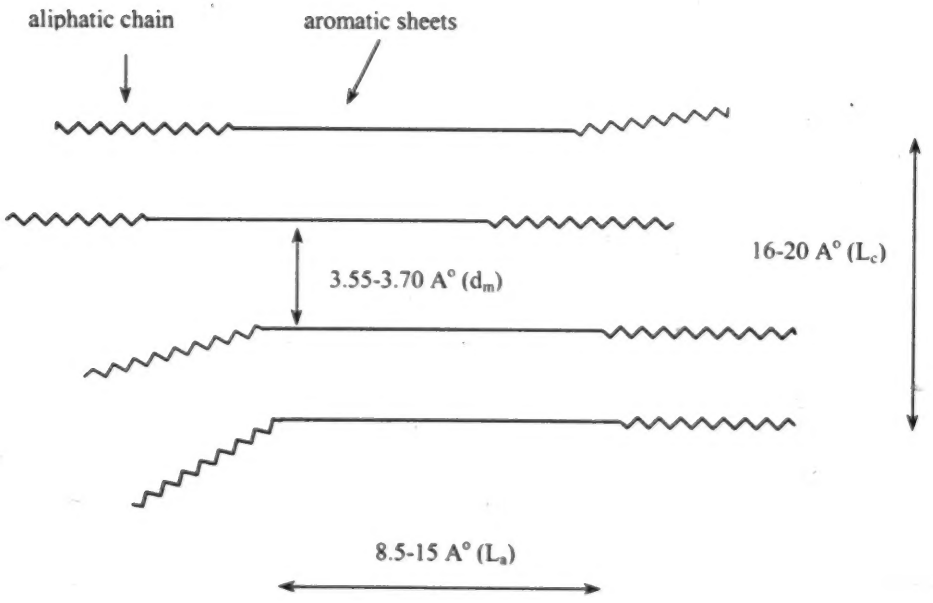

Other researchers have questioned the reliability of using XRD to determine aromaticity. Ebert *et al.* (1985) pointed out that the method fails for a number of reasons. The band due to interference from the naphthenes was not considered. Also, the diffraction band arising from an infinite aromatic stack is different from a cluster of small aromatics, which was not taken into account by the model.

The aromatic ring size distribution of asphaltenes has never been directly measured. Although estimates range from a few to twenty condensed rings, the only agreement among researchers today is that there are less than ten fused rings. Speight (1991) has estimated that there is a maximum of six rings with a preponderance of one to four ring structures whereas other reseachers claim an average of 7 rings (Groenzin and Mullins, 2000). Still, this is much smaller than the highly condensed ring structures (six to twenty fused rings) initially proposed by various researchers (Yen, 1972; Speight and Moschopedis, 1981). It is important to note that the stacking pattern shown by asphaltenes does not require huge condensed ring systems. Discotic liquid crystals that contain a one to four ring aromatic core with aliphatic side chains, also tend to display similar stacking behaviour (Wiehe, 1994).

Strausz *et al.* (1992) have extensively characterised Athabasca bitumen asphaltene using various chemical means like ruthenium ion catalysed oxidation (RICO). RICO is capable of selectively oxidising aromatic carbon and removing it as $CO_2$. From their studies they concluded that large pericondensed ring systems were absent in Athabasca asphaltene. They found that length of the paraffinic chain attached to the asphaltene molecules extends beyond $C_{27}$ with a maximum at $C_1$. The

length of the bridges between aromatic rings varies from $C_{24}$ to $C_2$ with a maximum at $C_3$. There is twice as much carbon in chains as in bridges and three times as many chains as bridges. A substantial amount of carbon was also found as chains or bridges attached to naphthenic rings. They also noted that the position of the chain substituents is such that that ring structure can be opened up so that the ring skeleton and alkyl chain form a non branched alkyl chain. They estimated that 25% sulphur in the asphaltene is present as sulphide and the rest as thiophenes. The asphaltene model compound proposed by Strausz *et al.* (1992) is shown in Figure 2.7.

**Figure 2.7 Asphaltene molecule as proposed by Strausz *et al.* (1992)**
**Molecular formula:- $C_{420}H_{496}N_6S_{14}O_4V$**

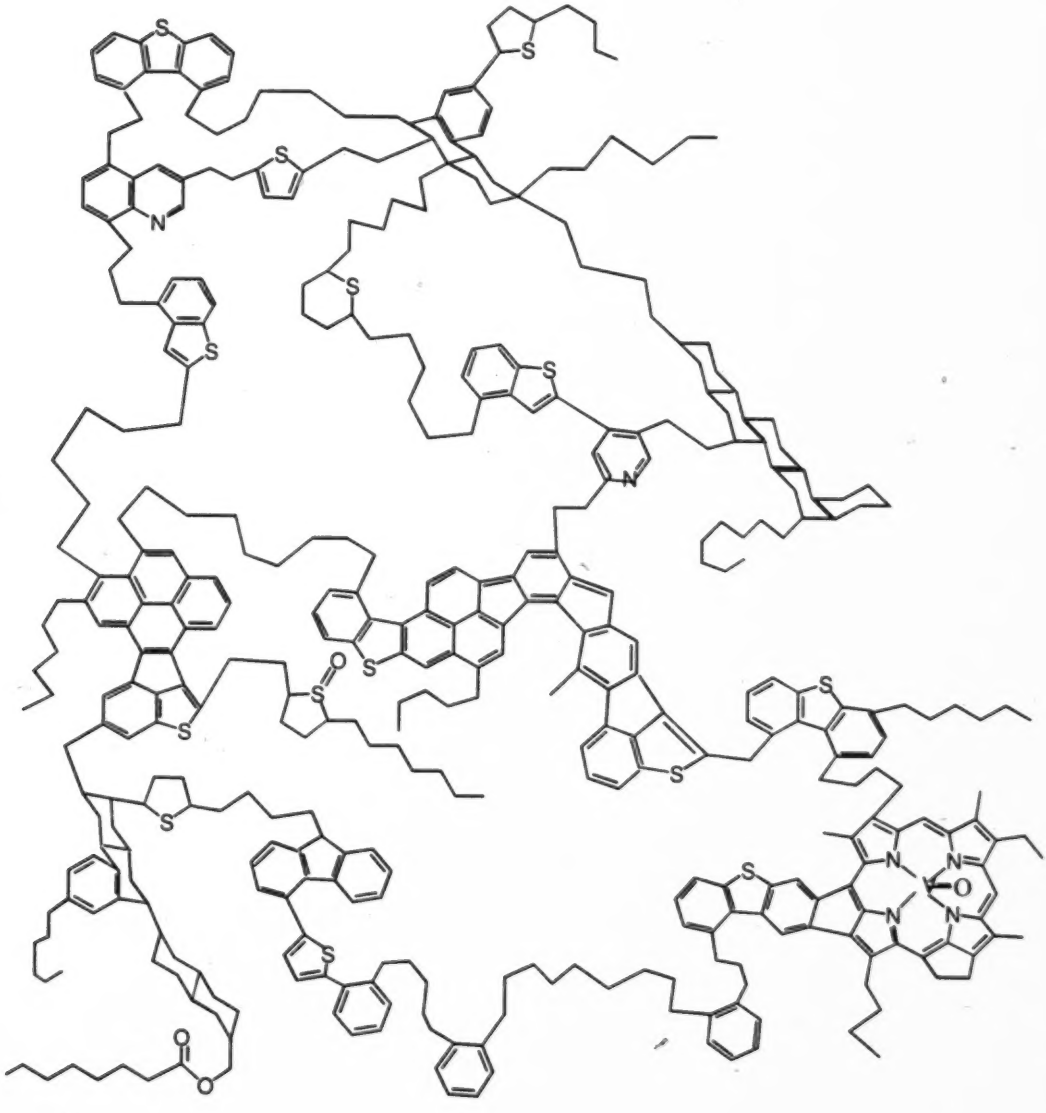

### *2.3.4.2 Molecular Weight*

Another contentious area regarding the asphaltene structure is the determination of the average molecular weight. Molecular weights of asphaltene as high as 300,000 dalton have been claimed (Speight and Moschopedis, 1981). Depending on measurement technique, asphaltene concentration and solvent used for the determination molecular weights can vary considerably even for the same asphaltene. For example, the molecular weight of Athabasca asphaltene has been reported to range from 885-10910 (Champagne *et al.*, 1985).

It is well known that asphaltenes tend to associate even in dilute solutions. The presence of relatively high concentration of heteroatoms leads to significant molecular associations via hydrogen bonding in addition to van der Waals interactions. These associations are weak and can be broken by using a good solvent at temperatures of 120°C to 150°C. Wiehe (1992) showed that using *o*-dichlorobenzene and temperatures of 130°C increased concentrations did not cause aggregation effects seen at the lower temperature of 70°C (Figure 2.8).

Asphaltenes are a solubility class and any asphaltene contains a number of compounds having a wide range of molecular weights and structures. Cyr *et al.* (1987) separated various asphaltene fractions using gel permeation chromatography. They showed that though the average molecular weight was 3600 they could separate various fractions having molecular weight ranging from 1200 to 16900. The highest molecular weight fraction had the lowest aromaticity and the lowest molecular weight fraction had the highest aromaticity.

**Figure 2.8 Molecular weight of Arabian Heavy oil asphaltene in *o*-dichlorobenzene at different temperatures (Wiehe, 1992)**

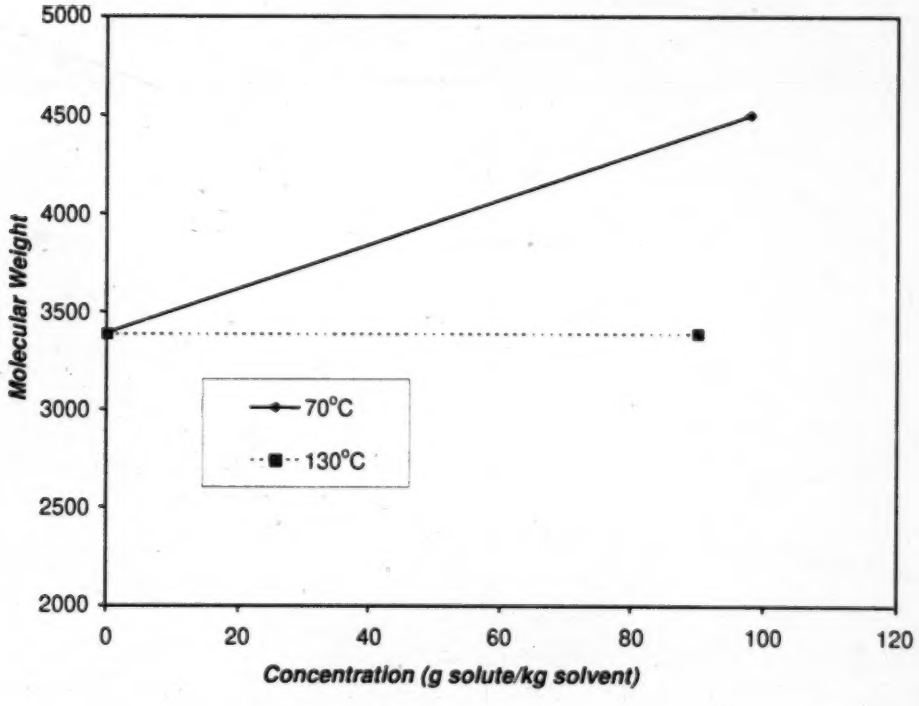

## 2.4 Thermal Cracking

Bitumen upgrading is achieved mainly by thermal cracking reactions. When hydrocarbons are brought to high temperatures they undergo thermal cracking via free radical reaction mechanisms. Cracking involves breaking down the large molecules into smaller ones. When petroleum compounds are heated to 320°C the aliphatic C-S bonds, one of the weakest bonds in the petroleum molecule start breaking and produce $H_2S$. Over 410°C, C-C bond breaking reactions start taking place within the petroleum molecule (Gray 1994; Poutsma 1990). The bond energies determine the degree of difficulty of breakage of the bonds and thus the selectivity with respect to the product formed.

**Table 2.2 Bond dissociation energies (Benson, 1976; Gray 1994; Greinke 1992)**

| Bond type | Bond dissociation energy (kcal/mol) |
|---|---|
| *i*-$C_3H_7$-$CH_3$ | 84 |
| $C_3H_7$-$C_2H_5$ | 82 |
| $C_6H_5$-$CH_2$-$CH_3$ | 90 |
| $C_6H_5$-$CH_2$-$CH_3$ | 72 |
| $C_6H_5$-$C_6H_5$ (aromatic) | 116 |
| $C_3H_7$-H | 98 |
| $C_6H_5$-H (aromatic) | 110.5 |
| $CH_3S$-$CH_3$ | 77 |

All free radical chain reactions go through initiation, propagation and termination steps. As an illustration the mechanism of thermal cracking of an alkane is shown below (Gray, 1994):

| | | |
|---|---|---|
| Initiation: | $M \longrightarrow$ | $2\,R^{\bullet}$ |
| Propagation: | | |
| Hydrogen extraction: | $R^{\bullet} + M \longrightarrow$ | $RH + M^{\bullet}$ |
| β–scission: | $M^{\bullet} \longrightarrow$ | $R^{\bullet}$ + Olefin |
| Termination: | Radical + Radical $\rightarrow$ | Products |

Here M is the parent compound, and $R^{\bullet}$ is the smaller hydrocarbon radical formed as a result of cracking. In cracking reactions paraffins decompose to form paraffin and olefins. At high temperature and low pressure, radicals tend to break all the way down to $CH_3^{\bullet}$ or $H^{\bullet}$, giving one molecule of 1-olefin, several molecules of $C_2H_4$ and $CH_4$ or $H_2$. This is described as the Rice-Kossiakoff mechanism. At low temperature and high pressure, the radical formed by β-scission will tend to undergo hydrogen abstraction giving one molecule of an olefin and one molecule of an alkane. This is known as the Fabuss-Smith-Satterfield mechanism (Poutsma, 1990).

Naphthenes are generally less reactive as compared to paraffins. In model compound experiments by Savage *et al.* (1988) on tridecylcyclohexane the major pair of reaction products were cyclohexane and 1-tridecene as well as methylenecyclohexane and dodecane. The study indicated that ring opening reactions were of minor consequence.

The major reactions of hydroaromatics can be represented using tetralin as the model compound (Figure 2.9). The preferred product under thermal cracking conditions was naphthalene (de Vlieger *et al.*, 1984). For alkylhydroaroamtics similar reactions were seen. In a study by Savage and Baxter (1996) on the alkylhydroaromatic 2 dodecyl-9,10-dihydrophenanthrene it was shown that under thermal cracking conditions the primary reaction product is 2-dodecylphenanthrene at reaction times stretching to 120 minutes. Polycyclic hydroaromatics are even more reactive than tetralin. It should be noted however that for polycyclic hydroaromatics at higher reaction temperatures (450°C) there were significant amounts of ring contracted product, even in the presence of coal (Collin *et al.*, 1985).

**Figure 2.9 Reactions of hydroaromatics with tetralin as model compound**

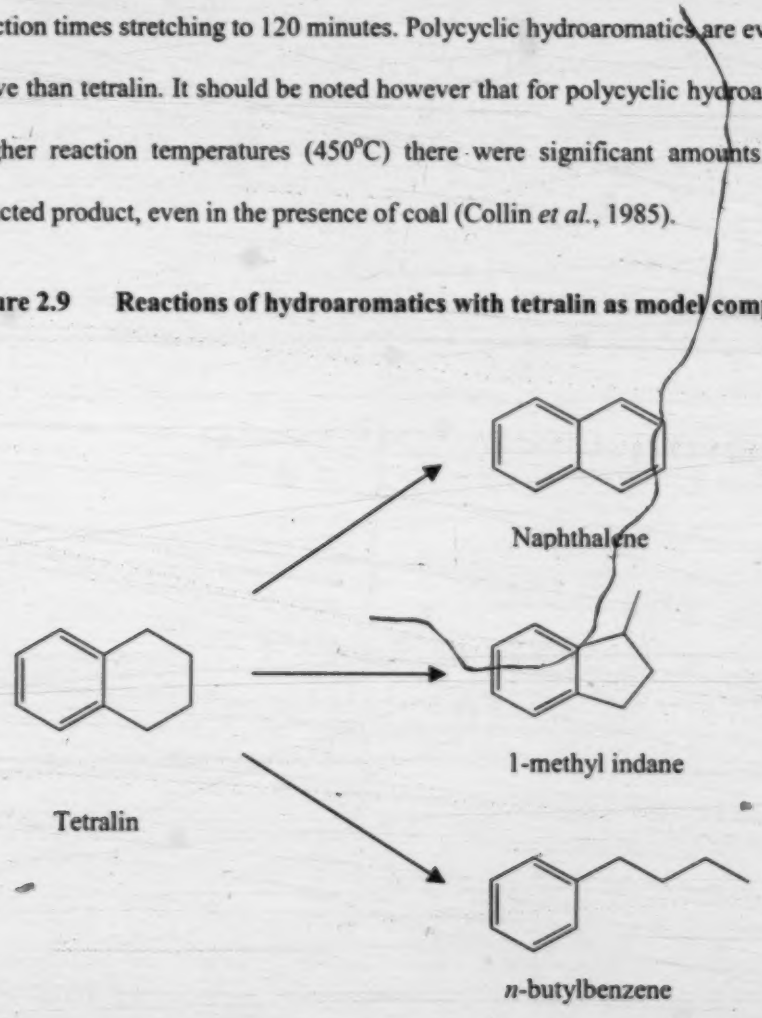

The aromatics are resonance stabilised and therefore have higher bond energies (Table 2.2). There is some disagreement among researchers whether aromatics can crack under reaction conditions, but most agree that this is unlikely below 700°C (Gray, 1994; Poutsma, 1990; Speight, 1991; Sanford, 1994; Fitzer *et al.*, 1971). Unsubstituted aromatics can react by chemical condensation to form polynuclear aromatics along with their respective hydrogenated derivatives (Poutsma, 1990; Fitzer *et al.*, 1971).

Alkyl-substituted aromatics are more reactive than unsubstituted ones, the effect being more pronounced the greater the number and length of the alkyl groups. Since the bond dissociation energy of small alkylaromatics indicated that the alkyl bond β to the benzene ring is easier to thermally fracture than the α bond (Table 2.2), it was generally believed that cracking took place at the carbon β to the aromatic for all alkylaromatics (Savage and Klein, 1987; Mushrush and Hazlett, 1984; Stalick *et al.* 1994). This was supported by the fact that pyrolysis of alkyl benzenes led to formation of an olefin and toluene and styrene and *n*-alkanes at typical processing conditions. On the other hand model compound studies on polycyclic alkyl aromatics pointed out the relatively facile cleavage of the alkyl-aryl C-C bond which led to the formation of an aromatic core and an alkane chain. (Savage *et al.*, 1989; Grienke, 1992; Freund *et al.*, 1991; Stalick *et al.* 1994). For example, the pyrolysis of dodecyl pyrene gave pyrene and dodecane as the major products (Figure 2.10). Obviously the alkyl-aryl C-C bond is susceptible to cleavage and could be a significant route in cracking of petroleum residue.

**Figure 2.10 Major reaction products from dodecyl pyrene pyrolysis (Savage *et al.*, 1989)**

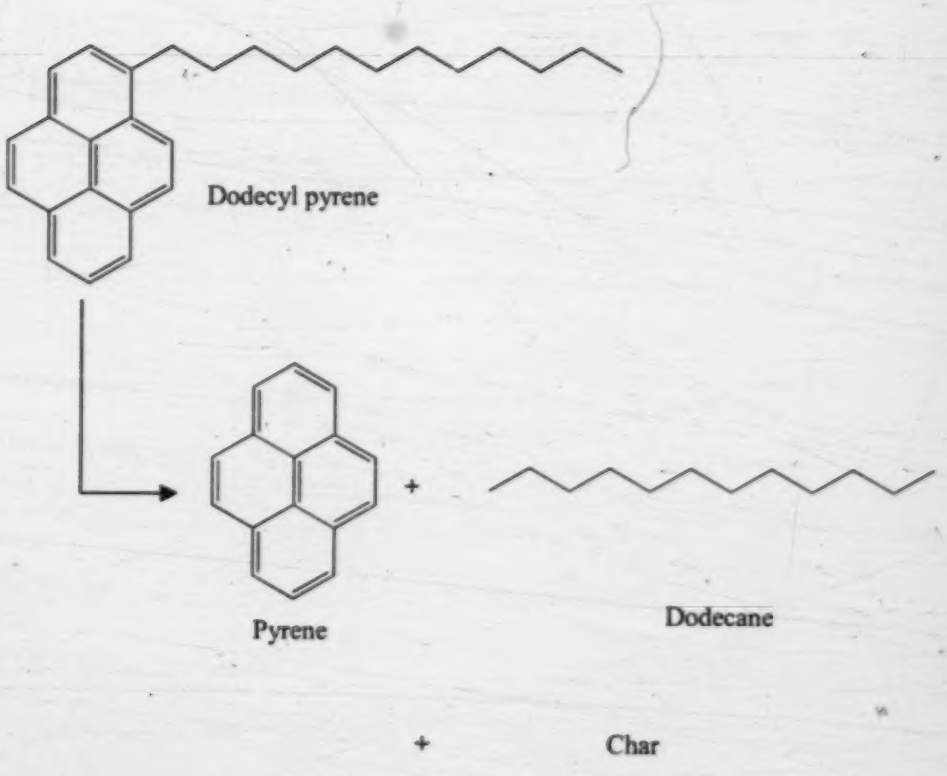

Substituted cyclic structures make up the bulk of the petroleum residue fraction. Besides dehydrogenation of cycloparaffins, thermal cracking reactions comprise mostly of dealkylation of side chains. Residue conversion may be viewed as cracking of the side chains of alkylaromatics and alkylnaphthenes compounds leaving behind a refractory aromatic core. This is also the major reason that a high degree of correlation is seen between degree of conversion of unprocessed residue and the fraction of α-carbon (Gray *et al.*, 1991).

## 2.5 Mechanism of Coke Formation

Coke is defined in terms of its solubility. In most laboratories toluene insolubles are called coke, although any solid carbonaceous material produced during the processing of hydrocarbons is generally termed coke. Structurally coke produced from one process, say fluid coking, may be quite different from that produced in another process, for example, coke produced on hydrotreater catalyst (Egiebor *et al.*, 1989). All thermal upgrading processes, whether in the presence or absence of catalyst, can ultimately lead to the formation of coke. For most bitumen upgrading processes, coke formation is an undesirable by-product and every effort is made to reduce coke formation. Coking processes aim to form the minimum amount of coke to eliminate the most refractory portions of the feed. In catalytic hydrocracking or visbreaking processes, where coke formation often leads to serious problems, it has to be avoided altogether.

### 2.5.1 MCR as indicator of coke formation in reactor

Micro Carbon Residue (MCR) is a standard test technique (ASTM 4530) often used in the industry to measure coke forming propensity of a feedstock. MCR (Noel, 1984) was designed to replace the Conradson Carbon Residue (CCR) test and gives similar values as the CCR test (Wiehe, 1994). In an MCR test a weighed quantity of a sample is placed in a glass vial and the temperature ramped up to 500°C in a nitrogen atmosphere. Nitrogen is used as the carrier gas and helps remove the volatile materials. The carbonaceous residue left behind is reported as the %MCR.

MCR or CCR has been correlated with the 524°C+ pitch content (Ternan and Kriz, 1990), the amount of asphaltene present (Nelson, 1958; Trasobares *et al.*, 1998), the aromaticity (Gray *et al.* 1991) as well as hydrogen content (Wiehe 1994; Trasobares *et al.*, 1998). The method most often used to predict coke yields in a given process is via empirical correlations relating MCR to coke yields (Martin and Wills, 1959; Gary and Handwerk, 1984). The correlations shown below have been proposed by Martin and Wills (1959).

Delayed Coking

$$\left.\begin{aligned} W_c &= 2.0 + 1.66\,K \\ W_{cg} &= 5.5 + 1.76\,K \end{aligned}\right\} \qquad (2.1)$$

Fluid Coking

$$\left.\begin{aligned} W_c &= 1.15\,K \\ W_{cg} &= 5.0 + 1.30\,K \end{aligned}\right\} \qquad (2.2)$$

*where* $K$ = *Conradson Carbon*

$W_c$ = *coke yield, weight %*

$W_{cg}$ = *coke plus gas yield, weight %*

As seen above MCR is related to the yield of coke via empirical correlations. MCR or CCR yields have in turn been correlated to H/C ratios. Roberts (1989) has shown that a linear correlation exists between the H/C ratio and the CCR make (also see Wiehe, 1994). He also showed that for a given crude whether processed or unprocessed, a straight-line correlation was also seen with nitrogen content. Furthermore, distillation curves, API gravity, pour point and bitumen viscosity are all related to H/C ratio (Speight, 1991). Aromaticity also shows a linear correlation with the H/C ratio (Ouchi, 1985). This makes the variation of the H/C ratio another important indicator of processability of the petroleum fraction.

### 2.5.2 Pendant Core Model

The pendant core model proposed by Wiehe (1994) was derived based on the fact that for both processed and unprocessed streams above a molecular weight of 700, a linear relation is obtained between MCR and hydrogen content. In the model the petroleum molecule is considered to be a copolymer made up of two blocks: one called pendant and the other the core. Assuming a fixed hydrogen content for coke ($H_C$) and determining the hydrogen content of the pendants ($H_P$) which is constant

for given feed, the Micro Carbon Residue (*MCR*) content of any feed of intermediate hydrogen content (*H*) can be determined.

$$100H=(100-MCR)H_P+MCR.H_C$$

$$MCR=0 \qquad H \geq H_C$$

$$\mathbf{MCR= 100(H_P-H/H_P-H_C)} \qquad H_P \geq H \geq H_C \qquad (2.3)$$

$$MCR=100 \qquad H \leq H_C$$

One of the drawbacks of the Wiehe model is that it places a limitation that the molecular weight of the feed material to the reactor be higher than 700 dalton. This limit is placed to allow for the fact that lower molecular weight feeds will volatilise out of the reactor without reacting and should therefore give lower coke make or MCR contents. Unfortunately, cracked refinery streams always have a molecular weight less than 700 dalton and this limits the applicability of the model.

The two major factors that influence coke yield, are molecular weight and aromaticity. The Wiehe pendant core model has attempted to simplify the model by substituting hydrogen content for aromaticity as a measure of coke forming tendency and excluded all data where volatilisation may be an issue.

### 2.5.3 Other factors influencing coke formation

#### *2.5.3.1 Phase separation*

The formation of solid coke from liquid petroleum necessitates phase separation. As a petroleum molecule is subjected to cracking reactions the material becomes more aromatic as a result of the cracking of the side chains (Gray *et al.*, 1989). The

material undergoing cracking slowly becomes chemically dissimilar and therefore incompatible with the surrounding medium resulting in phase separation. The formation of this heavy aromatic 'coke precursor' liquid is thus the first step in the formation of coke.

Even in simple mixtures, liquid-liquid phase separation was observed by Shaw *et al.* (1988). When pyrolysing a mixture of tetralin and pyrene, at temperatures exceeding 418°C and a hydrogen pressure exceeding 12 MPa they found that the liquid separated into two phases, one rich in pyrene and the other rich in tetralin and other degradation products. Evidence for the formation of a second liquid phase also comes from work done by Liu *et al.* (1998). They showed the existence of coke microspheres indicating the past liquid behaviour of the coke.

Phase separation results in a second phase that does not have access to the hydrogen donor oil (Wiehe 1993; Gray, 1994). Once this second liquid phase, which is rich in coke precursors is formed, rapid condensation reactions can take place leading to coke formation.

#### *2.5.3.2 Fine solids*

Tanabe and Gray (1997) found that naturally occurring fine solids in vacuum residue reduced coke formation compared with the solid-free feeds. It was postulated that the fine solids accumulated on the interface of the new 'coke precursor phase' and thereby stabilised the coke precursors from coalescence. The existence of the dispersed phase led to better contact with the hydrogen donor compounds in the oil phase and consequently reduced the rate of coke formation.

## 2.6 Upgrading Processes

Typically, bitumen obtained from extraction of oil sands needs to be upgraded to synthetic crude before it can be utilised or sold to refineries which process conventional crude. There are a variety of processes that are used to upgrade heavy feeds. These processes may be divided into carbon rejection processes, e.g. coking and deasphalting, and processes without carbon rejection, e.g. visbreaking or catalytic hydrogen addition processes such as LC Fining or the H-Oil process (Speight, 2000; Le Page *et al.*, 1992). The bulk of the residue processing is done by thermal upgrading and coking is the resid upgrading process of choice for today's heavy oil refiners (Wiehe, 2000). A standard upgrading scheme involves coking the bitumen followed by hydrotreating to obtain the synthetic crude. The varying properties of a typical gas oil fraction undergoing these processes is tabulated in Table 2.3.

**Table 2.3 Properties of oil before and after upgrading (Wang, 2000)**

| Property | Bitumen | Coker gas oil | Hydrotreated gas oil |
|---|---|---|---|
| Carbon (Weight %) | 83.3 | 83.5 | 86.0 |
| Hydrogen (Weight %) | 10.38 | 10.5 | 12.9 |
| Sulphur (ppm) | 47770 | 41500 | 301 |
| Nitrogen (ppm) | 5041 | 3400 | 5.0 |
| Asphaltene (Weight %) | 16.9 | 0.6 | n.d. |
| Density ($kg/m^3$ at 15 °C) | 1015.8 | 990.2 | 880 |
| Viscosity (MPa-S at 20 °C) | | 492 | 6.5 |
| Boiling range (°C) | 323 - >720 | 275 – 540 | 177 – 433 |

### 2.6.1 Coking Processes

Coking is essentially a severe thermal cracking reaction to break residue molecules to lower boiling components. At the same time, coking separates catalyst poisons and other undesirables in the form of a solid by-product called coke. Coking processes may broadly be divided into delayed coking and fluid coking. The major coking processes are listed in Table 2.4.

**Table 2.4 Different kinds of coking processes (Le Page *et al.*, 1992)**

| Delayed Coking and similar processes | Fluid Coking and similar processes |
|---|---|
| Delayed Coking | Fluid Coking |
| ACTIV | Flexi Coking |
| EUREKA | LR Coking |
| CHERRY P | ART process |
| | KK process |

#### *2.6.1.1 Delayed Coking*

In the delayed coker, the feed enters the bottom of a fractionator where it mixes with the hot vapours from the coke drum (Figure 2.11). The heavy ends from the vapour stream are condensed and recycled into the coke drums along with the fresh feed. Before being fed into the coke drums, the combined feed is first sent to a furnace that raises the temperature to about 500°C. The heated feed is then fed into coke drums where the residence time for the vapours is about a few minutes.

**Figure 2.11 Delayed coker flowsheet**

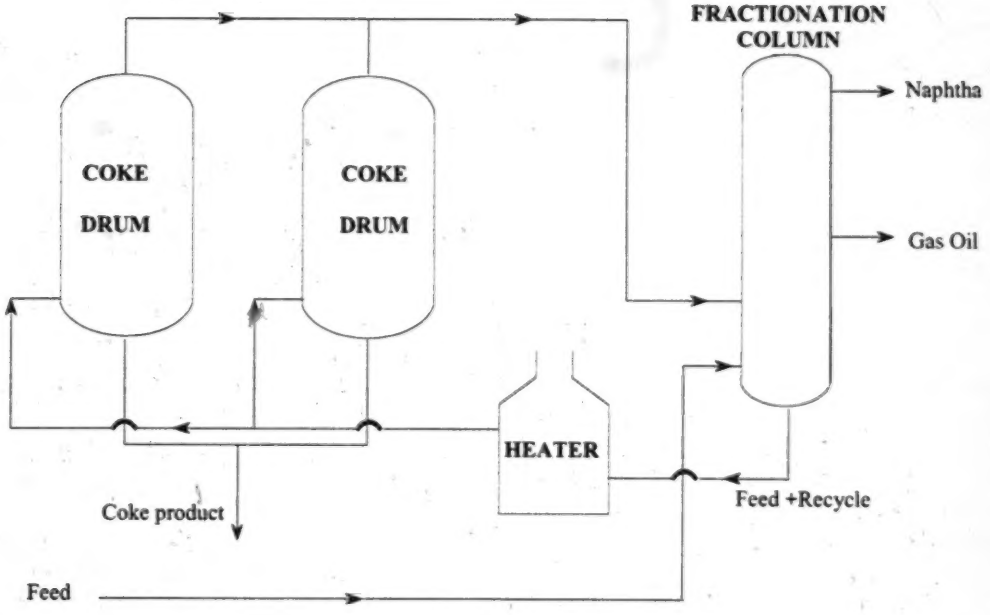

Cracking and polymerisation take place in the coke drum for a 24-hour period. The cracked overhead products are sent to the fractionator and the naphtha and gas oil fractions are recovered.

Coking is a batch operation carried out in two coke drums. Coking takes place in one drum while the other the drum is cooled and decoked. The coke is removed using high-pressure water jets to cut the coke from the drum.

#### *2.6.1.2 Fluid Coking*

Fluid coking is a continuous process in which the feed is preheated and sprayed into a fluidised bed of hot coke particles maintained at 450°C to 550°C. The feed liquid forms a film on the coke particles and cracks to give vapours and coke. The particles thus grow by layers as coke is deposited. The cracked vapours pass through cyclones on top of the reactor to remove the entrained coke particles and the vapours move on to the scrubber section, where they are quenched by fresh feed. The high boiling portion of the vapour stream is recycled into the reactor. The coke is removed from the bottom of the reactor where it is steam stripped and sent to a burner. The heat for the endothermic cracking process and for heating the feed comes from burning some of the coke and returning the hot coke to the reactor.

**Figure 2.12 Fluid coker flowsheet**

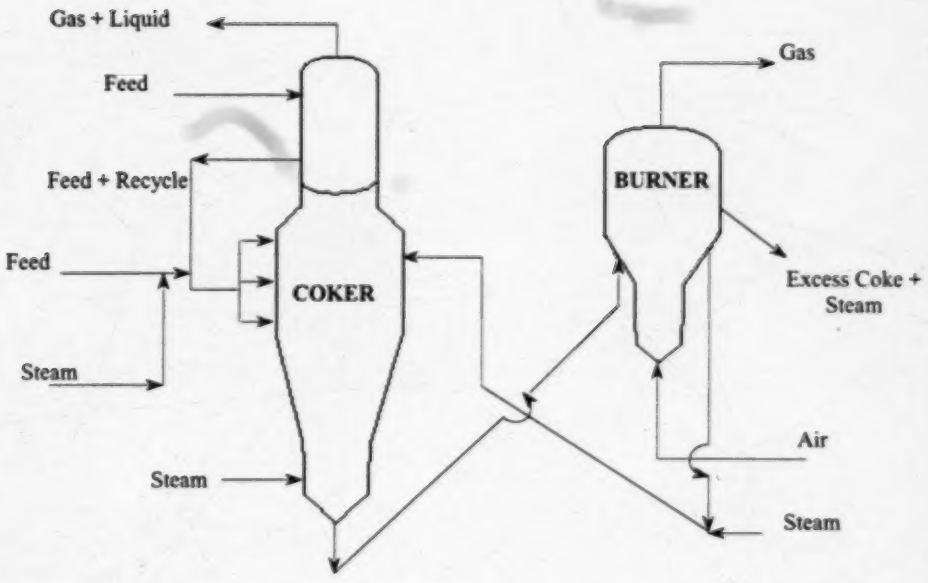

### *2.6.1.3 Recycle Stream*

A characteristic feature of most coking processes is a recycle stream where the unconverted residue fraction (524°C+) is returned to the reactor. The recycle stream affects the product quality to a great extent, but inspite of this, limited research has been done to determine the changing characteristics of this stream. Sachanen (1940) observed that on repeated thermal cracking at 450°C of the fraction boiling between 200 to 350°C the API gravity of the 200°C- fraction produced decreased to 30.6°API on the sixth cycle from 58.2°API at the first cycle. Martin and Wills (1959) reviewed the early literature on coking. Realising the importance of the recycle stream they compared the product quality from the once through process with recycle to extinction. They showed that recycling increased the gas oil yield by up to 15% with a small increase in CCR and API gravity of the gas oil. They calculated the Conradson decarbonising efficiency (CCR in feed-CCR in liquid product/CCR in feed) that could be obtained from a fluid coker on recycling could be increased to about 91-96% from 61-65% based on once through operation.

The first fundamental structural analysis of coker recycle material was done by Kirchen *et al.* (1989) and Gray *et al.* (1989). A combined coker recycle stream, consisting of condensed recycled residue from the coker and unconverted residue, was compared to feed bitumen, atmospheric residue (343 °C+) and vacuum residue (427 °C+). An analysis of the coker recycle showed that there was a significant decrease in the paraffinic groups compared to topped fresh bitumen. An increase was observed in the aromatic content of the recycle stream compared to topped fresh

bitumen (Figure 2.13). Considering that the coker recycle was composed of both topped fresh bitumen and actual recycle material these trends would be more pronounced for the recycle stream alone.

In a typical upgrading plant the gas oil fraction has to be sent for hydrotreating. A highly condensed aromatic stream is undesirable, as it would accelerate the poisoning of the catalyst in the downstream hydrotreaters.

**Figure 2.13 Aromaticity and concentration of paraffinic groups in feed and recycle residue samples (Gray *et al.*, 1989).**

**ATH – 1 = feed bitumen, ATH-2 = 343°C+ residue, ATH-3 = 427°C+ vacuum residue, ATH-4 = coker recycle**

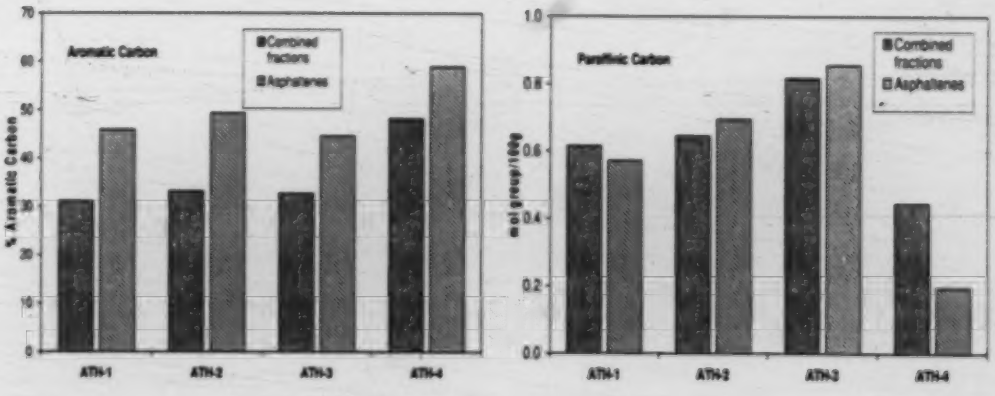

## 2.7 Hydrotreating of cracked products

### 2.7.1 Feed and product properties

The liquid products obtained from thermal cracking must be hydrotreated to meet the specifications for synthetic crude oil (see Table 2.5 and Table 2.6). Catalytic hydrotreating is a hydrogenation process used to remove contaminants such as nitrogen, sulphur, oxygen, and metals from liquid petroleum fractions. In addition, hydrotreating converts olefins and aromatics to saturated compounds.

### 2.7.2 Process flow description

The feed is mixed with hydrogen and heated to temperatures in the range of 300-400°C (Figure 2.14). The feed enters the top of a fixed bed reactor. In the reactor, the sulphur and nitrogen compounds in the feedstock are converted into $H_2S$ and $NH_3$. The olefins present are saturated with hydrogen and polyaromatics and diaromatics are hydrogenated. The reaction products leave the reactor and after cooling to a low temperature enter a liquid/gas separator. The hydrogen-rich gas from the high-pressure separation is recycled to the reactor. A purge is maintained to control the amount of light gases building up in the gas stream due to cracking.

**Table 2.5 Properties of synthetic crude oil (Gray, 1990)**

| Property | Syncrude | Husky Oil | Alberta Light |
|---|---|---|---|
| Gravity, °API | 32.4 | 32 | 38.5 |
| Sulphur, wt.% | 0.11 | 0.15 | 0.4 |
| Naphtha (82-177°C) | | | |
| Vol.% | 16 | 8 | 25 |
| Nitrogen, ppm | 1.1 | 1.0 | |
| Sulphur, ppm | 2.2 | | |
| Mid Distillate (177-343°C) | | | |
| Vol.% | 49 | 40 | 40 |
| Sulphur, wt.% | 0.04 | 0.2 | |
| Gas Oil (343°C+) | | | |
| Vol.% | 33 | 40 | 24 |
| Sulphur, wt.% | 0.24 | 0.5 | |
| Nitrogen, wt.% | 0.14 | 0.1 | |

**Table 2.6 Properties of products from primary upgrading (Gray, 1990)**

| Property | LC-Fining[1] | H-Oil[1] | Fluid Coker[2] |
|---|---|---|---|
| Sulphur, wt.% | 1.66 | | 4.12 |
| Nitrogen, ppm | 332 | | 3050 |
| Naphtha (82-177°C) | | | |
| Weight % | 17.4 | 16.9 | 0.5 |
| Nitrogen, ppm | 300 | 430 | |
| Sulphur, ppm | 900 | 2000 | |
| Mid Distillate (177-343°C) | | | |
| Weight % | 27.2 | 38.5 | 40 |
| Sulphur, wt.% | 0.36 | 1.14 | |
| Nitrogen, wt.% | 0.14 | 0.086 | |
| Gas Oil (343-525°C) | | | |
| Vol.% | 41.4 | 31.0 | 61.6 |
| Sulphur, wt.% | 1.05 | 2.07 | |
| Nitrogen, wt.% | 0.45 | 0.38 | |
| Residue (525°C+) | | | |
| Weight % | 7.68 | 4.1 | |
| Sulphur, wt.% | 3.0 | | |
| Nitrogen, wt.% | 1.4 | | |

1 Product from Cold Lake bitumen
2 Product from Athabasca bitumen

**Figure 2.14 Hydrotreater flowsheet**

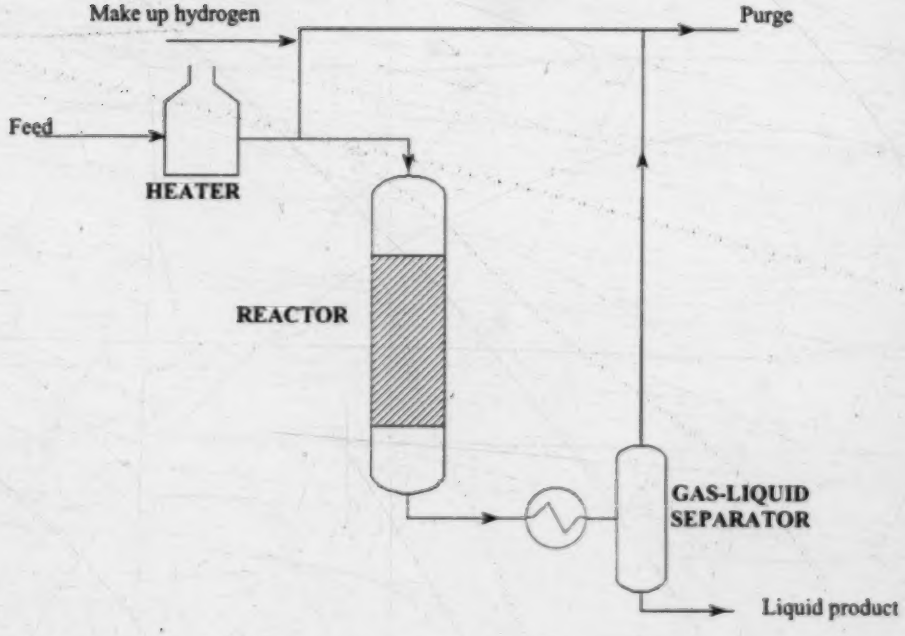

### 2.7.3 Catalyst deactivation

One of the major problems in the hydrotreaters is catalyst deactivation, which depends on the quality of the distillates being sent from primary upgrading. The catalyst used in the reactor is continuously deactivated and to maintain the catalyst activity the temperature of the reactor must be raised from about 320°C when the catalyst is fresh and to a maximum of 400°C at the end of the catalyst life cycle. Above 400°C thermal cracking reactions will occur and the product quality deteriorates.

In comprehensive surveys on hydrotreating catalysts by Halabi *et al.* (1991) and Thakur and Thomas (1985), PAHs, asphaltenes, metals and heteroatoms were identified as the major sources of catalyst deactivation in the hydrotreaters. Stohl and Stephens (1986) performed various experiments to study the impact of the chemical constituents of coal liquid on hydrotreating catalysts. They found that the catalyst activity decreased by 95% after a 2-hour reaction with nitrogenous extract and by 41% after reaction with polyaromatic hydrocarbons.

Vital information about the deactivation process comes from the composition of the carbonaceous deposits on the hydrotreating catalyst. The deposits from gas oil and naphtha hydrotreating catalysts are dramatically enriched in nitrogen and oxygen relative to feed concentrations. Obviously adsorption of these compounds is an important factor in catalyst deactivation (Furimsky, 1978; Furimsky 1982; Choi and Gray, 1988).

# 3 Materials And Methods

## 3.1 Materials

Athabasca vacuum residue provided by Syncrude Canada Limited was used as the first stage feed. Table 3.1 lists some of the important properties of the material. The simulated distillation curve for the residue is shown in Figure 3.1. Carbon disulphide (99.9%) was supplied by Fisher Scientific and nitrogen (99.998%) was supplied by Praxair. 0.22 μm Millipore filter papers were used to filter the carbon disulphide insoluble material from the reaction products.

**Table 3.1 Properties of Athabasca vacuum residue**

| | |
|---|---|
| Carbon, wt.% | 81.4 |
| Hydrogen, wt.% | 9.6 |
| Sulphur, wt.% | 5.8 |
| Nitrogen, wt.% | 0.7 |
| Toluene Insoluble, wt% | 1.8 |
| Average Molecular Weight | 1012 |
| Asphaltene Content, wt.% | 24.7 |
| MCR, wt.% | 25.4 |

**Figure 3.1 Simulated distillation curve for Athabasca vacuum residue**

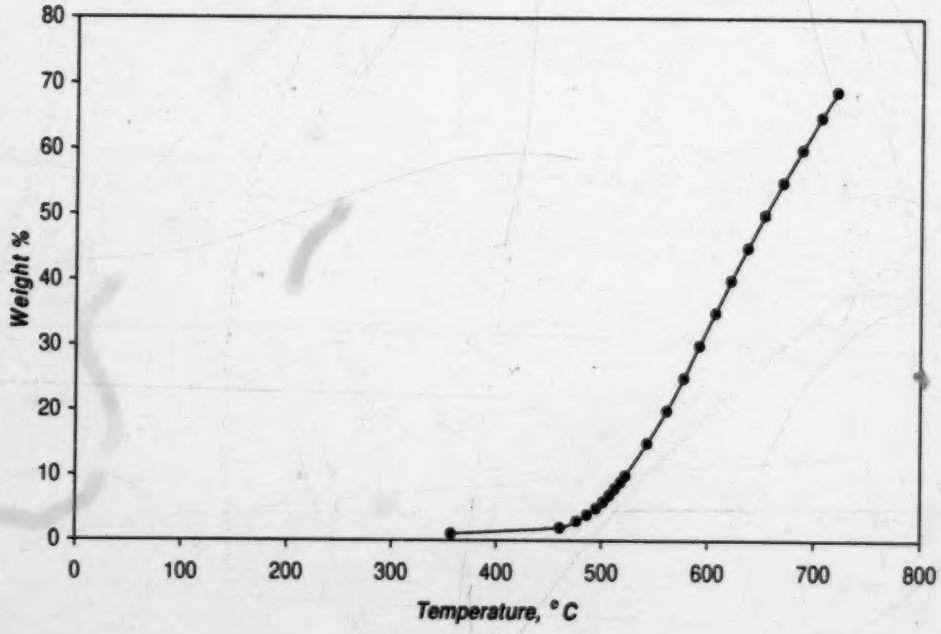

## 3.2 Quartz Tube Reactor

### 3.2.1 Introduction

The quartz tube reactor was designed as an open system for high temperature thermal cracking reactions. The evolved products accumulated in the downstream collection assembly that was maintained at dry ice-acetone temperature (-78°C).

### 3.2.2 Apparatus

A schematic of the quartz tube reactor is shown in Figure 3.2. The main reactor was a 1" quartz tube with an internal volume of approximately 60mL. It was dipped in a molten salt bath maintained at the reaction temperature of 530°C. The salt used was provided by APCO Industries Co. Limited and was a mixture of sodium and potassium nitrate. The heat up profile for the quartz tube is shown in Figure 3.3. The collection assembly consisted of a U-tube filled with glass wool that acted as a demister. Flexible metal tubing was used to connect the quartz tube reactor to the U-tube. When required, gas bags were used directly after the U-tube to collect the gaseous products.

### 3.2.3 Procedure

The quartz tube was filled with approximately 4 g of the feed material and the apparatus assembled. After it was purged with nitrogen for about five minutes the U-tube was dipped into an acetone-dry ice mixture. The nitrogen purge continued for a total of 30 min before the reaction was started by dipping the quartz tube into the salt bath reactor. Nitrogen was used as the sweep gas at a flow rate of 0.17 L/min, which

**Figure 3.2 Quartz Tube Reactor**

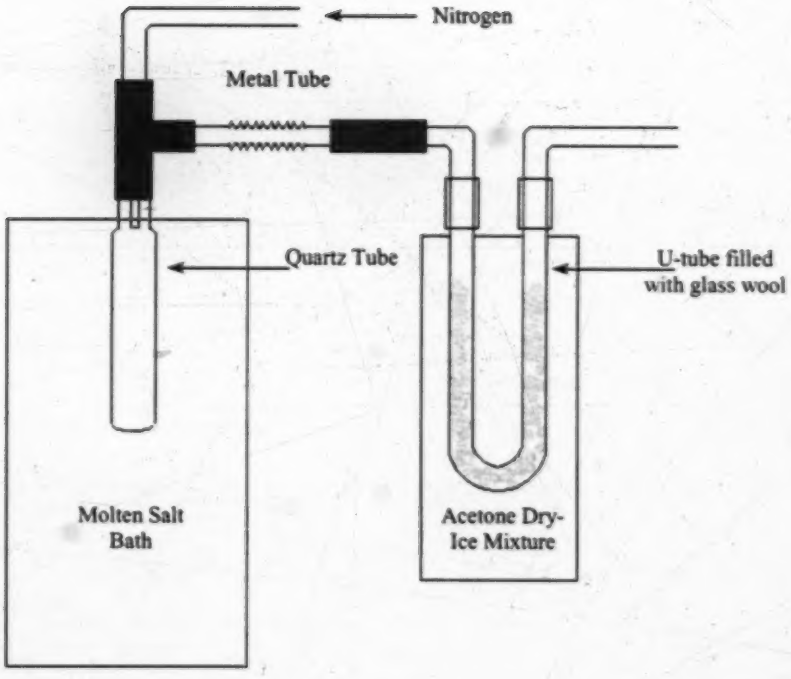

**Figure 3.3 Salt bath heat up profile**

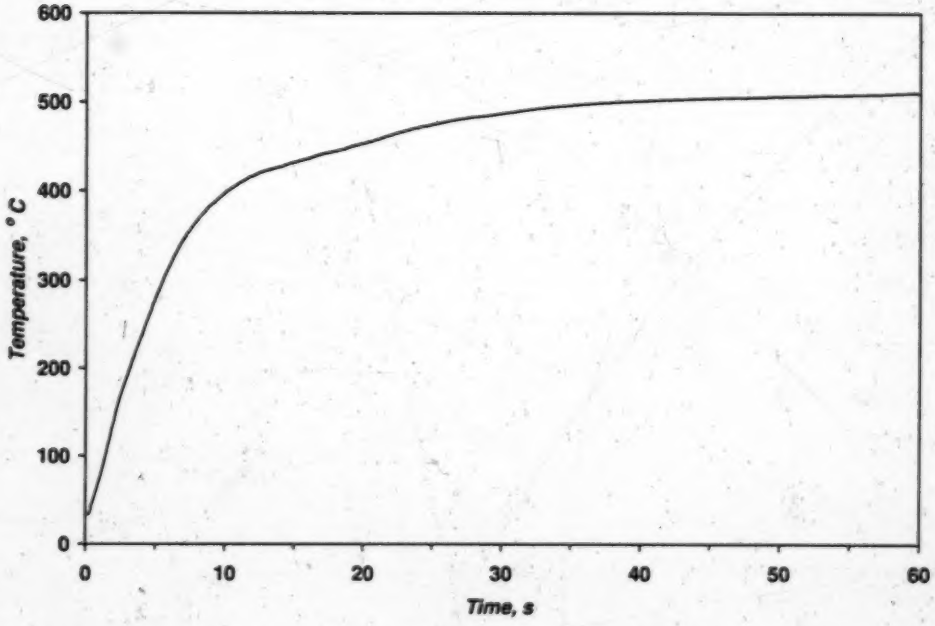

corresponds to a residence time of 7.9 s at 530°C. After exactly 10 min the tube was quenched in water at room temperature and the nitrogen purge stream was shut off. The system was allowed to cool for a few minutes. The quartz tube, along with the Swagelok fitting and glass insert, were removed and replaced with another similar assembly and the cycle repeated. Each individual part of this assembly was weighed and then washed in $CS_2$. The weight of the feed and liquid products was determined gravimetrically. The collected liquid was filtered through a 0.22 μm filter paper to separate the $CS_2$ insoluble material. Note that no variation was seen in the coke yield, whether determined as toluene insoluble or $CS_2$ insoluble (Appendix 2). The filter paper and quartz tubes were dried in a vacuum oven overnight and weighed to determine coke yield.

$$\%coke_yield = \frac{m_{CS_2 I} - m_{fCS_2 I}}{m_{feed} - m_{fCS_2 I}} \times 100 \qquad (3.1)$$

where $m_{CS_2 I}$ = weight of $CS_2$ insoluble

$m_{fCS_2 I}$ = weight of $CS_2$ insoluble in the feed

$m_{feed}$ = weight of feed

Distillate yields were determined as the fraction of liquid product collected on condensation while the amount that did not volatilise during vacuum distillation was called residue. The loss of weight during product handling i.e., the difference in weight of liquid after the thermal cracking experiment and before vacuum distillation was assumed to represent yield of naphtha. For a typical experiment, the gas produced was collected in a gas bag and the gases analysed by gas chromatography. Since the amount of nitrogen was known the gas yields were determined by calibration with the concentration of nitrogen determined by the gas chromatograph.

$$\left.\begin{aligned} \%distillate_yield &= \frac{m_d}{m_{feed} - m_{fCS_2l}} \times 100 \\ \%residue_yield &= \frac{m_r}{m_{feed} - m_{fCS_2l}} \times 100 \end{aligned}\right\} \qquad (3.2)$$

where $m_d$ = weight of liquid condensed on the entire assembly

$m_r$ = weight of liquid not volatilised during distillation

## 3.3 Micro scale distillation at reduced pressure

### 3.3.1 Introduction

A laboratory-scale vacuum distillation apparatus based on ASTM D-1160 was built to distil small quantities of material. The technique was first validated and checked for repeatability using samples of bitumen (details in Appendix 3). To prevent thermal degradation the maximum temperature was restricted to 325°C. The

small quantities and thermal instability of the bitumen fractions involved made it essential to minimise liquid hold up. Therefore, every effort was made to avoid long distillation paths. The conditions of distillation are such as to provide approximately one theoretical plate fractionation.

### 3.3.2 Apparatus

The vacuum distillation system is shown schematically in Figure 3.4. It consists of a flask containing the feed material to be distilled, a condenser tube and a collection flask. The feed material was filled to only about 50% of the flask capacity to provide sufficient headspace. This approach ensured that any problems due to entrainment or bumping were minimised. The empty space in the flask was packed with glass wool that acted as a demister to trap the entrained particles. A thermocouple was dipped into the flask such that it touched the lowermost portion of the flask, thus ensuring an accurate measurement of the highest liquid temperature. The flask was placed in a heating mantle that was controlled by an Omron E5CK controller. The riser assembly, which served as an inlet for the thermocouple and a McLeod vacuum gauge, connected the flask to the condenser. The vacuum takeoff, placed between the condenser and the collection flask, was connected to a rotary vane vacuum pump capable of maintaining a pressure of approximately 0.5 mm of Hg. The application of silicone grease to the ground glass joints ensured a vacuum tight seal.

**Figure 3.4 Vacuum distillation apparatus**

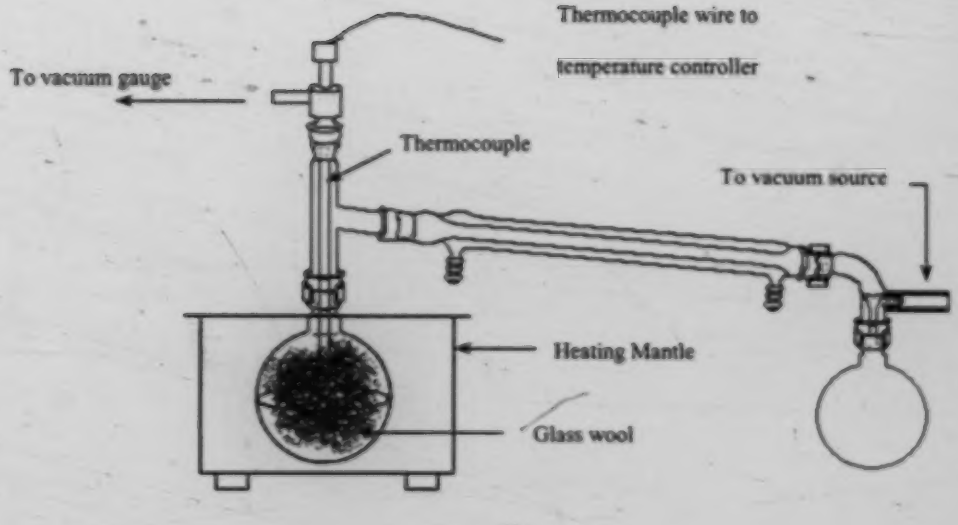

### 3.3.3 Procedure

Distillation was performed on the liquid samples using a 50 mL flask for stage 1 and stage 2 distillations and a 10 mL flask for stage 3 distillation. The headspace was filled with glass wool and the apparatus was evacuated by applying a vacuum. A cold trap kept in liquid nitrogen was used to collect any light product not condensed in the collection flask. After the required pressure was reached the heating mantle was switched on. The temperature was increased rapidly to 100°C and then ramped up at a rate of 5°C/min to 325°C. The flask was weighed before and after distillation to obtain the weight fraction of residue. The distillate was measured by weighing the entire assembly before and after distillation. The total recovery was approximately 100% for all samples used.

## 3.4 Analytical Techniques

### 3.4.1 Nuclear Magnetic Resonance Spectroscopy (NMR)

The samples for $^{1}H$ NMR spectroscopy were prepared by mixing approximately 20 mg of the sample with 700 µL deuterochloroform ($CDCl_3$). The distillate $^{13}C$ NMR samples used approximately 100mg of material in 600 µL $CDCl_3$ and the residue $^{13}C$ NMR spectroscopy used the same amount of material in 700 µL $CDCl_3$. The NMR spectroscopic analyses was performed at room temperature (20 ± 1°C) on a Varian XL-300 NMR spectrometer, operating at 299.943 MHz for proton and 75.429 MHz for carbon.

The proton spectra were collected with an acquisition time of 2.1 s, a sweepwidth of 7000 Hz, a pulse flip angle of 30.8° (8.2 μs), and a 1 s recycle delay. These pulse recycle conditions permit the collection of quantitative spectra for all protonated molecular species in the petroleum samples. The spectra, resulting from 128 scans and using 0.3-Hz line broadening, were referenced to the residual chloroform resonance at 7.24 ppm.

The quantitative carbon spectra were acquired using an acquisition time of 0.9 s and a sweepwidth of 16,500 Hz. A flip angle of 26.2° (4.6μs) and a recycle delay of 10 s were used for the distillate, while for the residue samples, a flip angle of 31.9° (5.7μs) and a 4 s delay were used. These parameters are quantitative for carbons with spin lattice relaxation times ($T_1$) of the order of 100 s in distillate and 30 s in the residue (Dettman, manuscript in preparation). Reverse-gated waltz proton decoupling was used to avoid nuclear Overhauser effect enhancements of the carbon signals. The spectra were the result of 5000 scans for the distillate. The distillate spectra used 5-Hz line broadening to improve the signal-to-noise ratio of the spectra. The residue spectra resulted from 15,000 scans and used 10 Hz line broadening. All spectra were referenced to the $CDCl_3$ resonance at 77.0 ppm.

The nomenclature used to describe the various carbon functionalities is shown in Figure 3.5. The chemical shift assignments for the $^1H$ and $^{13}C$ NMR spectra are shown in Table 3.2 and Table 3.3 respectively. These assignments were based on model compound assignments, 2-D NMR spectroscopic techniques like HETCOR (Heteronuclear chemical shift correlation) and COSY (Correlation Spectroscopy) as well as 1-D techniques such as DEPT (Dettman, manuscript in preparation).

**Figure 3.5 Hypothetical molecule to represent different carbon functionalities**

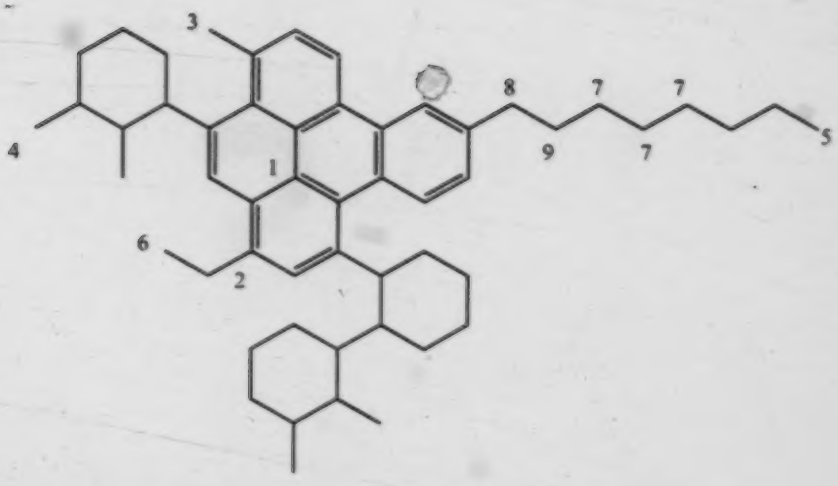


1. Bridgehead aromatic C (Qar-P)
2. Substituted aromatic C (Qar-S)
3. Methyl group on aromatic C ($Ar\text{-}CH_3$)
4. Methyl group on cycloparaffinic C ($Cy\text{-}CH_3$)
5. Terminal chain methyls ($C\text{-}CH_3$)
6. Methyl groups on aromatic ethyls ($E\text{-}CH_3$)
7. $CH_2$ that are atleast $\gamma$ from aromatic or terminal methyl or atleast $\beta$ to cycloparaffin or branch point (CHAIN)
8. $\alpha$ to aromatic $CH_2$
9. $\beta$ to aromatic $CH_2$

The final calculations performed to obtain the different carbon functionalities are shown in Table 3.4. The aromatic CH's, terminal methyls and the methyl of aromatic ethyls were determined directly from the carbon spectra. These groups are based on minimal assumptions and may be considered to be very accurate.

The other groups listed below were calculated using data from both proton and carbon spectra or had to be estimated due to spectral overlap and are therefore subject to larger margins of error. The substituted quaternary carbon (Qar-S) was determined from the proton spectra by converting the α to aromatic $CH_2$ and $CH_3$ protons to their respective amounts of carbon. The remaining amount of quaternary carbon was considered to be bridgehead carbon (Qar-P). The methyl carbons attached to aromatic (Ar-$CH_3$) were determined by evaluating the respective proton spectral region HP2. The remaining α to ring $CH_3$'s were assumed to be attached to cycloparaffinic rings (Cy-$CH_3$). The olefinic carbon was also obtained indirectly by converting the proton spectra. Half of region CP2 was estimated to be paraffinic CH's and the total CH's were calculated as the sum of region CP1 and one-half of region CP2. The CHAIN carbon were calculated from region CP4 after the contributions of $CH_2$ carbon from aromatic attached ethyls and α to aromatic cycloparaffinic $CH_2$ was removed. The α to aromatic cycloparaffinic $CH_2$ were estimated as half of the cycloparaffinic region CP5. Finally, NAPH fraction was evaluated from region CP5 only as an indicator of cycloparaffinic content.

**Table 3.2 Chemical shifts of proton spectral regions**

| Region | Chemical Shifts (ppm) | Structural type |
|---|---|---|
| HA1 | 10.7 to 7.4 | Polyaromatic |
| HA2 | 7.4 to 6.2 | Monoaromatic |
| HO1 | 6.2 to 5.1 | Olefinic CH |
| HO2 | 5.1 to 4.8 | Olefinic $CH_2$ |
| HO3 | 4.8 to 4.3 | Olefinic $CH_2$ |
| HP1 | 4.3 to 2.4 | $\alpha$ to aromatic $CH_2$ |
| HP2 | 2.4 to 2.0 | $\alpha$ to aromatic $CH_3$ |
| HP3 | 2.0 to 1.09 | Paraffinic $CH_2$ |
| HP4 | 1.09 to -0.5 | Paraffinic $CH_3$ |

**Table 3.3 Chemical shifts of carbon spectral regions**

| Region | Chemical Shifts (ppm) | Structural Type |
|---|---|---|
| CA1 | 190 to 170 | Oxygenated |
| CA2 | 170 to 129 | Quaternary aromatic |
| CA3 | 129 to 115.5 | Aromatic CH |
| CA4 | 115.5 to 113.5 | Olefinic $CH_2$ |
| CA5 | 113.5 to 100 | Olefinic $CH_2$ |
| CP1 | 70 to 45 | Paraffinic CH |
| CP2 | 45 to 32.7 | Paraffinic CH & $CH_2$ |
| CP3 | 32.7 to 30.8 | Chain $\gamma$-$CH_2$<br>$\beta$ to aromatic $CH_2$ |
| CP4 | 30.8 to 28.5 | Chain $\delta$-$CH_2$<br>$\alpha$ to aromatic naphthenes<br>Aromatic-attached ethyl $CH_2$ |
| CP5 | 28.5 to 25 | Cycloparaffin $CH_2$ |
| CP6 | 25 to 21.9 | Chain $\beta$-$CH_2$<br>$\alpha$ to aromatic or isobutyl $CH_3$ |
| CP7 | 21.9 to 17.6 | $\alpha$ to Ring $CH_3$ |
| CP8 | 17.6 to 14.7 | Aromatic-attached ethyl $CH_3$ |
| CP9 | 14.7 to 12.3 | Chain $\alpha$-$CH_3$ |
| CP10 | 12.3 to 0 | Branched-chain $CH_3$ |

**Table 3.4 Group classifications of chemical species**

| Chemical Species | Spectral Region |
|---|---|
| Oxygenated carbon (C=O) | CA1 |
| Aromatic CH (CHar) | CA3 |
| Methyl of an aromatic ethyl (E-$CH_3$) | CP8 |
| Terminal methyl of a paraffinic chain | CP9 |
| Paraffin-substituted Qar (Qar-S) | HP1 + HP2 converted to C wt.% |
| Polyaromatic quaternary (Qar-P) | CA2 – Qar-S |
| $\alpha$ to Aromatic ring methyl (Ar-$CH_3$) | HP2 converted to C wt.% |
| $\alpha$ to Cycloparaffin ring methyl | (CP7 + CP6/2) - Ar-$CH_3$ |
| Olefin CH | HO1 converted to C wt.% |
| Olefin $CH_2$ | HO2 converted to C wt.% |
| Paraffinic CH (CH) | CP1 + CP2/2 |
| > C5 chains (CHAIN) | CP4 – CP8 – CP5/2 |
| Cycloparaffin $CH_2$ (NAPH) | CP5 |

### 3.4.2 Simulated distillation by gas chromatography (SIMDIST)

The high temperature simulated distillation was performed at Syncrude Research laboratory. The technique used a MXT-1 column which is a crossbonded 100% dimethyl polysiloxane column with a coating of 0.15 μm. The column was heated from 40°C to 430°C at 10°C per minute with a final hold time of 3 minutes. A relationship between boiling point and retention time was defined by calibration with *n*-paraffins from $C_5$ through to $C_{120}$. A flame ionisation detector was used and 100% recovery of the samples was assumed (see Appendix 4).

### 3.4.3 High performance liquid chromatography (HPLC)

The separation of various fractions based on number of aromatic rings was done by HPLC at the Syncrude Research laboratory. The HPLC method used two detectors; an Alltech model 500 evaporative light scattering detector (ELSD) run at 35°C and 1.2 L/min of nitrogen and a polychrom 9065 diode array detector (DAD). The two columns used were the PAC (Whatman Partisil 5) and the RingSep (ES Industries) column. Hexane, methylene chloride and isopropyl alcohol were used as the solvents. The solvents with their respective flowrates are listed in Appendix 5.

### 3.4.4 Refinery gas analysis

A Hewlett Packard 5890 Series II type gas chromatograph was used for the hydrocarbon gas analyses. It used different types of porous layer open tubular columns with columns being isolated or reversed and their orders changed by means of valves.

The inorganic gases ($CO_2$, CO, $N_2$, $H_2$ and $H_2S$) were analysed by a three column chromatographic system and a thermal conductivity detector (TCD). Two different Hewlett Packard Poraplot Q columns and a Hewlett Packard MS5A column were used. The organic gases ($C_1^*$ hydrocarbons) are separated by a two column (Hewlett Packard $Al_2O_3$/KCl) system and were analysed using a flame ionisation detector.

Quantitative results were obtained from the measured areas of the recorded peaks and the application of individual response factors.

### 3.4.5 Molecular weight

The average molecular weights were obtained using vapour pressure osmometry (Westcan Corona Model 232A) at the Micro Analytical Laboratory at the University of Alberta. The solvent used was *o*-dichlorobenzene at a temperature of 130°C.

### 3.4.6 Elemental analysis

Elemental analysis was performed on a Carlo Erba Elemental Analyser 1108 at the Micro Analytical Laboratory, University of Alberta. The elements were first burnt in oxygen at 1800°C and the gas produced separated by gas chromatography and analysed by a thermal conductivity detector. Sulphur was detected by the Schöniger oxygen flask combustion method.

### 3.4.7 Ash Content

The ash content was determined on a Perkin Elmer Pyris 1 TGA Thermogravimetric Analyzer. The sample was heated in a stream of air from 50°C to 750°C at 15°C/min and then held at 750°C for 180 minutes.

# 4 Results

## 4.1 Yield of product fractions

### 4.1.1 Cumulative yields

The cumulative product yields and residue conversions are shown in Figure 4.1 and Figure 4.2. Mass balance closures in excess of 98% were obtained for all three stages of coking (Appendix 6). Nevertheless; the figures presented in the following graphs have been normalised. Stage 1 of coking achieved almost 82% conversion of the residue fraction. Recycling the residue to achieve a residue conversion of 99% gave a 12% increase in liquid yield and an increase of 5% in the coke and gas yields. A substantial increase in liquid yields was thus obtained by recycling the unconverted residue.

**Figure 4.1 Cumulative product yields**

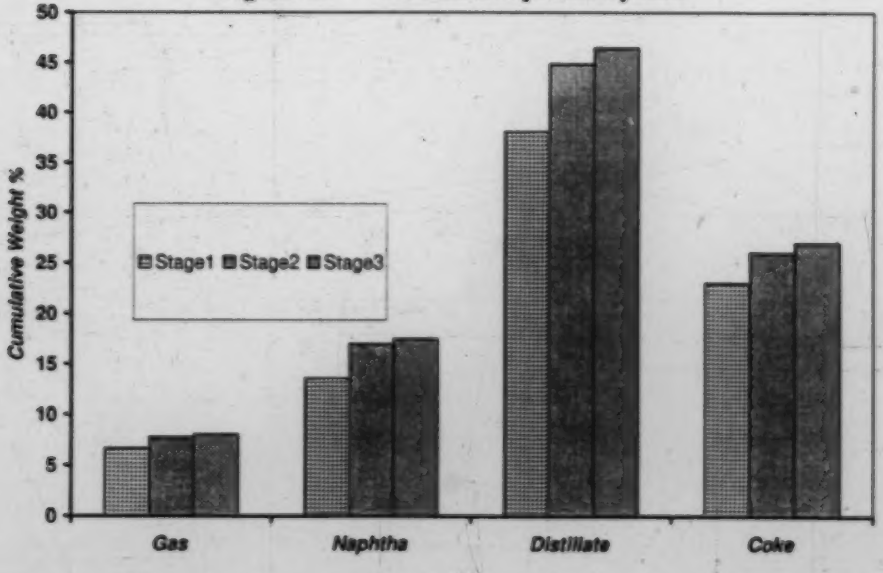

**Figure 4.2 Cumulative residue conversion**

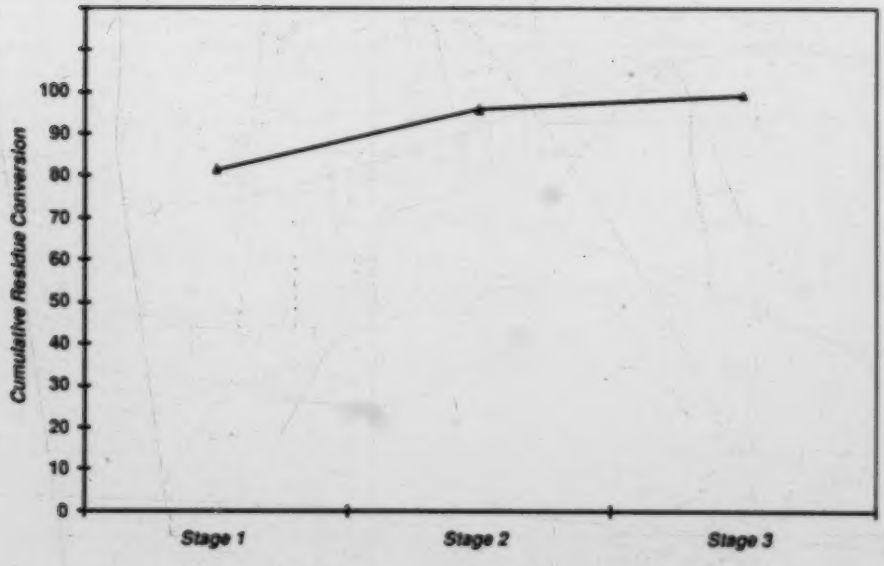

### 4.1.2 Stagewise yields

The gas, liquid and coke yields from repeated coking are shown in Figure 4.3. The error bars on coke represent the 95% confidence limits after repeat experiments. The naphtha yields reached a maximum at the second stage of coking. The gas and distillate yields were constant and did not change from stage to stage within experimental error. A minimum was seen in the yield of coke in the second stage of reaction.

**Figure 4.3 Product yields for the three stages of coking**

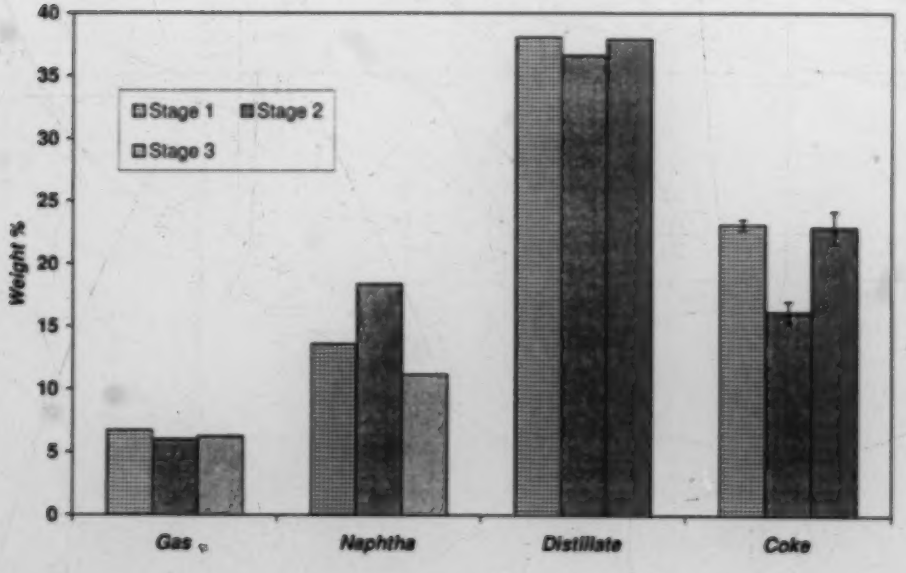

Figure 4.4 shows that the amount of residue material that volatilised out of the reactor increased from stage 1 to stage 2 but then remained constant (within the margin of error) from stage 2 to stage 3. The shift in the fraction of residue vaporised from feed to stage 1 residue was one of the major factors contributing to the drop in the coke yields.

**Figure 4.4 Feed vaporisation at each stage of coking**

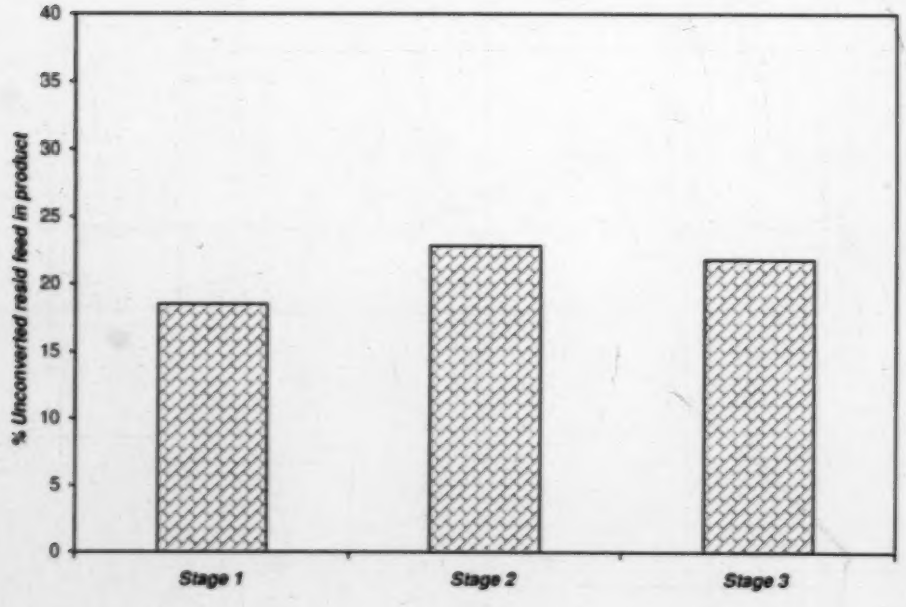

## 4.2 Analytical Data

### 4.2.1 Simulated distillation by gas chromatography (SIMDIST)

The simulated distillation curves for residue from the three stages of reaction are shown in Figure 4.5. The boiling point distribution was determined after normalising the data assuming 100% recovery of distillate and residue from the gas chromatograph (details in Appendix 4). The first stage feed was significantly different from the other residue fractions, and had about 40% of the material boiling above 700°C. In contrast, the residue from the subsequent stages had an end point of 700°C. The distillate fraction (Figure 4.6) displayed similar 95% cut points of 500°C but the boiling point distribution shifted to higher temperatures from stage 1 distillate to stage 3 distillate.

### 4.2.2 Elemental analysis and ash content

The results from the elemental analysis are shown in Table 4.1. The carbon content did not show a wide variation for the liquid samples. The hydrogen content of the distillate and residue fractions decreased from stage to stage, although hydrogen content for the coke was almost constant. Nitrogen showed an increasing trend and it more than doubled for the distillate fraction from stage 1 to stage 3. The sulphur content of the residue and distillates did not display any major trends.

Problems with $SO_x$ emissions and ash content limit the possible uses of the coke formed from bitumen. Upon recycling it was found that the quality of the coke formed from the later stages of the experiments showed significant improvement.

**Figure 4.5 Simulated distillation curve for residue fractions**

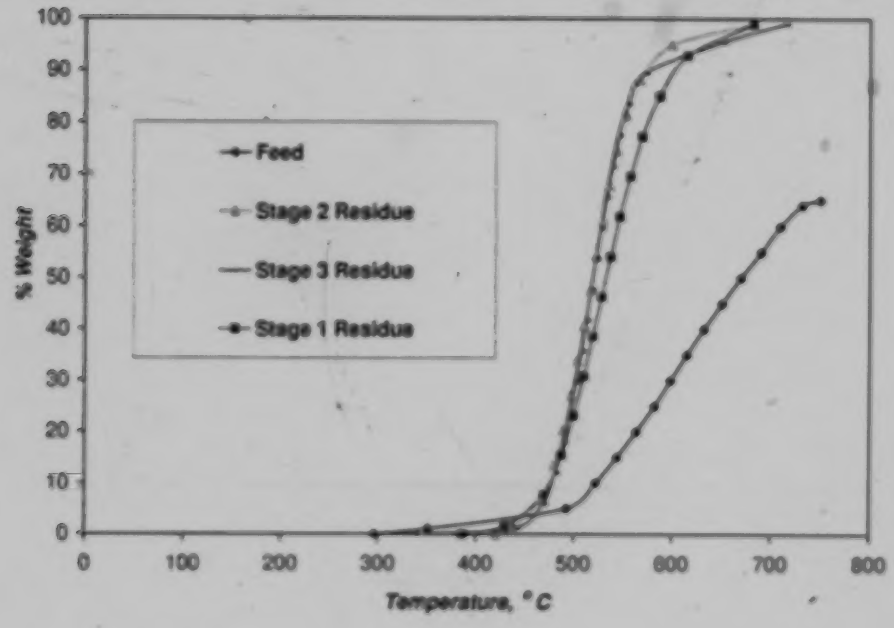

**Figure 4.6 Simulated distillation curves for distillate fraction**

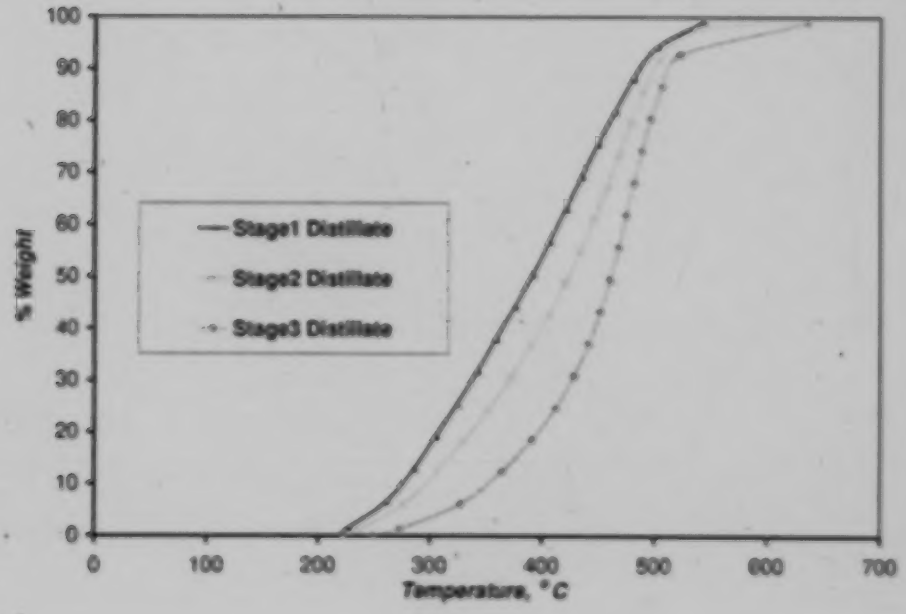

The sulphur content and the ash content of the coke dropped rapidly from stage 1 to stage 2.

The sulphur content dropped from 6.6 to 2.6 wt.% and the ash content dropped from 5.5 wt.% to 1.6 wt.%. The final stage produced coke with an ash content of 0.5 wt.%. Although the coke produced from the recycled residue represents less than 4 wt.% of the total feed, it does have the potential to produce better quality coke.

Although coking is generally called a carbon rejection process, the carbon content of the coke in the first stage was actually lower or similar to the carbon content of the residue feed. The distillate carbon content was also slightly higher than the residue feed.

**Table 4.1 Elemental analysis and ash content**

| | Carbon (wt.%) | Hydrogen (wt.%) | Nitrogen (wt.%) | Sulphur (wt.%) | H/C ratio | Ash (wt.%) |
|---|---|---|---|---|---|---|
| Feed | 81.4 | 9.6 | 0.7 | 5.8 | 1.42 | |
| Stage 1 residue | 83.7 | 9.5 | 0.7 | 5.0 | 1.36 | |
| Stage 2 residue | 84.2 | 8.2 | 0.9 | 5.8 | 1.17 | |
| Stage 3 residue | 84.5 | 6.6 | 1.3 | 6.6 | 0.94 | |
| Stage 1 distillate | 83.7 | 10.6 | 0.3 | 4.9 | 1.52 | |
| Stage 2 distillate | 83.3 | 9.9 | 0.5 | 5.6 | 1.42 | |
| Stage 3 distillate | 83.9 | 9.0 | 0.8 | 5.3 | 1.29 | |
| Stage 1 coke | 79.4 | 3.1 | 1.8 | 6.6 | 0.47 | 5.5 |
| Stage 2 coke | 86.9 | 3.5 | 1.4 | 2.6 | 0.48 | 1.6 |
| Stage 3 coke | 86.4 | 3.4 | 1.4 | 2.7 | 0.47 | 0.5 |

The cumulative values for the distillate fraction are shown in Table 4.2. On a cumulative basis the distillate properties displayed little variation. For example, the H/C ratio constantly decreases, indicating the deteriorating quality of the fractions, but on a cumulative basis only a small decrease in the distillate H/C ratio was observed (Table 4.2). Comparing Table 4.1 and Table 4.2 it can be seen that the distillate quality was deteriorating yet when viewed on a cumulative basis, these variations were small and likely to be overlooked.

**Table 4.2 Cumulative distillate properties on recycle coking**

| | Distillate1 | Distillate2 | Distillate3 |
|---|---|---|---|
| Cumulative wt.% | 38.1 | 44.9 | 46.5 |
| Wt. % carbon | 83.7 | 83.6 | 83.6 |
| Wt. % nitrogen | 0.3 | 0.4 | 0.4 |
| Wt. % sulphur | 4.9 | 5.0 | 5.0 |
| Wt. % hydrogen | 10.6 | 10.5 | 10.4 |
| H/C | 1.52 | 1.50 | 1.49 |

### 4.2.3 Molecular Weight

The molecular weight sharply dropped after the initial feed material was first cracked (Table 4.3). Subsequently, the residue fraction showed a gradual decrease in molecular weight with every reaction stage. Although the variation of molecular weight for the distillate fraction was small, a maximum was observed in the second stage.

From the elemental analysis and molecular weights, the average molecular formulas were calculated and are shown in Table 4.3. The average molecular weight showed that the residue and distillate materials were quite similar and the removal of five to ten carbon atoms can convert the residue to distillate.

Calculation of average molecular formulas:

$$\left.\begin{aligned} C &= \frac{wt\%Carbon \times MW}{1201} \quad H = \frac{wt\%Hydrogen \times MW}{100} \\ S &= \frac{wt\%Sulphur \times MW}{3206} \quad N = \frac{wt\%Nitrogen \times MW}{1401} \end{aligned}\right\} \qquad (4.1)$$

where C – number of carbon atoms per molecule

H – number of hydrogen atoms per molecule

S – number of sulphur atoms per molecule

N – number of nitrogen atoms per molecule

**Table 4.3 Molecular weight and average molecular formula**

| | MW (dalton) | Average Molecular formula |
|---|---|---|
| Feed | 1013 | $C_{68.6}H_{96.9}N_{0.3}S_{1.8}$ |
| Stage 1 residue | 543 | $C_{37.8}H_{50.9}N_{0.1}S_{0.8}$ |
| Stage 2 residue | 457 | $C_{32.0}H_{37.2}N_{0.1}S_{0.8}$ |
| Stage 3 residue | 428 | $C_{30.1}H_{27.9}N_{0.2}S_{0.9}$ |
| Stage 1 distillate | 350 | $C_{24.4}H_{36.7}N_{0.0}S_{0.5}$ |
| Stage 2 distillate | 393 | $C_{27.3}H_{38.4}N_{0.1}S_{0.7}$ |
| Stage 3 distillate | 306 | $C_{21.3}H_{27.4}N_{0.1}S_{0.5}$ |

### 4.2.4 Refinery Gas Analysis

The composition of the gas obtained from all three stages is shown in Figure 4.7. The methane content increased slightly from stage 1 to stage 3. The yield of $C_2^+$ hydrocarbon gases and yield of hydrogen sulphide decreased. The TCD detected no hydrogen in the gas samples. The absence of a hydrogen signal could be the result of the low concentrations because of the dilution of the gas sample with nitrogen.

**Figure 4.7 Gas composition for all three stages**

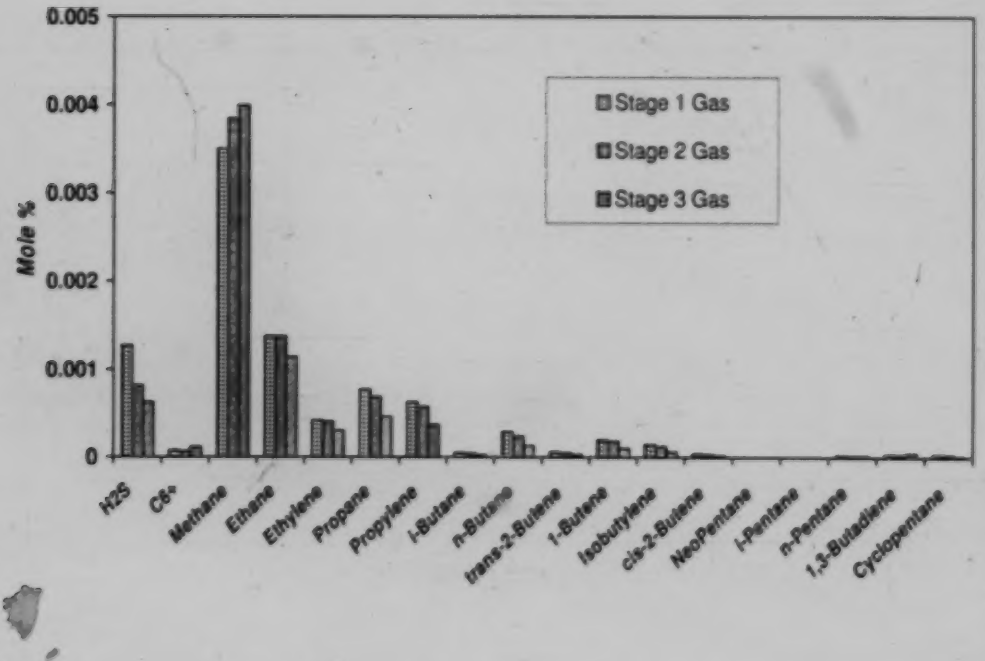

### 4.2.5 Nuclear Magnetic Resonance Spectroscopy (NMR)

#### *4.2.5.1 Spectra from $^1$H NMR Spectroscopy*

The $^1$H NMR spectra for the residue fractions are shown in Figure 4.8. The spectra distinctly indicated the growing aromaticity of the fractions from stage to stage as indicated by the broad peak centred at 7.3 ppm. Although the $^1$H NMR spectra indicated a general decrease in paraffinic carbon (peaks at 1.3 ppm and 0.9 ppm) it also pointed to an increasing fraction of α-carbon (peak at 2.6 ppm). Deuterated chloroform was used as the solvent and consequently a sharp peak was seen at 7.24 ppm due to the residual hydrogen in the chloroform. The silicone grease that was used in the experimental apparatus to seal the joints was also seen in the spectra as a sharp peak at 0.1 ppm. The distillate $^1$H NMR spectra shown in Figure 4.9 reflected the same trends as were seen in the residue spectra. The major difference was the presence of olefins (from 4.3 to 6.2 ppm) that were absent from the residue spectra. The distillate $^1$H NMR spectra also indicated a clear peak at 2.0 ppm due to the α to olefinic carbons (Rodriguez *et al.*, 1994).

**Figure 4.8** $^{1}$H NMR spectra for residue fractions

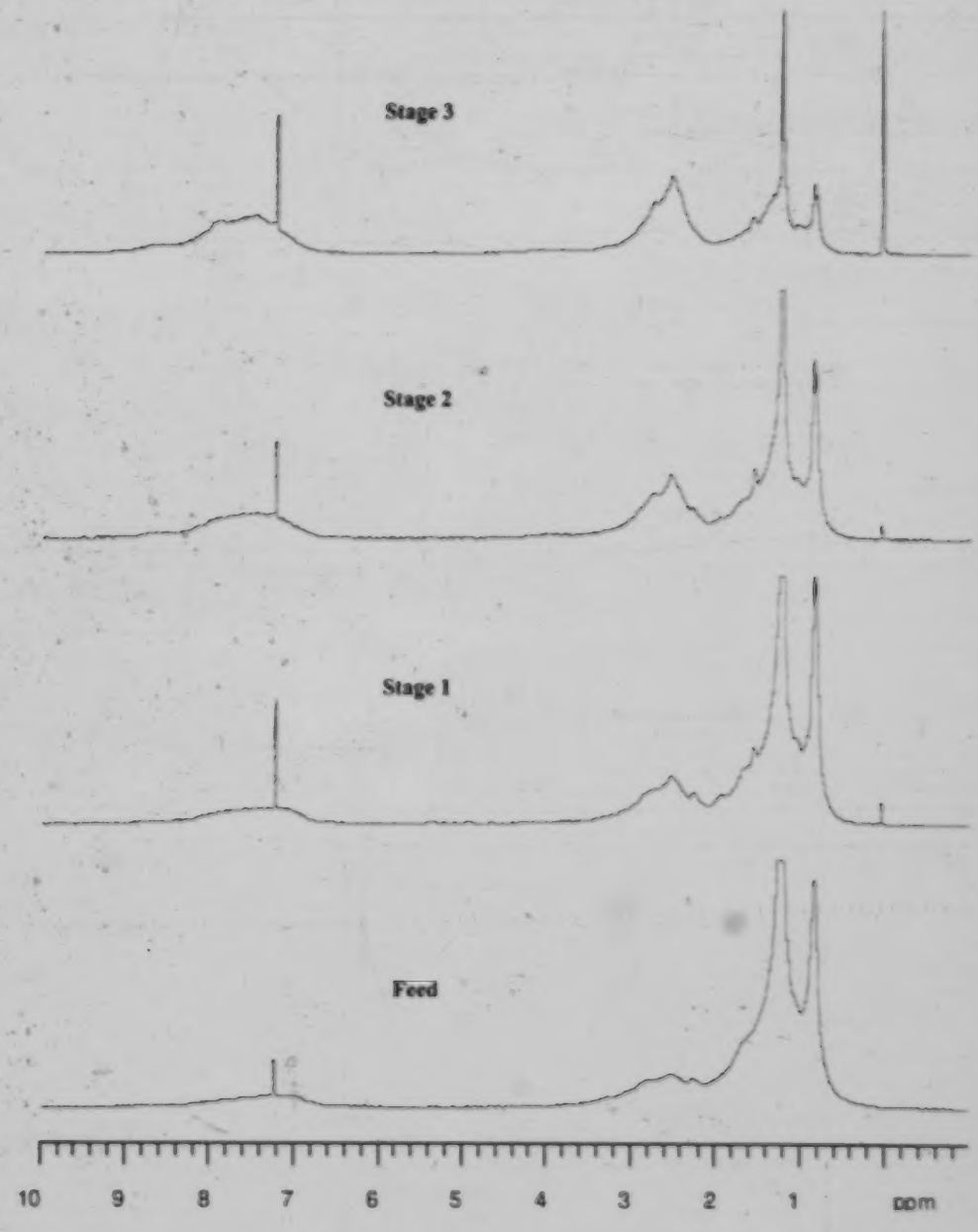

**Figure 4.9** $^{1}H$ NMR spectra for distillate fractions

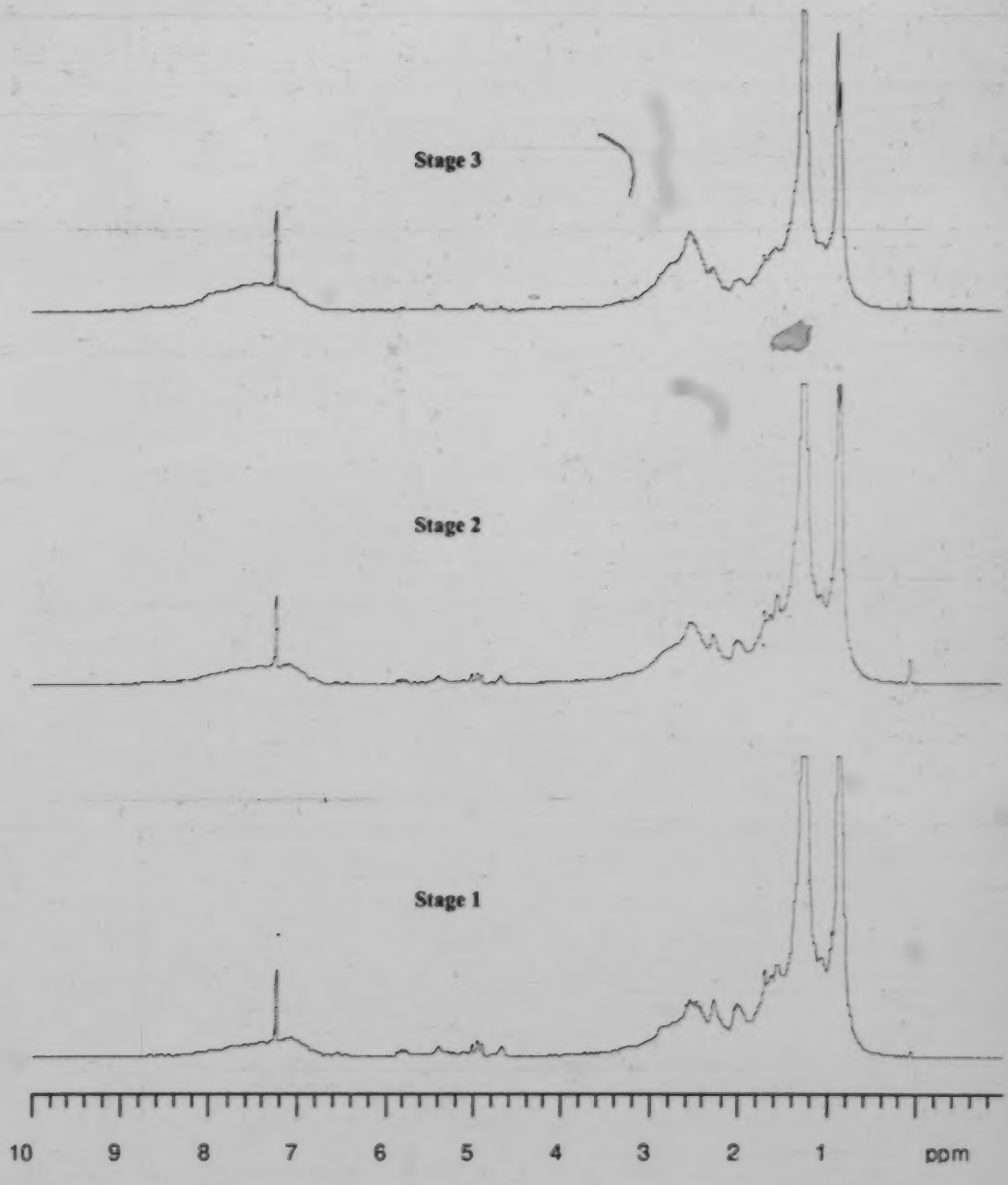

#### 4.2.5.2 *Spectra from $^{13}C$ NMR Spectroscopy*

The aromatic regions of the residue and distillate $^{13}C$ NMR spectra for all the fractions are shown in Figure 4.10 and Figure 4.11 respectively. In spite of the baseline noise, an unavoidable feature of the $^{13}C$ NMR spectra of complex mixtures, the spectra clearly displayed the same increasing trend of aromaticity indicated in the $^{1}H$ NMR spectra. The paraffinic regions of the distillate and residue $^{13}C$ NMR spectra are shown in Figure 4.12 and Figure 4.13. The peaks at 14, 23, 32 and 30 ppm traditionally assigned to terminal $C_1$, $C_2$, $C_3$ and central methylene groups of paraffinic chains (Thiel and Gray, 1988) were clearly visible. There was a gradual decrease in the intensity of these peaks from stage to stage, such that the smaller peaks disappeared in the baseline noise for the spectra from the third stage product. The peak round 20 ppm due to aromatic attached methyls (Snape *et al.*, 1979) did not show any significant trend. The stage 3 fraction shows a sharp peak at 0.5 ppm due to the presence of vacuum grease.

The spectra indicated that the hump, which forms underneath the sharp peaks, disappeared as the residue was repeatedly subjected to thermal cracking. Young and Galya (1981) allotted this region to naphthenic groups. Although the α and β to aromatic paraffinic chains also contribute to the signal in this region, it is still a useful indicator of the naphthenic content.

**Figure 4.10 $^{13}C$ NMR spectra for residue fractions – aromatic region**

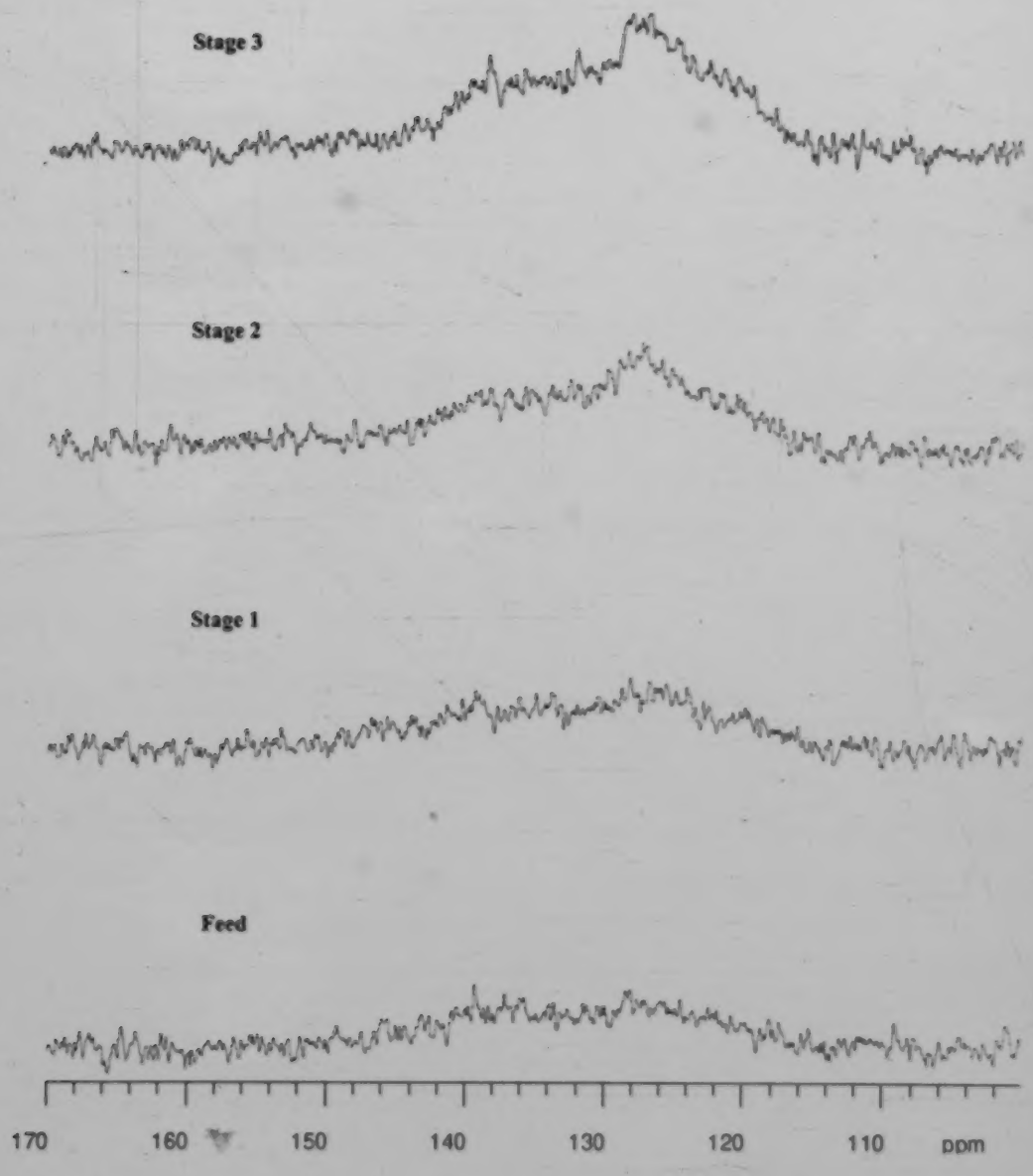

**Figure 4.11** $^{13}C$ **NMR spectra for distillate fractions - aromatic region**

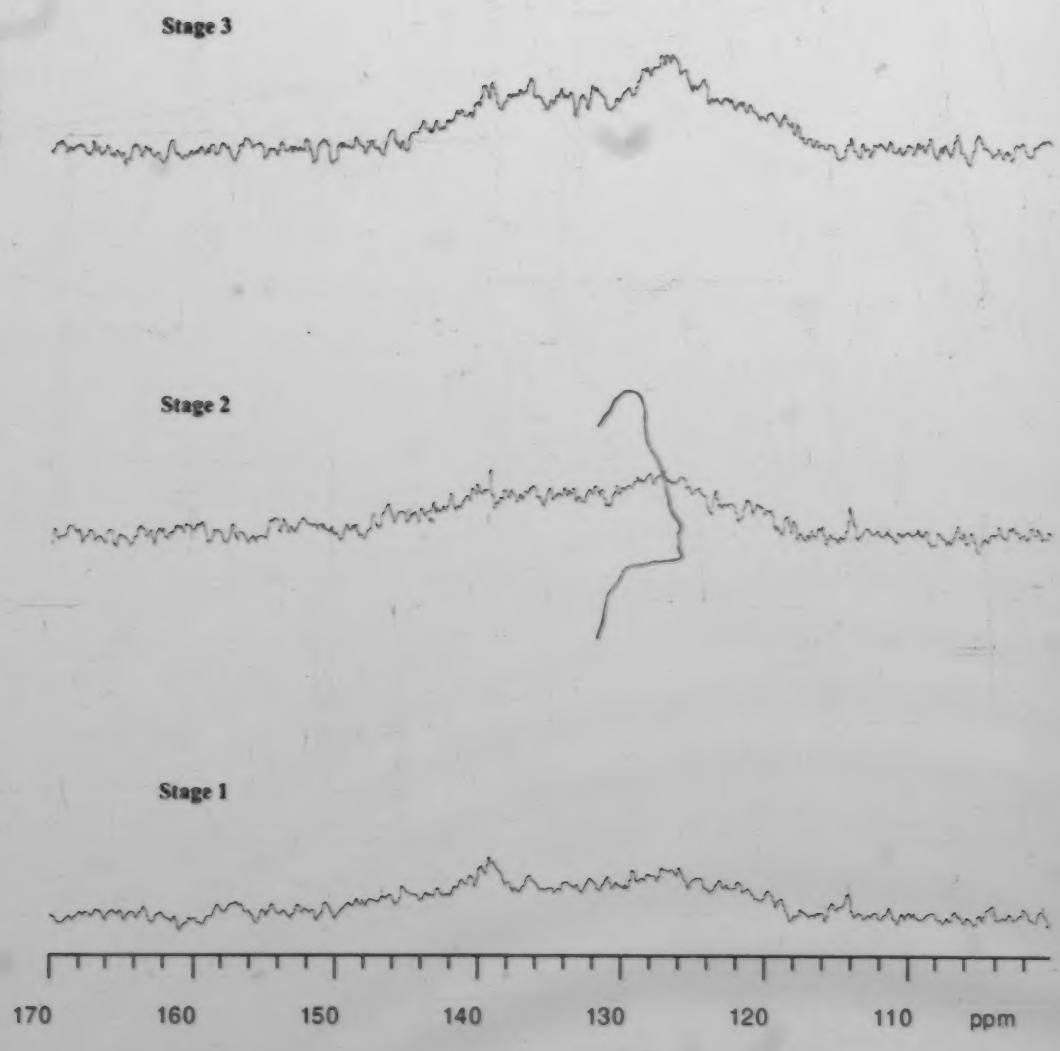

**Figure 4.12** $^{13}C$ **NMR spectra for residue fractions - paraffinic region**

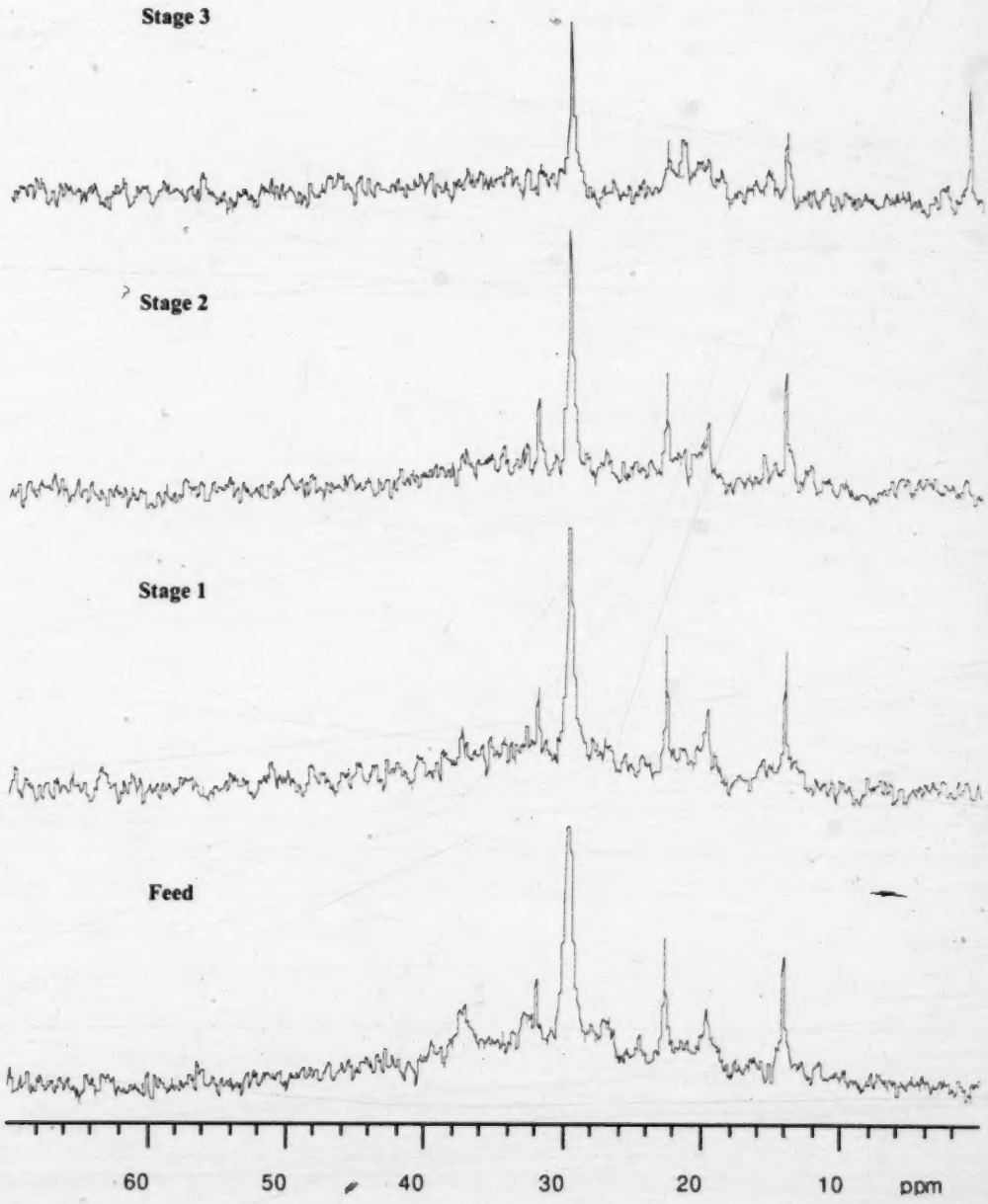

**Figure 4.13** $^{13}C$ **NMR spectra for distillate fractions - paraffinic region**

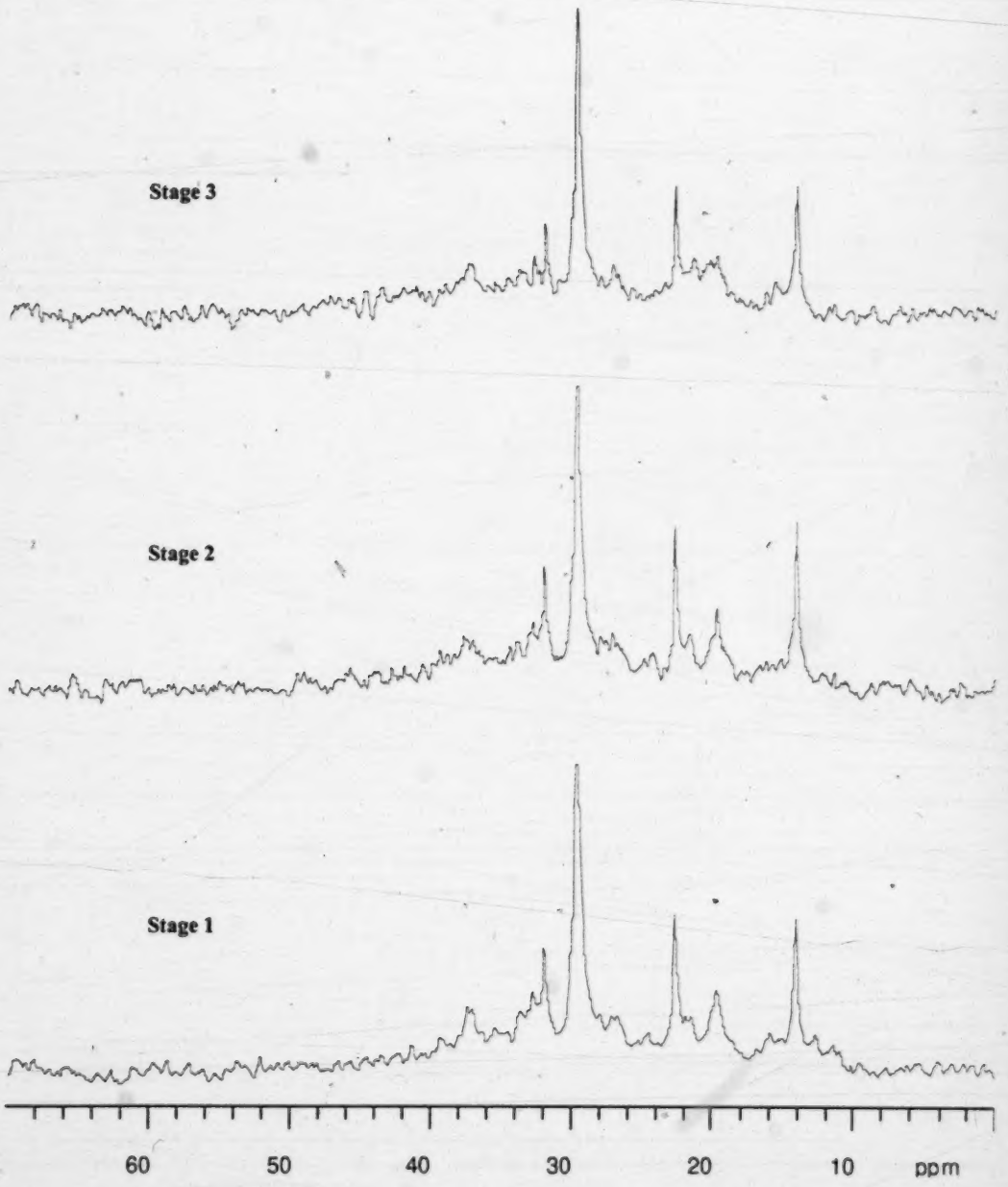

#### *4.2.5.3 Advanced NMR spectroscopic techniques*

The Distortionless Enhancement by Polarisation Transfer (DEPT) spectra of the last stage residue fraction shown in Figure 4.14 and Figure 4.15 distinguished between quaternary, CH, $CH_2$, and $CH_3$ carbons. The DEPT spectra indicated that $\delta$ = 129 ppm was a reasonable division line between the quaternary aromatic carbons and the protonated aromatic carbons. The DEPT spectra of the paraffinic region shown in Figure 4.15, subspectra B, detected little CH in the sample. Subspectra A of the same figure showed that downfield of 22 ppm, $CH_2$ carbon makes up the major part of the NMR signal.

The 2-D NMR spectra used to characterise the stage 3 residue sample are shown in Figure 4.16 and Figure 4.17. The HETCOR spectra shown in Figure 4.17 is plotted with the proton spectra on the top and a carbon spectra along the side. The intersection between these spectra represents a correlation between the carbon and its attached protons. Similarly, in the COSY spectra the cross peaks represent a correlation between coupled protons.

The COSY spectra clearly showed the correlation between the $\alpha$ and $\beta$ to aromatic protons as well as the terminal $\alpha$ $CH_3$ and $\beta$ chain $CH_2$. The HETCOR spectra demonstrated that the 29.7 ppm peak consisted not only of $\delta$ carbon but also various other carbon functionalities. The peak at 14 ppm was confirmed as the terminal $CH_3$ peak and the peak around 22 ppm indicated not only $\beta$-$CH_2$ but also $\alpha$-$CH_3$. The $CH_2$ carbon $\beta$ to terminal chain methyls (chain $\gamma$ $CH_2$) was confirmed at 32 ppm.

**Figure 4.14 DEPT Spectra for stage 3 residue fractions – aromatic region**

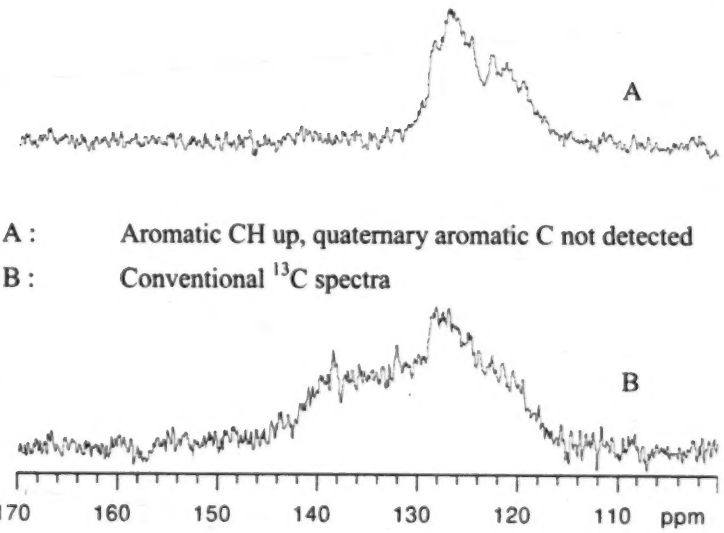


Subspectra A : Aromatic CH up, quaternary aromatic C not detected

Subspectra B : Conventional $^{13}C$ spectra

**Figure 4.15 DEPT Spectra for stage 3 residue fractions - paraffinic region**

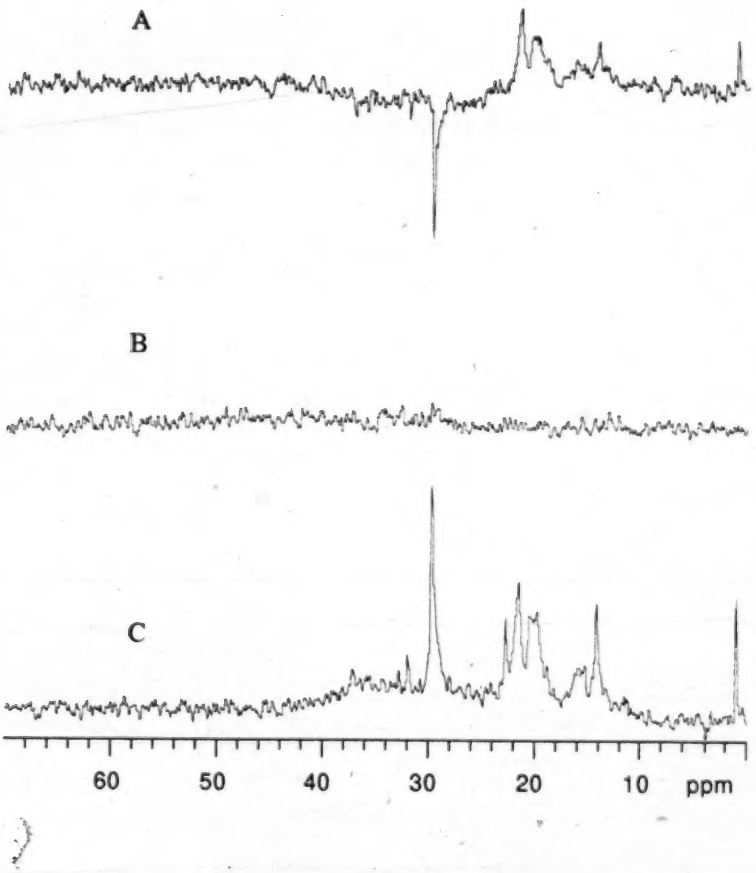


| | |
|---|---|
| Subspectra A : | $CH_2$ down, $CH_3$ and CH up |
| Subspectra B : | CH up, $CH_2$ & $CH_3$ suppressed |
| Subspectra C : | Conventional $^{13}C$ spectra |

**Figure 4.16 COSY Spectra for stage 3 residue fraction**

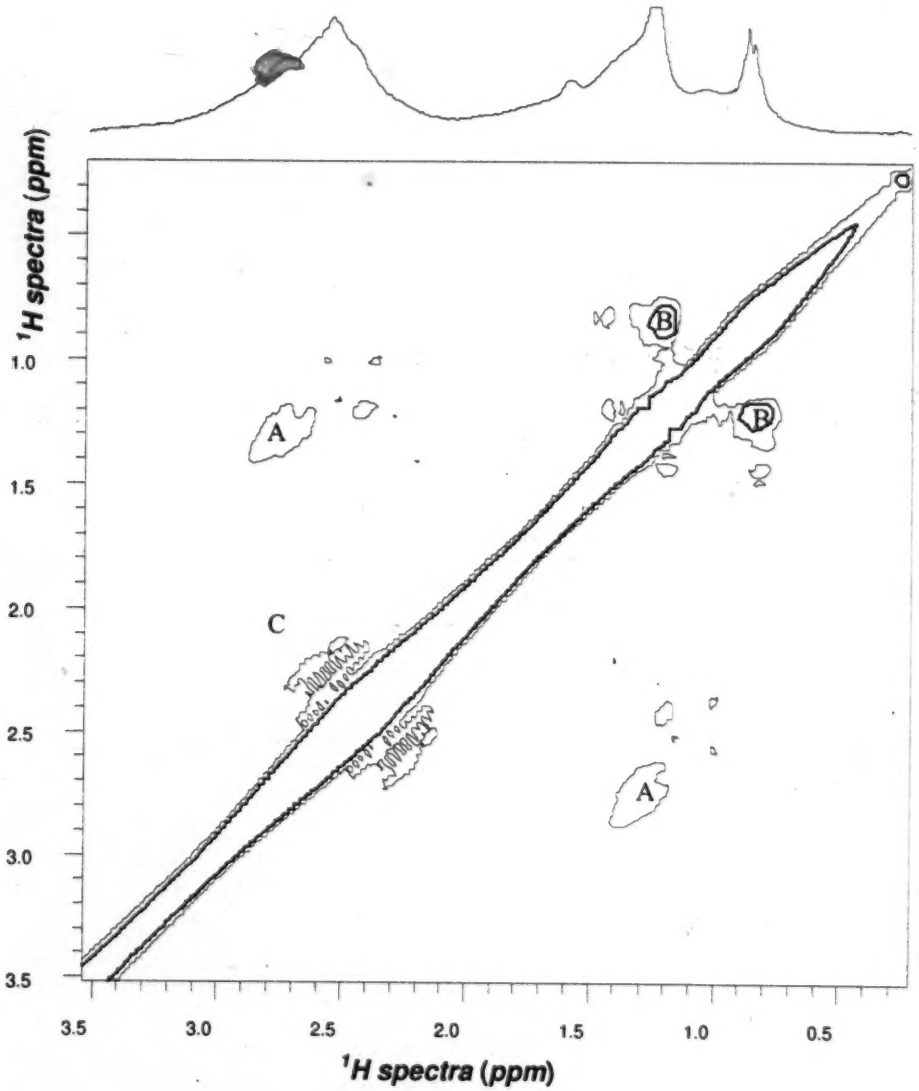


Region A : Coupling of protons α and β to aromatic

Region B : Coupling of terminal α $CH_3$ protons to β $CH_2$

Region C : Coupling of α $CH_2$ protons on adjacent aromatic carbons

**Figure 4.17 Paraffinic region of the HETCOR spectra for stage 3 residue fraction**

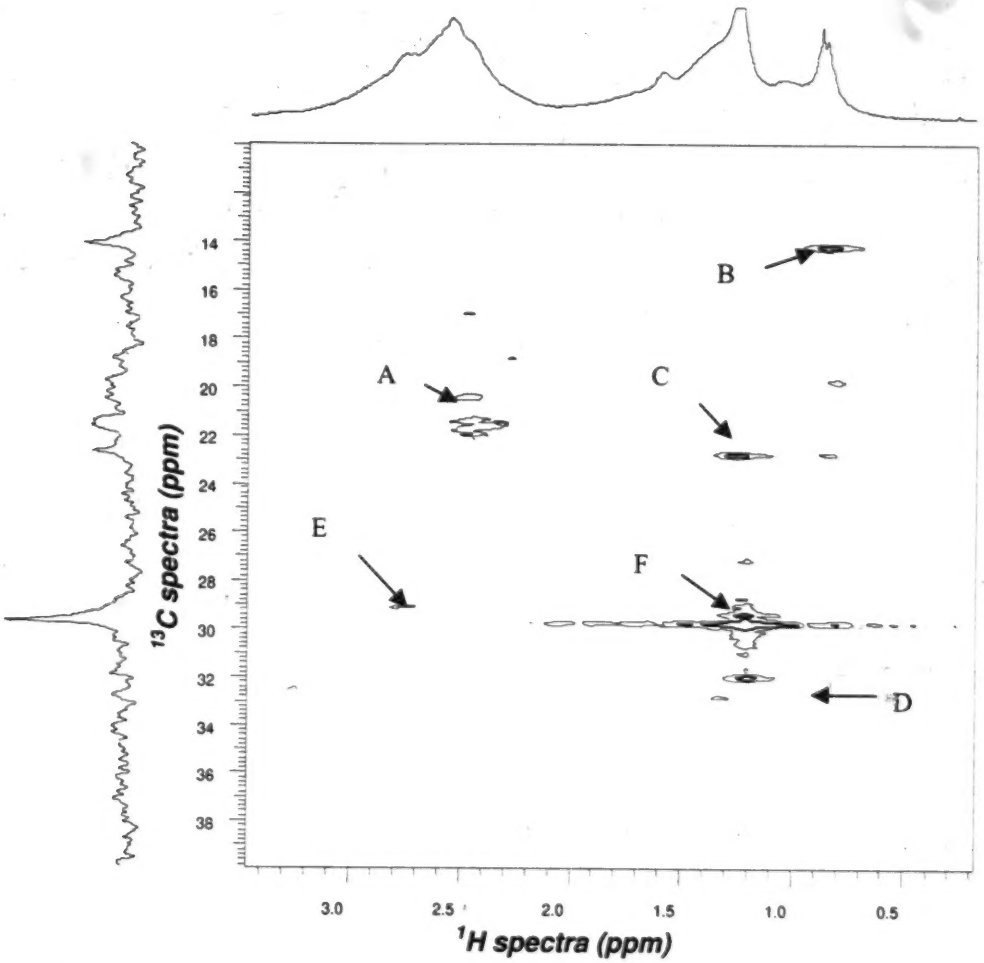


Region A: α to aromatic $CH_3$

Region B: Terminal chain methyls

Region C: Chain β $CH_2$

Region D: Chain γ $CH_2$

Region E: α to aromatic $CH_2$

Region F: 30 ppm peak traditionally assigned to chain δ $CH_2$

#### *4.2.5.4 Quantitative data analysis*

The NMR spectroscopic data gave quantitative confirmation of the increase in aromatic carbon from the feed stage to the final stage 3 (Figure 4.18). The aromaticity increased from 40% in the virgin feed to 78% for stage 3 residue fraction. It was observed that the fraction of both quaternary carbon (Qar) and protonated carbon (CHar) increased. The substituted quaternary carbon (Qar-S) showed little or no variation and thus the increase in quaternary carbon is almost entirely due to quaternary bridgehead carbon (Qar-P). The paraffinic residue fraction, shown in Figure 4.19, indicated a small but steady decrease in Ar-$CH_3$. The NAPH fraction, which may be considered to be an indicator of the total naphthenic carbon, displayed a significant decrease. The chain carbon (CHAIN) as well as terminal methyls (C-$CH_3$) gradually decreased with every reaction stage. Significant decreases were seen in all other paraffinic carbon functionalities except E-$CH_3$. The distillate fractions followed a trend similar to the residue fractions (Figure 4.20 and Figure 4.21). The only exception was the CH functionality that did not decrease from the second stage distillate fraction to the third stage distillate fraction. The concentration of the different carbon functionalities in the feed residue and the corresponding distillate product showed a strong one to one correlation.

**Figure 4.18** $^{13}C$ NMR data for residue fraction - aromatic region

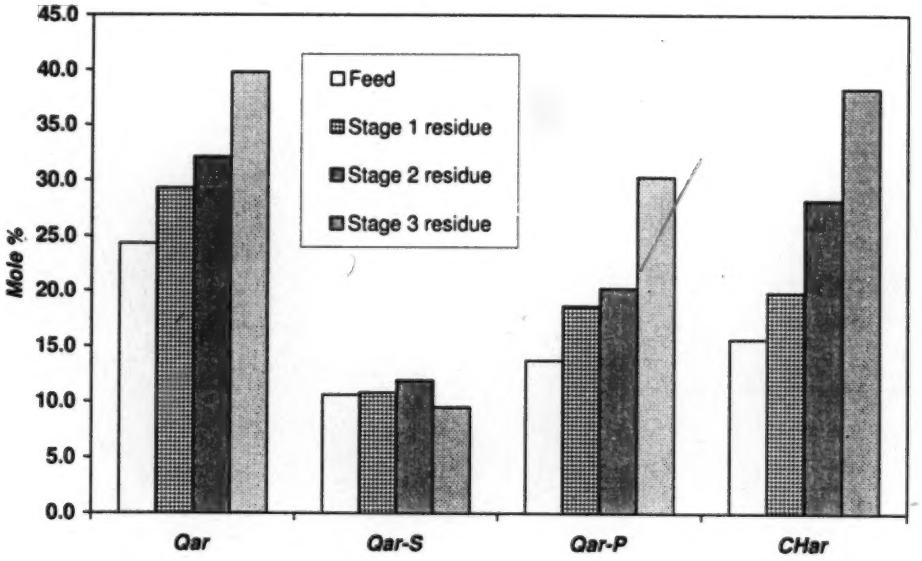


**Figure 4.19** $^{13}C$ NMR data for residue fraction - paraffinic region

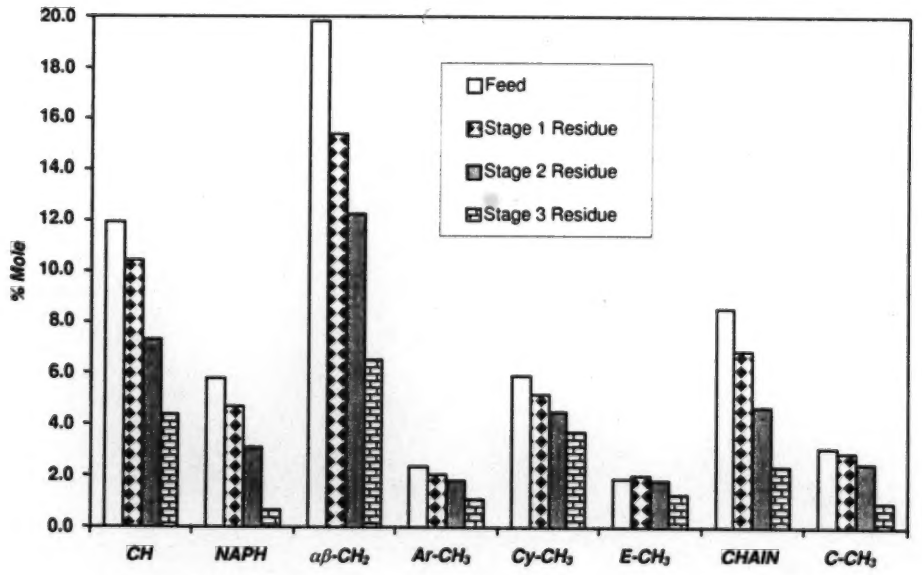

**Figure 4.20** $^{13}C$ **NMR data for distillate fraction - aromatic region**

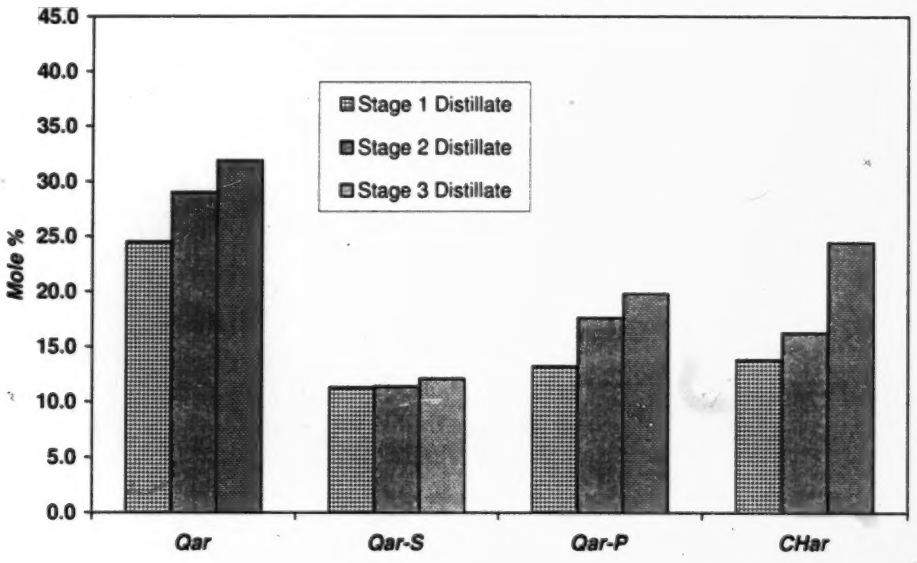


**Figure 4.21** $^{13}C$ **NMR data for distillate fraction - paraffinic region**

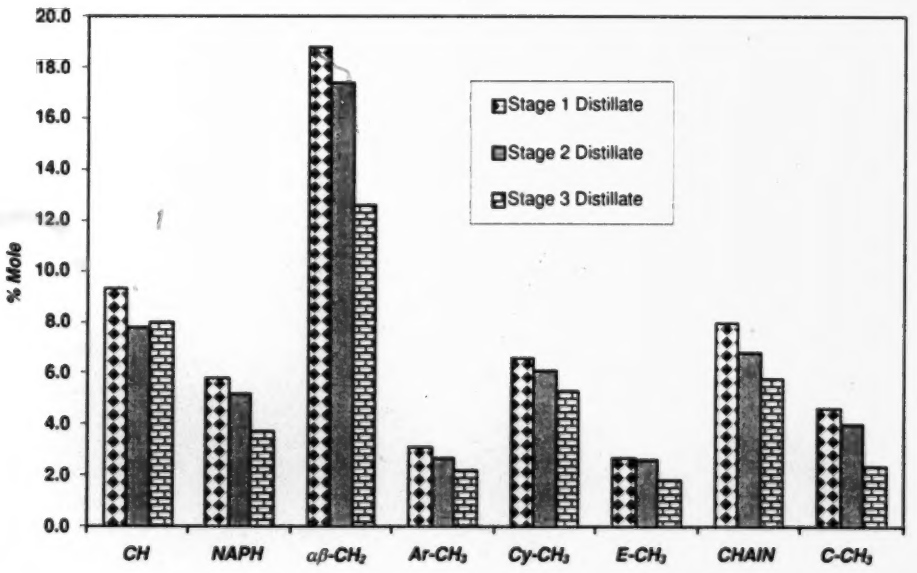

#### 4.2.5.5 *Other estimated parameters*

The NMR data were also used to estimate various other parameters. Chain length can be calculated from the ratio of CHAIN/C-$CH_3$ (Netzel *et al.*, 1981). As seen in Figure 4.22, the variation in this ratio is small and can be considered to be within the margin of error. Another important parameter calculated from the NMR data was the ratio of bridgehead to aromatic carbon, which is useful as an indicator of the degree of condensation (Snape and Bartle, 1984; Solum *et al.*, 1989). The variation of this ratio was minimal, indicating no build-up of large condensed aromatic structures.

**Figure 4.22 Chain length and cluster size**

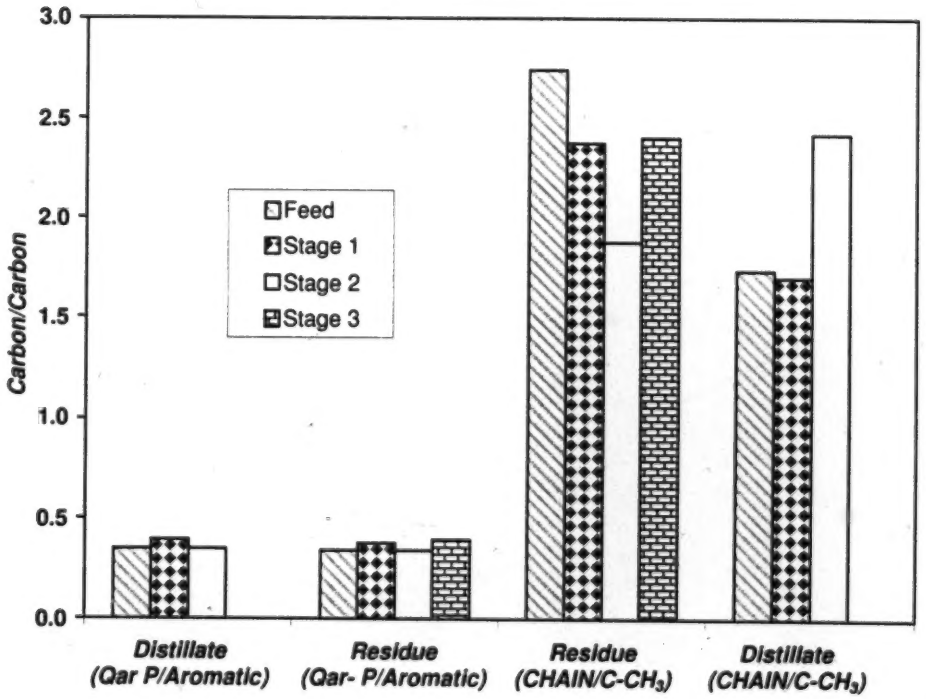

#### 4.2.5.6 *Mass balance on aromatic carbon*

The NMR data, elemental analysis and the yields of the product fractions enabled the calculation of an aromatic carbon mass balance. The calculation was based on the assumption that the aromaticity of the coke was 91% and that the naphtha and gas fractions were all paraffinic. The value of the aromaticity was determined by Egiebor *et al.* (1989) using $^{13}C$ NMR Spectroscopy with CP/MAS and dipolar dephasing technique. The coke analysed was from a commercial delayed coking unit. Hepler (1989) showed that the H/C ratio for the coke obtained from the same delayed coking unit is 0.52, which is comparable to the H/C ratio of the coke produced from the coking experiments (Table 4.1), therefore the aromatic carbon content would be circa 91%. The carbon content of the liquid fractions and the coke was obtained from the elemental analysis. The gas composition allowed the determination of the carbon content of the gas. The total aromatic carbon (*TAC*) in a given fraction was determined as:

$$\left.\begin{aligned} TAC_{fraction} &= Weight \times \frac{\%Aromaticity}{100} \times \frac{Weight\%Carbon}{100} \\ \%\ Feed\ aromatic\ carbon\ in\ product &= \frac{TAC_d + TAC_r + TAC_c}{TAC_f} \times 100 \end{aligned}\right\} \qquad (4.2)$$

where $TAC_r$ = Weight of aromatic carbon of residue

$TAC_d$ = Weight of aromatic carbon of distillate

$TAC_c$ = Weight of aromatic carbon of coke

$TAC_f$ = Weight of aromatic carbon of feed

The aromatic carbon mass balance is shown in Figure 4.23. The figure showed that within the margin of error, total aromatic carbon increased only for the first stage of coking, then remained constant.

The mass balance calculation was repeated assuming the aromaticity of the naphtha fraction was 35% and it contained 83.5 wt.% carbon. The literature suggests values of coker naphtha range from as low as 5.4% to as high as 26.1% (Abu-Dagga and Rüegger, 1988; Gray *et al.*, 1992). A still higher value of 35% was chosen here to represent the upper bound on the aromatic carbon balance. The carbon content was estimated from the average carbon content of all the liquid fractions obtained in the coking reactions (Table 4.1).

The additional aromatic carbon thus estimated to be in the naphtha fraction is shown in Figure 4.23 in dotted lines. The figure shows that even with this relatively high value for aromaticity of naphtha no significant increase was observed in the net amount of aromatic carbon produced in stage 2 and stage 3.

**Figure 4.23 Mass balance for aromatic carbon on all three coking stages**

**Dashed line represents the change in aromatic carbon mass balance with the variation of naphtha aromaticity from 0 to 35%**

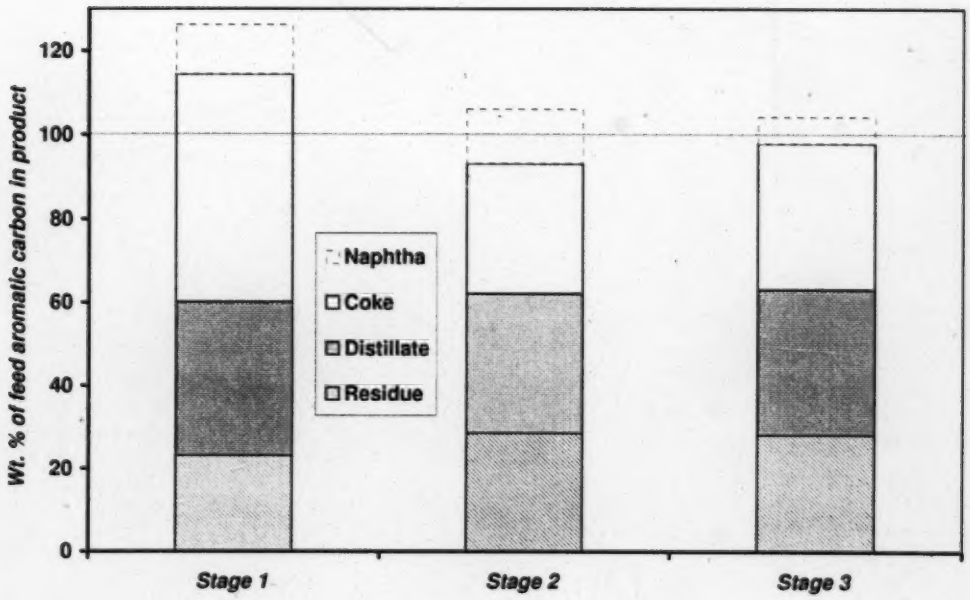

### 4.2.6 Micro Carbon Residue (MCR)

The bar charts in Figure 4.24 indicate the variation of the distillate MCR over the various stages of coking. The cumulative MCR after each stage is also shown in the figure as a solid line. Although the last stage feed showed a very high MCR (6.3%) for a volatile 'non-MCR' distillate fraction, on a cumulative basis there was little change in distillate MCR.

**Figure 4.24 MCR for distillate fractions**
**(Bars - stagewise product properties; points - average cumulative properties)**

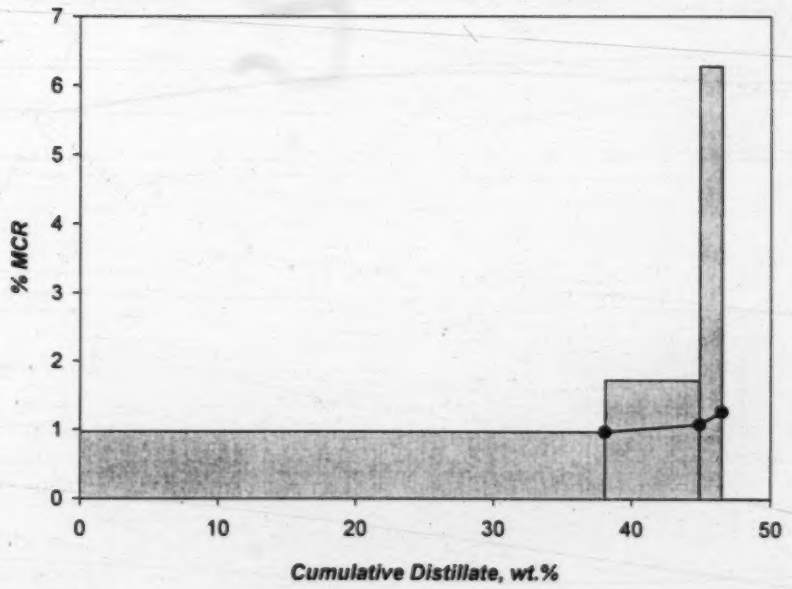

The residue fraction MCR data are shown in Figure 4.25. A monotonic increase was seen in the MCR given by the residue from the first stage to the residue of the third stage from 16.4 % to 33.9%. As explained in Section 4.1.2, the high MCR in the feed to the first stage was a result of the higher boiling components. Note that the first stage MCR content has been corrected for fine solid content. A one to one correlation was found between the MCR content and the yield of coke (Figure 4.26) for all three stages of coking. The one to one correlation enabled the prediction of the third stage coke yield.

There was a linear correlation between the aromaticity of the residue fraction and the MCR for the recycled residues (Figure 4.27), although it should be noted that the fresh feed did not fall on the same trend. Other researchers (Gray *et al.*, 1991) have also seen a similar linear correlation. Many researchers have correlated the H/C ratio with the MCR or CCR of the given feed material (Roberts, 1989; Trasobares *et al.*, 1998). A plot of H/C vs aromaticity is shown in Figure 4.28. The H/C ratio is largely dictated by the aromaticity. Ouchi (1985) showed that there is a linear relationship between aromaticity and H/C ratio. The hydrogen to carbon ratio and its relationship to the aromaticity for the samples in this study is shown in Figure 4.29.

**Figure 4.25 MCR for residue fractions**

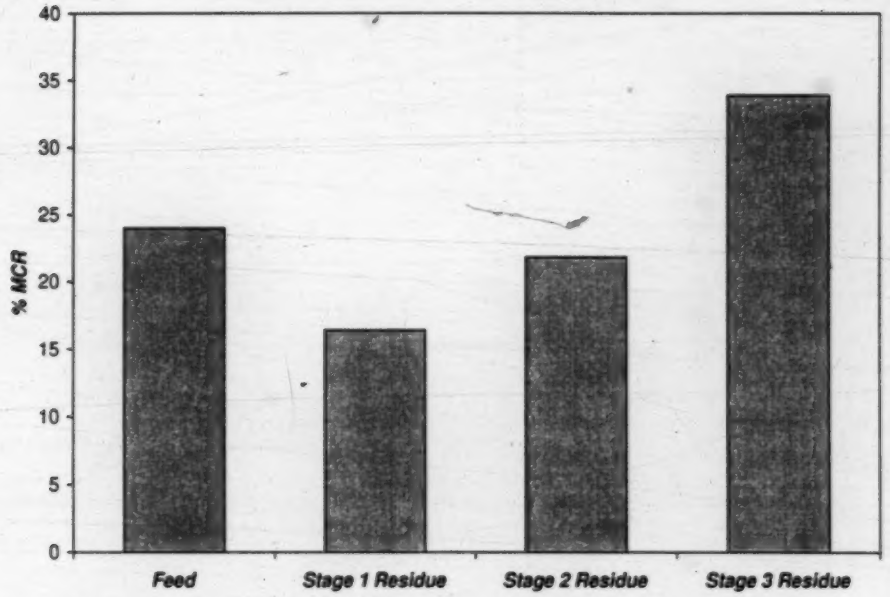


**Figure 4.26 MCR content of residue fractions vs. coke yield**

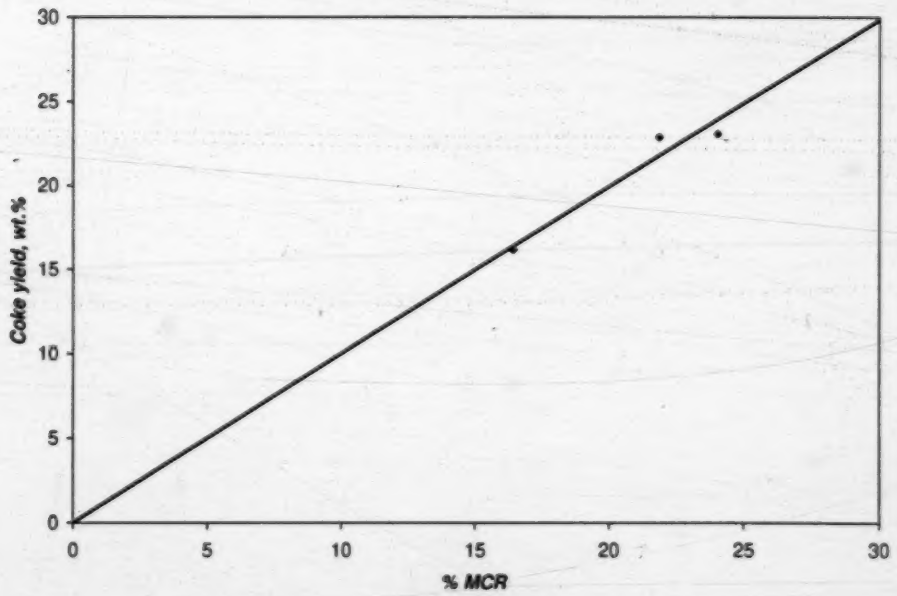

**Figure 4.27 MCR vs. aromaticity for residue fractions**

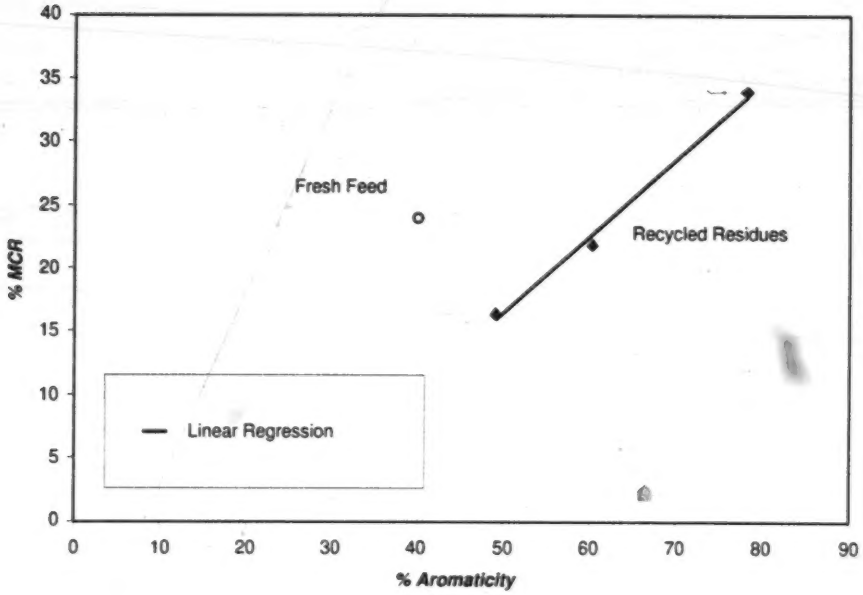


**Figure 4.28 MCR vs. H/C for residue fractions**

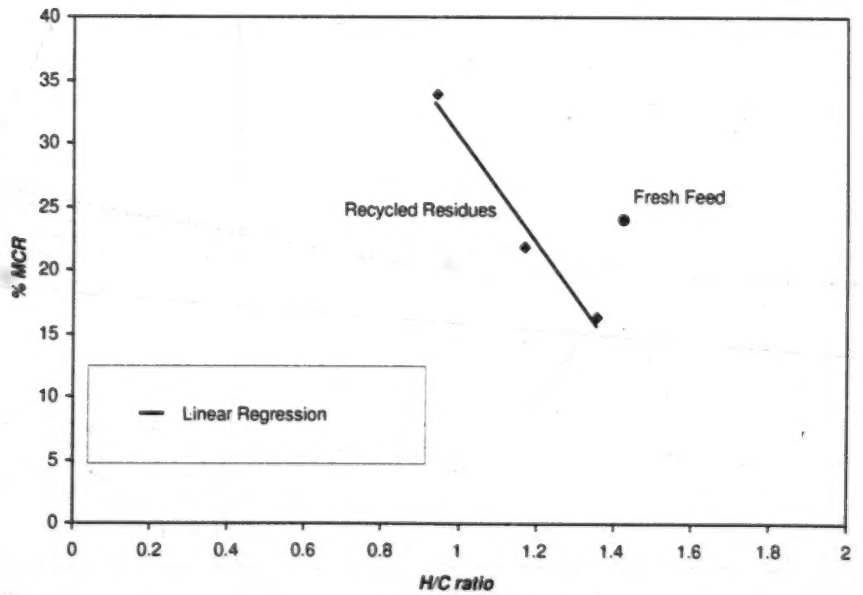

**Figure 4.29 Aromaticity vs. H/C ratio for residue and distillate fractions**

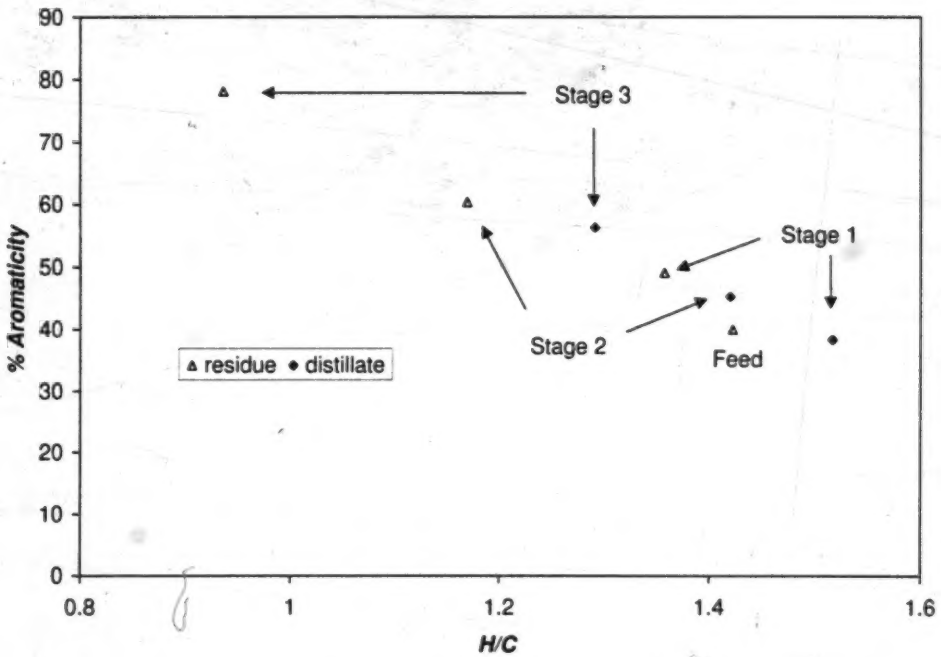

### 4.2.7 High performance liquid chromatography (HPLC)

The HPLC data shown in Figure 4.30 indicated an increase in the tri and polyaromatic hydrocarbons (PAHs) and a decrease in the diaromatics with each successive stage of coking. All other parameters showed little or no variation. Note that using the ELSD, unsatisfactory material balance closures ranging from 79 to 107% were obtained for the three distillate fractions (details in Appendix 5). Fortunately, the UV absorption spectra at 282nm (Figure 4.31) also confirmed the build up of PAHs from stage 1 to stage 3. The absorption spectra at 210nm (Figure 4.32) also confirmed the decrease in diaromatics seen in the ELSD data. The absorption of UV light in the region demarcated as the saturate fraction indicated the presence of aromatics and thus explained the relatively high yield of saturates indicated by the ELSD. The UV data indicated a significant drop in the signal in the saturate and monoaromatic region, contrary to the ELSD data, which indicated only a slight decrease for these fractions (on a cumulative basis) with each stage. The spectra at 210 nm displayed a sudden jump in the signal at 20 min, which is due to the elution of the solvent, methylene chloride ($CH_2Cl_2$).

**Figure 4.30 HPLC data for the distillate fractions (ELSD)**

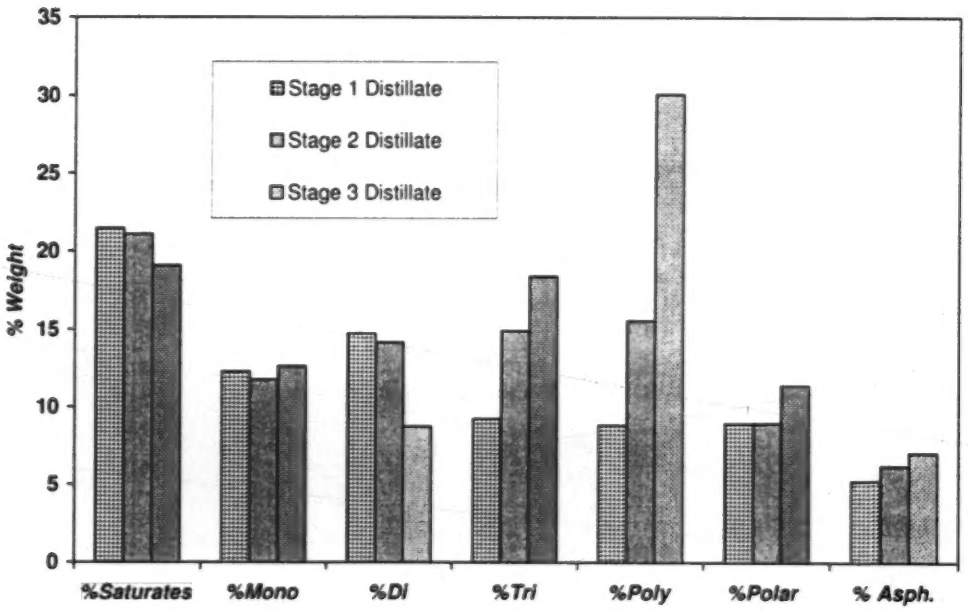

**Figure 4.31 Distillate fraction UV absorption spectra - 282 nm**

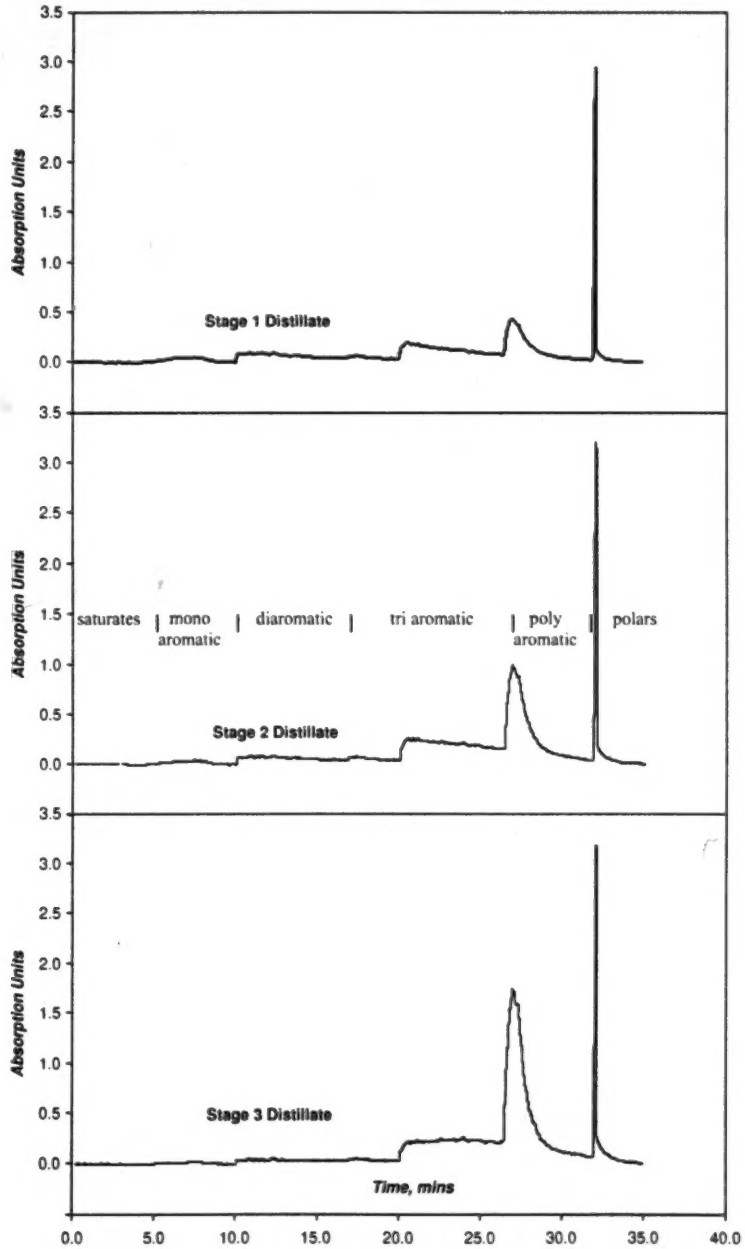

**Figure 4.32 Distillate fraction UV absorption spectra – 210 nm**

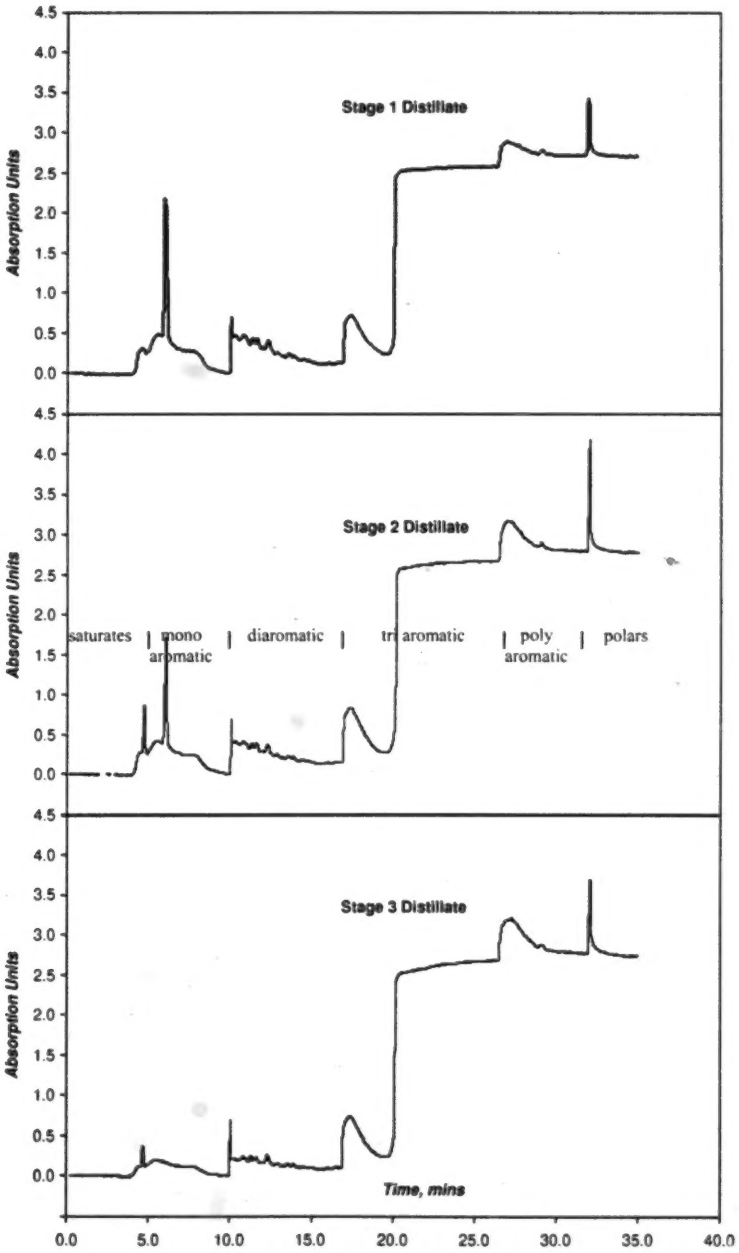

# 5 Discussion

## 5.1 Feed transformations during thermal cracking

Thermal cracking involves breaking up the petroleum macromolecules into smaller fragments. Some of the more reactive cracked molecules undergo secondary condensation reactions to combine and give even larger molecules than those in the original feedstock. Therefore, feed introduced into the reactor may follow any of the following paths (Figure 5.1):

1. Large molecules crack to form smaller molecules that vaporise.
2. Active products polymerise to form heavier molecules like coke.
3. The feed fed into the reactor can volatilise out of the reactor without significant reaction.

**Figure 5.1 Feed transformations**

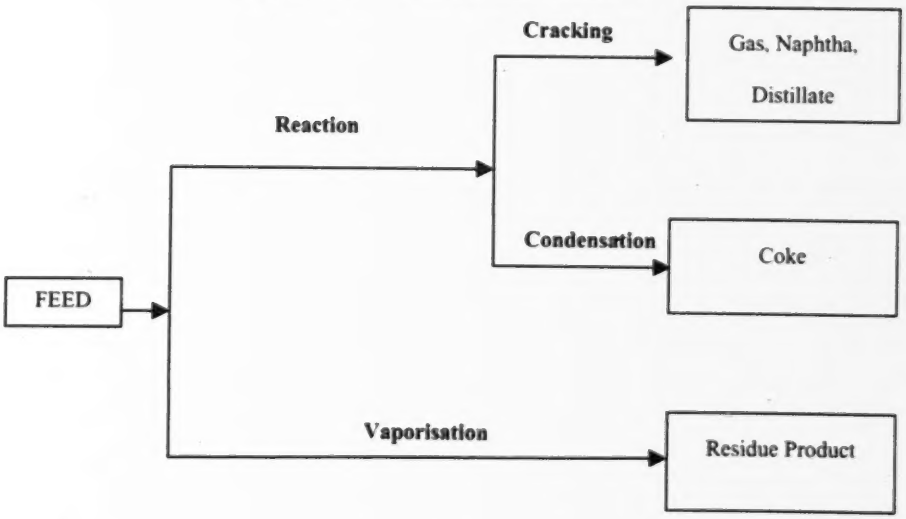

### 5.1.1 Yields on cracking

The yields of the various product lumps indicated in the previous figure are shown in Figure 5.2. All the lumps have been expressed on a 500°C+ basis. The yield of cracked products (gas, naphtha and distillate) show a monotonically decreasing trend with subsequent stages of cracking. The coke yields went through a minimum. Since the coke yields and MCR content showed a one to one correlation (Figure 4.26) the stage 4 coke yields could be estimated. The dotted bar in Figure 5.2 represents the estimated coke yield.

**Figure 5.2 Feed conversion at various stages**
**(See Figure 4.3, Figure 4.5 and Figure 4.6)**

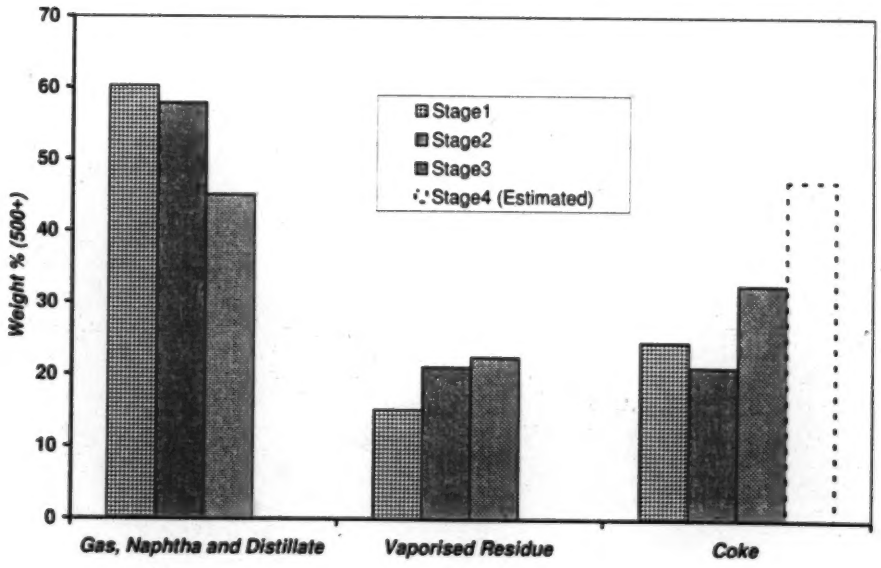

The product yields were dependent on the chemical composition and the physical characteristics of the feed. The aromaticity is one of the most important factors representing the changing chemical composition while the molecular weight is the major physical characteristics affecting product distribution (see Ternan and Kriz, 1998). The variation of these properties over the stages of conversion is shown in Figure 5.3. The residue collected from stage 1, stage 2 and stage 3 had similar molecular weights and boiling curves (Figure 4.5) and therefore aromaticity was the only significant factor affecting coke yields. Figure 5.4 shows a linear correlation between coke yield and aromaticities for these processed residues. The unconverted feed residue gave approximately 14% higher coke yield than that expected from the linear correlation. This exception was due to the fact that the extent of residue vaporisation significantly changed from stage 1 to stage 2 (Figure 5.2), as the molecular weight and boiling point distribution of the feed shifted. Furthermore, the feed fraction contains fairly large hydroaromatic and cycloparaffinic (3-5 rings) structures (Strausz *et al.*, 1992; Peters *et al.* 1992) that can undergo dehydrogenation reactions to form condensed aromatics. A mass balance on aromatic carbon (Figure 4.23) showed a significant increase in the net amount of aromatics in the first stage. The higher molecular weight allowed the material to stay in the liquid phase and undergo dehydrogenation reactions to give a net increase in aromatic carbon and therefore substantially higher coke yields.

**Figure 5.3 Variation of MW and aromaticity for feed and product residues (See Table 4.3 and Figure 4.18)**

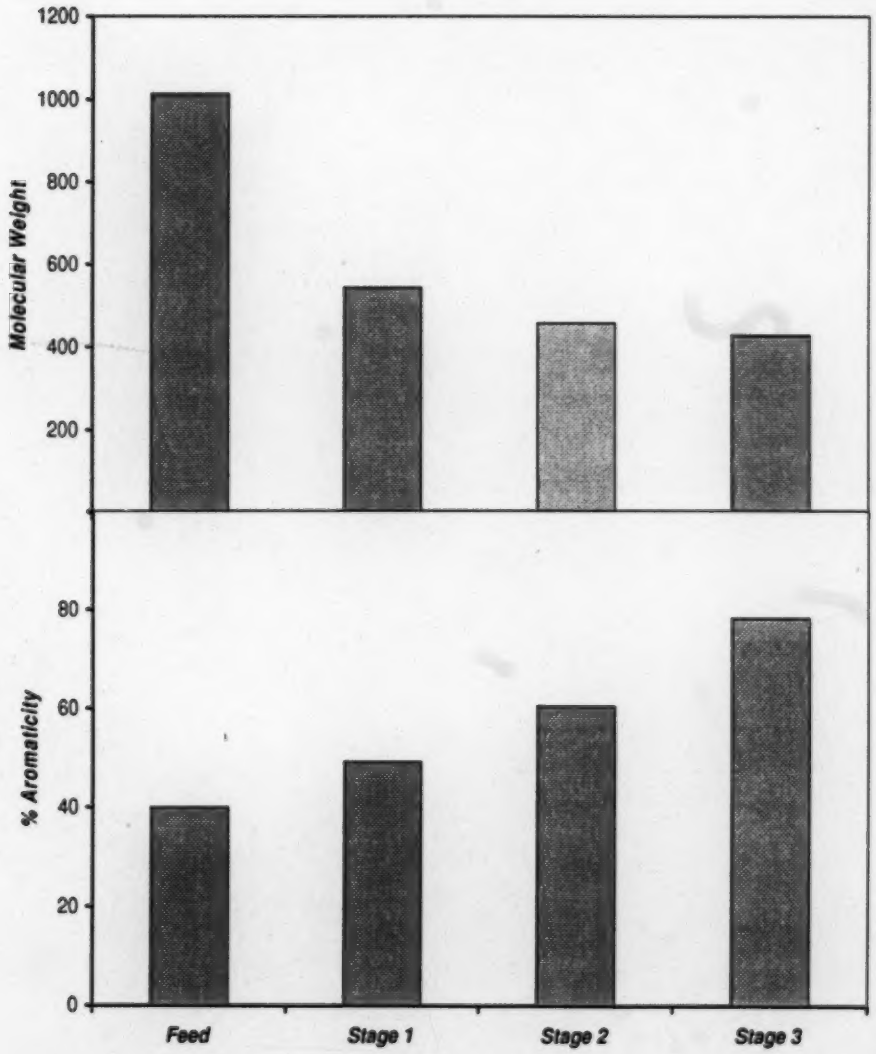

**Figure 5.4 Coke yield vs aromaticity**

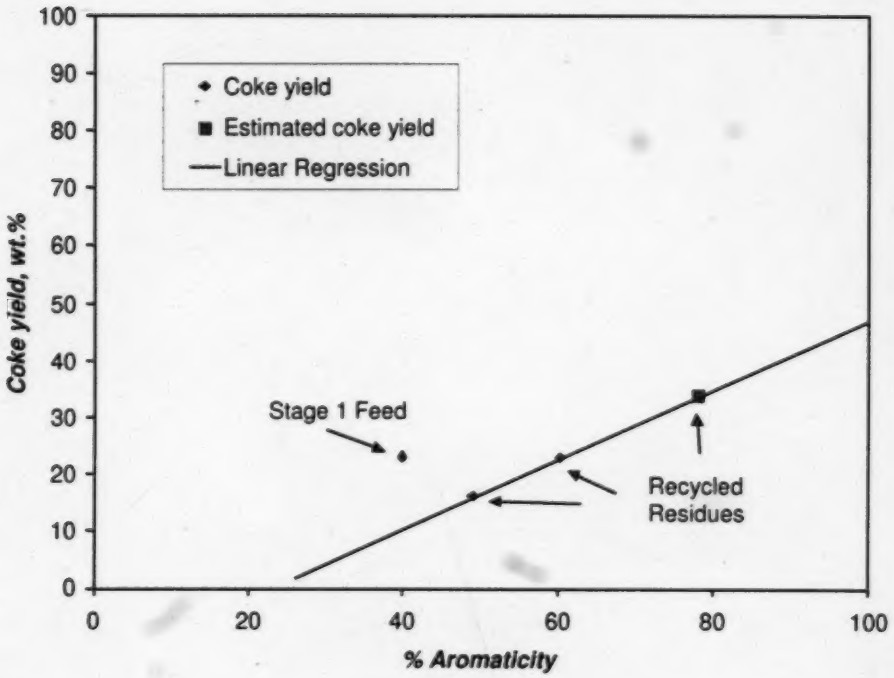

### 5.1.2 Major reactions and structural changes

The major reactions that occurred during thermal cracking included dealkylation of aromatic rings, ring growth and ring dehydrogenation. Our analysis indicated that although the number of alkyl side chains on aromatic rings decreased, the average chain length remained constant (Figure 4.22). The constant chain length and the almost constant amount of $\alpha$-$CH_3$ indicated that the preferred route for dealkylation of the alkyl aromatic moieties present in the residue was the cleavage of the alkyl-aryl bond. Model compound studies by Smith and Savage (1991), Greinke (1992) and Freund *et al.* (1991) showed that this was the preferred route for dealkylation of polycyclic alkyl aromatics. Alkyl benzenes on the other hand preferably undergo $\beta$ or $\gamma$ scission (Savage and Klein, 1987). The data thus indicated that there were significant quantities of polycyclic aromatic compounds (3-5 rings) and that the bulk of the dealkylation reactions involved removal of the side chains from these polycyclic aromatics.

The NMR data showed that the aromaticity of the distillate and residue fractions increased with each coking stage. However a mass balance on the aromatic carbon, showed that after the first stage of cracking no overall increase could be seen in the net amount of aromatic carbon (Figure 4.23). The net increase in aromaticity of the first stage was most likely due to the dehydrogenation of the hydroaromatics. The second and third stage residues were unlikely to have significant concentrations of these easily dehydrogenable compounds, and therefore no significant increase in aromatic carbon was observed. The NMR signal for the NAPH fraction in the

subsequent stages is probably due to cyclic naphthenes like steranes and terpanes (Figure 5.5), as well as aromatic steroids (Figure 5.6). These compounds do not easily dehydrogenate under reaction conditions, as observed by Peters *et al.* (1992) and Sullivan *et al.* (1989). In an extensive literature survey of dehydrogenation reactions of cyclic compounds it was shown that five membered naphthenic rings are difficult to dehydrogenate (Fu and Harvey, 1978). The naphthenic compounds present from stage 2 onwards cracked to give lighter products or underwent condensation reactions along with the aromatics to form coke.

**Figure 5.5 Tricyclic terpane**

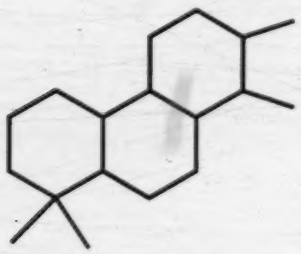

**Figure 5.6 Triaromatic steroid**

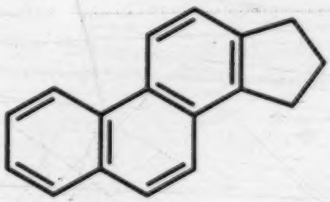

The HPLC data pointed to a build up of polycyclic aromatics in the distillate fractions (Figure 4.30). On the other hand, the NMR data showed that the ratio of bridgehead to total aromatic carbon remained constant (Figure 4.22). It is probable that the mono aromatics are lost to the naphtha fraction by cracking and the penta and higher aromatics are being lost to coke. This disproportination would lead to a build up of tri- and tetra-aromatic structures in the distillate products while maintaining a relatively constant ratio of bridgehead to total aromatic carbon.

By the last stage of cracking the residue molecules were highly aromatic, but it is important to note the considerable amount of leftover aliphatic carbon in the form of chains and methyl groups. Almost half of the non-aromatic carbon was non-cycloparaffinic. Structurally there was a continuous shift towards a more aromatic species due to the loss of naphthenic and paraffinic species. However there is no evidence to suggest the formation of a large, condensed naphtheno-aromatic structure as suggested in the literature (Sanford 1994, Zhao *et al.*, 2001).

## 5.2 Quality of the distillates

The analysis of the distillates obtained from repeated recycling of the residue showed that the quality of the distillates deteriorated with each coking stage. The high-performance liquid chromatography (HPLC) data indicated a build up of PAHs (Figure 4.31). The weight % of nitrogen in the distillate fraction more than doubled from stage 1 to stage 3 (Table 5.1). The SIMDIST results showed an increase in the average boiling points of the distillates with each successive stage. The increase in the coke forming potential of the distillate fraction can also be gauged from the fact that the MCR of the distillate fraction increased from 1.0% for stage 1 to 6.3% for the last stage (Table 5.1). Nitrogen and PAH's are identified catalyst poisons (Halabi *et al.* 1991; Thakur and Thomas *et al.* 1985) and therefore it is expected that the distillate fraction from the recycled residue would increase catalyst deactivation relative to distillate from fresh feed.

Recycling the residue fraction resulted in an increase in yield of distillate of almost 9 wt.%. On the other hand, by every quantitative measure of distillate product

quality the distillate fraction became progressively more refractory at every stage (Table 5.1).

**Table 5.1 Selected distillate properties on recycle coking**
**(See Table 4.2, Figure 4.20 & Figure 4.24)**

| | Distillate1 | Distillate2 | Distillate3 |
|---|---|---|---|
| %weight | 38.1 | 44.9 | 46.5 |
| % MCR | 1.0 | 1.7 | 6.3 |
| Wt. % nitrogen | 0.33 | 0.48 | 0.8 |
| % Aromaticity | 38.3 | 45.2 | 56.3 |

The variation of a few selected properties on a cumulative basis is shown in Figure 5.7. The nitrogen content and MCR showed a small increase but the change in cumulative hydrogen content was negligible. Although the properties of the cumulative distillate fraction may appear to be within acceptable limits, as shown in Table 5.1, the small amount of the final stage distillate was an extremely refractory fraction and had the potential for causing accelerated catalyst deactivation in the downstream hydrotreaters.

**Figure 5.7 Incremental distillate yield vs. distillate quality**

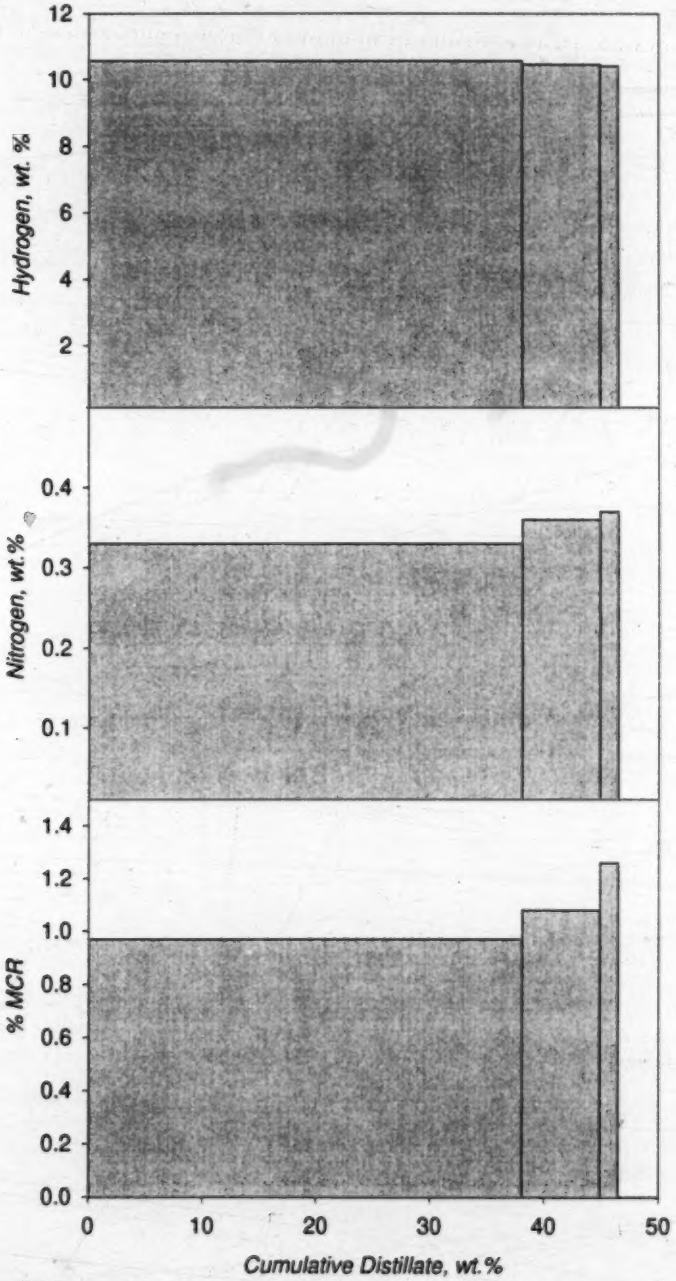

## 5.3 A building block model for bitumen

The complex bitumen macromolecules can be represented by various molecular building blocks. The structural changes and reactions taking place during the thermal cracking of bitumen can then be represented in terms of a rearrangement of these building blocks (Wiehe, 1994; Speight, 1991).

### 5.3.1 Identification and cracking of the building blocks

The different characterisation techniques used in this study identified the various structural parameters and the structural changes that occurred during the thermal cracking of residue. Based on this data the bitumen molecules were assumed to be made up of five different types of building blocks or groups, including aromatics, naphthenics and paraffinic side chains, all joined together by thermally labile bonds (Figure 5.8). Three different sizes of aromatic moieties in the residue structure were indicated by this study: large aromatic groups with more than five rings that were present only in the stage 1 unconverted feed, small aromatic groups with 1 to 2 rings that were lost to distillate fractions and intermediate size molecules containing 3-5 rings to account for the constant molecular weights from stage 2 onwards. The large aromatic groups have a larger heteroatom content and a high propensity to form coke under thermal cracking conditions. The coke formed from the first stage was therefore richer in heteroatoms. In spite of the loss of large aromatics to coke, the NMR data pointed to a constant bridgehead to aromatic ratio. The small aromatic groups are included in the building blocks so that the loss of these blocks from the

**Figure 5.8 Building block schematics for bitumen macromolecules**

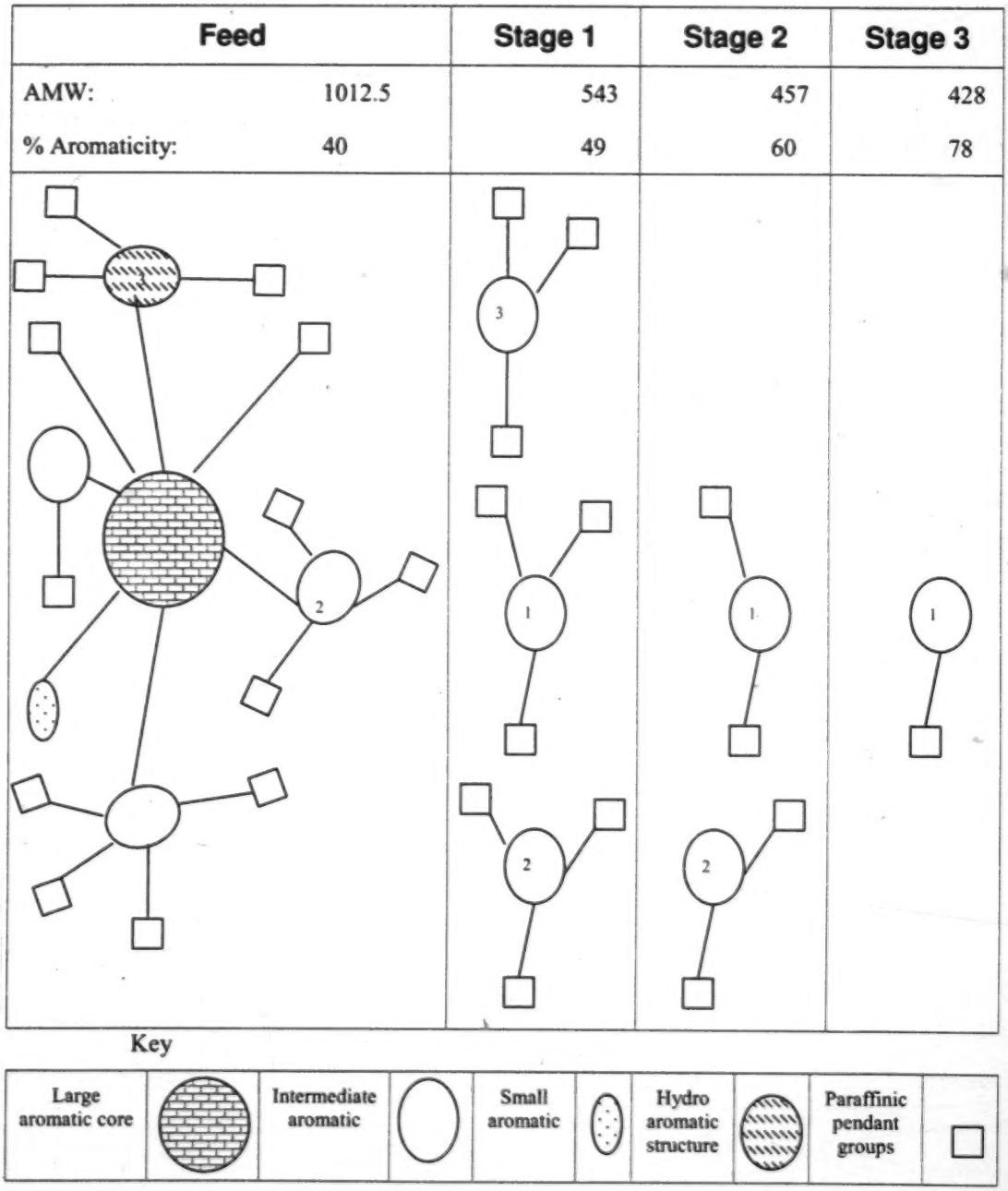

first stage feed can explain the constant bridgehead to aromatic carbon ratio from stage 1 to stage 2.

For stage 1, dehydrogenation of the hydroaromatics to form aromatics was an important reaction. The hydroaromatic group is included to account for these types of reactions as well as to explain the difference in coke yields for different thermal cracking reactors. In the quartz tube reactor these structures dehydrogenated to give the intermediate sized aromatic groups.

The sharp drop in molecular weight in the first stage resulted from the cracking of the thermally labile bonds (for example sulphur linkages) linking the building blocks. The separation of the building blocks did not result in any significant shift in the NMR data, which showed a similar variation of the various carbon functionalities for the residue across the stages.

The constant ratio of bridgehead to aromatic carbon (Figure 4.22) as well as the constant average molecular weight (Table 4.3) for the residue after the first coking stage indicated the absence of any significant ring condensation products in the recycled residue fraction. The average molecular formula (Table 4.3) for the distillate and residue fractions showed little difference. It is quite probable that the aromatic core of the molecule for the residue fraction does not change appreciably after stage 1. The structural differences from stage 2 onwards could simply be accounted for as the gradual disappearance of the paraffinic groups. The elemental analysis of the coke (Table 4.1) also showed that its composition was almost constant, thus indicating an origin from similar aromatic core groups. On thermal

cracking the building blocks are separated and the progress of the reaction (i.e. residue conversion) mainly involved the removal of side chains to leave behind an aromatic core.

The concept of building blocks essentially aims to segregate the bitumen molecule in terms of identifiable molecular structures following similar reaction paths. These building blocks were identified on the basis of the data obtained from the various analytical techniques, but can also be correlated to the molecular structures known to be present in bitumen. Figure 5.9 shows a typical asphaltene molecule proposed by Murgich *et al.* (1999). As illustrated in the figure, the building blocks shown in the schematic in Figure 5.8 can be identified as parts of this molecule.

**Figure 5.9 Strausz's asphaltene molecule (Murgich *et al.*, 1999)**

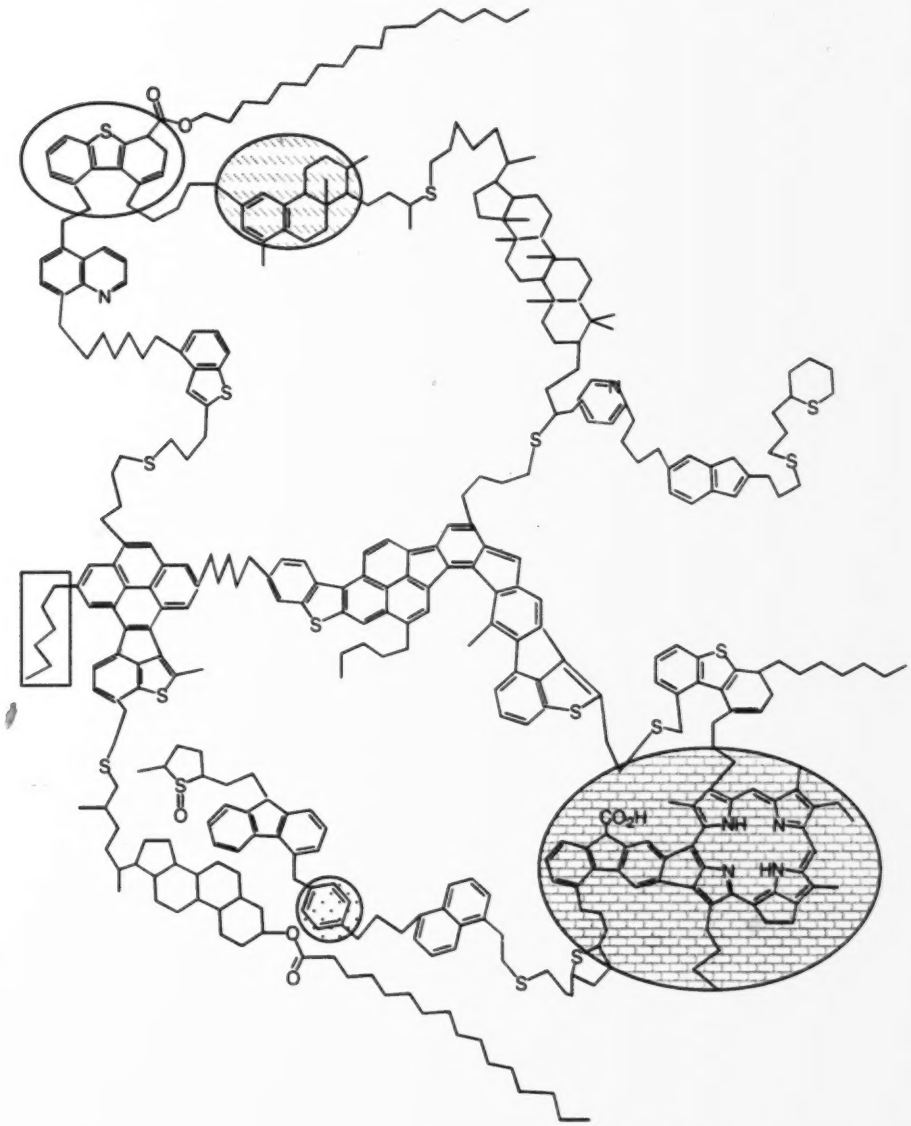

### 5.3.2 Phase Separation

The cracking of the bitumen molecule results in the release of the various building blocks. Some of the cracked structures thus produced were highly aromatic and thus incompatible with the remaining molecules. These highly aromatic structures would separate to from a second liquid phase (Figure 5.10). In the absence of abstractable hydrogen, the second phase would undergo rapid condensation reactions leading to coke formation.

**Figure 5.10 Schematic diagram representing phase separation**

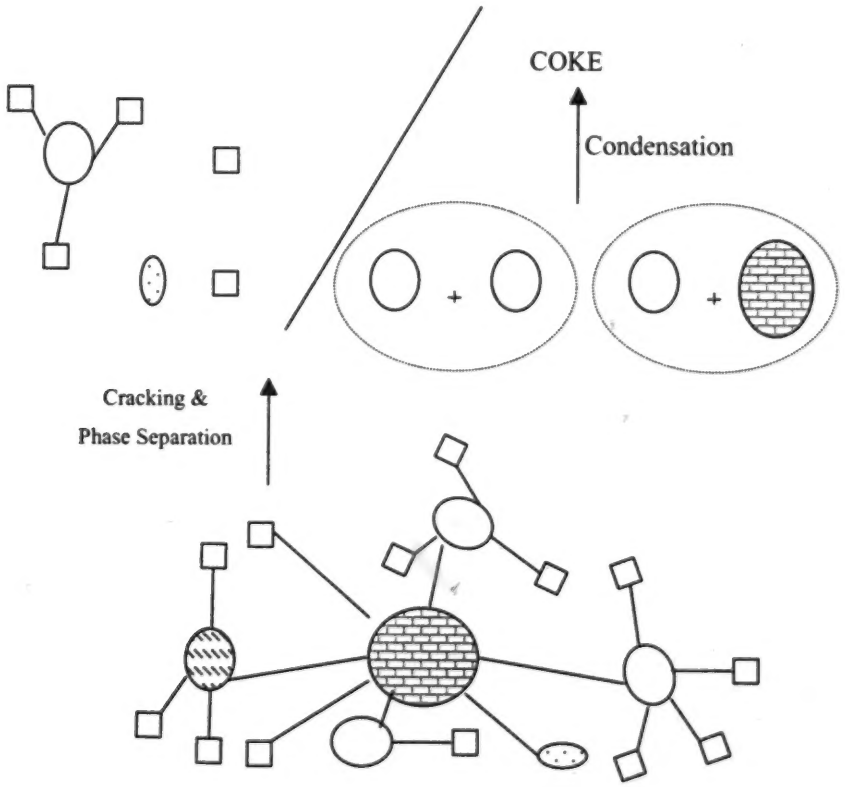

## 5.4 Process Implications

In the context of heavy oil upgrading, the purpose of the coker is to eliminate the undesirable constituents like metals, the heteroatoms and most of the PAH's in the form of coke while at the same time maximising the distillate yield for a given feed. On repeated recycle, the coker failed to achieve the separation between the desirable and undesirable constituents because the distillate product carried greater amounts of the undesirables in the second and third stages.

The coker could remove the undesirable constituents from the cumulative distillate fraction produced on recycle coking by the elimination of large amounts of the recycled residue in the form of coke, thus accepting a loss of distillate yield. As shown by Kirchen *et al.* (1989) this can be achieved by coking at lower temperatures, since the yield of coke increases with decreasing temperature. Figure 5.11 shows a possible flowsheet option that would allow the recycled residue stream to be processed separately at a lower temperature and thus increase coke yields in the second stage. The increase in coke yields can also be achieved by increasing the residence time for the recycle residue stream. A straightforward way to achieve this is by introducing the stream at the bottom of the coker.

**Figure 5.11 Two cokers in series**

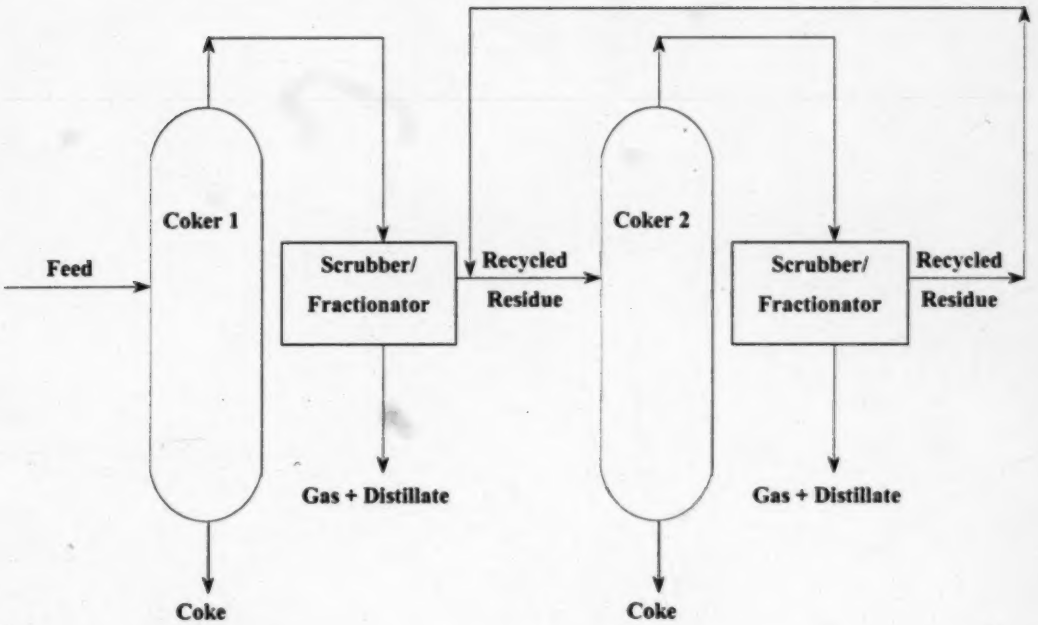

The selection of different processing conditions for the first stage (high temperature, low residence time) and second stage of coking (low temperature, high residence time) is required to ensure an optimum between liquid product yield and quality. The first stage requires rapid residue conversion and short residence times to minimise secondary reactions and maximise yield whereas the subsequent stages require lower temperatures to minimise vaporisation and maximise coke yields to improve distillate quality. The approach listed above would cause a decrease in liquid product yields, but would improve distillate quality. Other possible processing options to allow for a more selective removal of the heteroatoms and other undesirables from the recycled residue stream should also be explored.

The experimental results showed that the quality of the distillate produced on recycle coking approached that of the residue feed. This suggests that the recycle residue can be processed along with the distillate in the hydrotreaters. The majority of carbon functionalities identified by NMR data and the elemental analysis showed no significant difference between recycled residue and the corresponding distillate. The only distinction between the distillate and residue by the last stage was the slight difference in average molecular weights. The molecular weights would affect diffusion in the catalyst pores and thus the catalyst performance. But, the diffusivity is not highly sensitive to MW's ( $Diffusivity \propto \sqrt{MW}$ ) and it may be worthwhile to evaluate if there are any substantial differences in the effects of the residue versus the distillate on catalyst deactivation in the hydrotreaters

# 6 Conclusions and Recommendations

The main objective of the project was to determine the yields of gas, liquid and coke as a function of conversion of the residue fraction of bitumen and to ascertain the characteristics of the distillate products thus produced.

The cumulative yield of liquid increased by 12 wt.% from stage 1 of coking where 82% residue conversion was obtained, to stage 3 where 99% residue conversion was obtained. On the other hand, coke and the gas yields increased only by about 5 wt.%. On a stagewise basis, the higher yield of coke in the first stage was mainly attributed to the lower residue vaporisation due to the higher molecular weight. This subsequently allowed the hydroaromatic material to stay in the liquid phase and undergo dehydrogenation reactions to give a net increase in aromatic carbon and therefore substantially higher coke yields.

The analysis of the distillates obtained from repeated recycling of the residue showed that the quality of the distillates deteriorated with every coking stage. The distillate fractions showed an increasing trend of aromaticity. The extremely high concentration of nitrogen in the last stage distillate should especially be noted. The coke quality showed significant improvement in terms of lower ash and heteroatom content.

Although there was a sharp drop in molecular weight of the residue fraction only in the first coking stage, the carbon structural types as identified by NMR data showed a gradual change. On the basis of the analysis performed on the product

fractions, a building block model of the residue was presented to explain the analytical data. The initial stage of the reaction involved breaking up of the labile bonds that link up the bitumen macromolecule, giving a significant drop in molecular weight. As the reaction progressed, residue conversion involved mainly the removal of side chains from an aromatic core.

## 6.1 Directions for future work

The effect of the distillate on the hydrotreating catalyst needs to be quantified with more precision. The limited amount of time did not permit experiments on hydrotreating of the distillate products. The effect of the residue on catalyst deactivation versus the effect of the corresponding recycled residue feed also needs to be investigated.

It could be concluded from the experiments that the residue material is progressively more aromatic at each stage and thus potentially less reactive. The limited amounts of residue material produced and the large amount of time required unfortunately did not allow for kinetic studies to be performed on the successive residue fractions. A thorough study of the changing kinetics of the residue material versus the bitumen feed would be useful for better reactor design and operation. The development of a lumped kinetic model based on the building block structure of bitumen should also be explored.

The repetition of these experiments on a larger scale is necessary to allow sufficient material for a more detailed study involving kinetics and hydrotreater studies.

## BIBLIOGRAPHY


Abu-Dagga F. and Rüegger H., "Evaluation of low boiling crude oil fractions by n.m.r spectroscopy", *Fuel*, **1988**, 67, 1255-1262.

Altgelt K. H. and Boduszynski M. M., "Composition and Analysis of Heavy Petroleum Fractions", Marcel Dekker, New York, **1994**.

Benson S. W., "Thermochemical Kinetics", John Wiley & Sons, **1976**.

Brown J., "The end of the era of cheap oil", *Euromoney*, London, Nov. **2000**.

Boduszynski M. M., "Composition of Heavy Petroleum 1. Molecular Weight, Hydrogen Deficiency, and Heteroatom Concentration as a Function of Atmospheric Equivalent Boiling Point up to 1400°F (760°C)", *Energy & Fuels*, **1987**, 1, 2-11.

Campbell C.J. and Laherrere J.H., "The end of cheap oil", *Scientific American*, Mar **1998**, 278, 3, 78-84.

Champagne P.; Manolakis E. and Ternan M., "Molecular Weight distribution of Athabasca bitumen" *Fuel*, **1985**, 64, 423-425.

Choi J.H.K. and Gray M.R., "Structural Analysis of Extracts from Spent Hydroprocessing Catalysts" *Ind Eng. Chem. Res.*, **1988**, 27, 1587-1595.

Chung K. H.; Xu C.; Hu Y.; Wang, R., "Supercritical Fluid Extraction Reveals Resid Properties", *Oil Gas J.*, **1997**, 95(3), 66-69.

Collin. P.J.; Gilbert T.D.; Rottendorf H. and Wilson M.A., "Ring contraction and dehydrogenation in polycyclic hydroaromatics at coal liquefaction temperatures", *Fuel*, **1985**, 64, 1280-1285.

Cyr N.; McIntyre D.D.; Toth G and Strausz O. P., "Hydrocarbon structural group analysis of Athabasca asphaltene and its gpc fractions by $^{13}C$ NMR", *Fuel*, **1987,** 66, 1709-1714.

Domansky C.J., "Short Path Distillation of Athabasca Bitumen", *AOSTRA Journal of Research*, **1986,** 2, 3, 191-196.

de Vlieger J.J.; Kieboom A.P.G. and van Bekkum H. "Behaviour of tetralin in coal liquefaction" *Fuel*, **1984,** 63, 334-340.

Ebert L. B.; Scanlon J.C. and Mills D.R., "Structures of Liquid-Like Systems: X-Ray Diffraction of Model Organic Hydrocarbons" *Am. Chem. Soc. Div. Petrol. Chem. Prepr.*, **1985,** September 8-13, 636-640.

Egiebor N.O.; Gray M.R. and Cyr N., "$^{13}C$-NMR of Solid Organic Deposits on Spent Hydroprocessing Catalysts", *Chemical Engineering Communication*, **1989**, 77, 125-133.

Fitzer E.; Mueller K. and Schaefer W., "The Chemistry of the Pyrolytic Conversion of Organic Compounds to Carbon", *Chemistry and Physics of Carbon*, **1971**, 237-383.

Freund H.; Matturro M.G.; Olmstead W.N.; Reynolds R.P. and Upton T.H., "Anomalous Side-Chain Cleavage in Alkylaromatic Thermolysis", *Energy & Fuels*, **1991,** 5, 840-846.

Fu P.P. and Harvey P.G., "Dehydrogenation of polycyclic hydroaromatic compounds", *Chemical Reviews*, **1978,** 78, 317-361.

Furimsky E., "Chemical Origin of Coke Deposited on Catalyst Surface", *Ind Eng. Chem. Prod. Res. Dev.*, **1978**, 329-331.

Furimsky E., "Characterisation of Deposits formed on Catalyst Surfaces during Hydrotreatment of Coal-Derived Liquids", *Fuel Processing Technology*, **1982**, 6, 1-8.

Gary J. H. and Handwerk G. E., *Petroleum Refining, Technology and Economics*, Marcel Dekker Inc., New York, **1984**.

Gray M. R., "Upgrading Petroleum Residues and Heavy Oils", Marcel Dekker Inc., New York, **1994**.

Gray M. R.; Wanke S. E.; and Krzywicki A., "Chemical Transformation During Resid Upgrading: Catalytic and Thermal", CANMET, DSS Contract Serial No.: 23440-7-9011/01-SQ, NHRC Report #00746, **1992**.

Gray M. R.; Jokuty P.; Yeniova H.; Nazarewycz L.; Wanke S. E.; Achia U.; Krzywicki A.; Sanford E. C. and Sy O. K. Y., "The Relationship between Chemical Structure and Reactivity of Alberta Bitumens", *Can J. Chem. Eng.* **1991**, 69, 833-843.

Gray M.R., "Composition and Hydrotreating of Bitumen and Heavy Oil-Derived Distillates", *AOSTRA Journal of Research,* **1990**, 6, 185-197.

Gray M. R.; Choi J. H. K.; Egiebor N. O.; Kirchen R. P. and Sanford E. C. "Structural Group Analysis of Residues from Athabasca Bitumen", *Fuel Sci. & Tech. Int'l.*, **1989**, 7(5-6), 599-610.

Greinke R. A., "Chemical Bond Formed in Thermally Polymerized Petroleum Pitch", *Carbon,* **1992**, 30, 3, 407-414.

Groenzin H. and Mullins O.C., "Molecular Structure of Asphaltenes from Various Sources" *Energy & Fuels,* **2000**, 14, 677-686.

Halabi M. A.; Stanilaus A. and Trimm D. L., "Coke formation on Catalyst During the Hydroprocessing of Heavy Oils", *Applied Catalysis,* **1991**, 72, 193-215.

Hepler L.G., "Thermochemical and Thermodynamic Properties", *AOSTRA Technical Handbook on Oil Sands, Bitumens and Heavy Oils*, **1989**, 77-98.

Jewell D.M.; Albaugh E.W.; Davis B.E. and Ruberto R.G., "Integration of Chromatographic and Spectroscopic Techniques for the Characterization of Residual Oils", *Ind Eng. Chem. Fund.*, **1974**, 13, 278-282.

Kirchen R.P.; Sanford E.C.; Gray, M.R. and George Z.M., "Coking of Athabasca bitumen derived feedstocks", *AOSTRA Journal of Research*, **1989**, 5, 225-235.

Lachambre P.C., "The Oilsands Industry and Syncrude Canada Ltd. Growth Plans", *7th UNITAR International Conference on Heavy Crude and Tar Sands*, **1998**, October 27-30.

Lanier D., "Heavy Oil – A Major Energy Source for the 21st Century", *7th UNITAR International Conference on Heavy Crude and Tar Sands*, **1998**, October 27-30.

Le Page J.F.; Chatila S.G. and Davidson M., "Resid and Heavy Oil Processing", Editions Technip, Paris, **1992.**

Liu L.; Wang S.; Gray M. R. and McCaffrey W. C., "Thermal Processing of Heavy Petroleum Fractions: Coking as An Emulsion Process", *7th UNITAR International Conference on Heavy Crude and Tar Sands*, **1998**, October 27-30.

Martins S.W. and Wills L.E., "Coking Petroleum Residues", *Advances in Petroleum Chemistry and Refining*, **1959**, 357-433.

Meyer R.F. and Wallace de Witt, "Definition of World Resources of Natural Bitumens", *U.S. Geological Survey Bulletin*, No. 1944, **1990**.

Murgich J.; Abanero J.A. and Strausz O.P., "Molecular Recognition in Aggregates Formed by Asphaltene and Resin Molecules from the Athabasca Oil Sand", *Energy & Fuels*, **1999**, 13, 278-286.

Mushrush G. W. and Hazlett R. N., "Pyrolysis of Organic Compounds Containing Long Unbranched Alkyl Groups", *Ind. Eng. Chem. Fundam.*, **1984**, 23, 288.

Nelson W.L., 'Petroleum Refinery Engineering', Fourth Edition, McGraw-Hill Book Company, **1958**.

Netzel N.A.; McKay D.R.; Heppner R.A.; Guffey F.D.; Cooke S.D.; Varie D.L. and Linn D.E., "$^{1}$H and $^{13}$C-n.m.r. studies on naphtha and light distillate saturate hydrocarbon fractions obtained from *in-situ* shale oil", *Fuel*, **1981**, 60, 307-319.

Noel F. "Alternative to the Conradson Carbon Residue Test" *Fuel*, **1984**, 63, 7, 931-934.

Ouchi K., "Correlation of aromaticity and Molecular Weight of oil asphaltene and preasphaltene", *Fuel*, **1985**, 64, 426-427.

Peters K.E.; Scheuerman G.L.; Lee C.Y.; Moldowan J.M.; Reynolds R.N. and Pea M.M., "Effects of Refinery Processes on Biological Markers", *Energy and Fuels*, **1992**, 6, 560-577.

Poutsma L. M., "Free Radical Thermolysis and Hydrogenolysis of Model Hydrocarbons Relevant to Processing Of Coal", *Energy & Fuels*. **1990**, 4, 2, 113-131.

Precht P. and Rokosh C., "Oil Sands Development in Alberta: The New Paradigm", *7th UNITAR International Conference on Heavy Crude and Tar Sands*, **1998**, October 27-30.

Roberts I., "The Chemical Significance of Carbon Residue Data" *Symposium on Analytical Chemistry of Heavy Oils/Resids, American Chemical Society*, **1989**, April 9-14.

Rodriguez J., Tierney J.W. and Wender I., "Evaluation of a delayed coking process by $^{1}$H and $^{13}$C n.m.r. spectroscopy:2. Detailed interpretation of liquid n.m.r. spectra", *Fuel*, **1994**, 73, 12, 1870-1875.

Sachanen A.N., "Conversion of Petroleum", Reinhold Publishing Corporation, New York, **1940**.

Sanford E.C., "Molecular Understanding to Residuum Conversion" *Ind. Eng. Chem. Ref.*, **1994**, 33, 109-117.

Savage P. E. and Baxter K.L., "Pathways, Kinetics, and Mechanisms for 2-Dodecyl-9,10-dihydrophenanthrene Pyrolysis", *Ind. Eng. Chem. Res.*, **1996**, 35, 1517-1523.

Savage P. E.; Jacobs G.E. and Javanmardian M., "Autocatalysis and Aryl-Alkyl Cleavage in 1-Dodecylpyrene Pyrolysis", *Ind. Eng. Chem. Res.* **1989**, 28, 645-654.

Savage P. E. and Klein M. T., "Asphaltene Reaction Pathways 4. Pyrolysis of *n*-tridecyl-cyclohexane and 2-ethyltetralin", *Ind. Eng. Chem. Res.*, **1988**, 27, 1348-1356.

Savage P. E. and Klein M. T., "Asphaltene Reaction Pathways 2. Pyrolysis of *n*-penta-decyl-benzene", *Ind. Eng. Chem. Res.*, **1987**, 26, 488.

Shaw J.M.; Gaikwad R.P. and Stowe D.A., "Phase Splitting of Pyrene-Tetralin Mixtures Under Coal Liquefaction Conditions", *Fuel*, **1988**, 67,1554.

Smith C.M. and Savage P. E., "Reactions of Polycyclic Alkyl Aromatics: Structure and Reactivity", *AIChE Journal*, **1991**, 37, 11, 1613-1623.

Snape C.E. and Bartle K.D., "Definition of fossil fuel-derived asphaltenes in terms of average structural properties", *Fuel*, **1984**, 63, 883-887.

Snape C.E.; Ladner W.R. and Bartle K.D., "Survey of Carbon-13 Chemical Shifts in Aromatic Hydrocarbons and its Application to Coal-Derived Materials", *Analytical Chemistry*, **1979**, 51, 13, 2189-2198.

Solum M.S.; Pugmire R.J. and Grant D.M., "$^{13}C$ Solid-State NMR of Argonne Premium Coals", *Energy and Fuels*, **1989**, 3, 187-193.

Speight J. G., "The Desulfurisation of Heavy Oils and Residua", 2nd Edition. Marcel Dekker Inc., New York, **2000**.

Speight J. G., "The Chemistry and Technology of Petroleum", 2nd Edition. Marcel Dekker Inc., New York, **1991**.

Speight J. G. and Moschopedis S. E., "On the Molecular Nature of Petroleum Asphaltenes", *Chemistry of Asphaltenes*. Bunger, J. W. and Li, N. C. (Eds.), *Am. Chem. Soc. Div. Petrol. Chem. Prepr.*, **1981**.

Stalick W. M.; Mushrush G. W.; Murray J.H. and Zahadat N., "Pyrolysis Free Radical Reactions of Substituted Long Chain Alkyl Pyridines and Quinolines", *Am. Chem. Soc. Div. Petrol. Chem. Prepr.*, **1994,** August 21-26, 317-320.

Stohl F.V. and Stephens H.P., "The Impact of the Chemical Constituents of Hydrotreater Feed on Catalyst Activity *Am. Chem. Soc. Div. Fuel Chem. Prepr*, **1986,** 251-256.

Strausz O.P.; Mojelsky T.W. and Lown E.M., "The molecular structure of asphaltene: an unfolding story", *Fuel*, **1992,** 71, 1355-1363.

Sullivan R.F.; Boduszynski M.M. and Fetzer J.C., "Molecular Transformations in Hydrotreating and Hydrocracking", *Energy & Fuels*, **1989**, 3, 603-612.

Swain E.J., "Processed-crude quality in US continues downward trend", *Oil & Gas Journal*, Mar 13, **2000,** 98, 11, 44-48.

Syndor and Patterson, "Cracking Value of Straight-Run and Cycle Gas Oil", *Ind. Eng. Chem.*, **1930,** 22, 11, 1237-1240.

Tanabe K. and Gray M. R., "Role of Fine Solids in the Coking of Vacuum Residues", *Energy & Fuels*, **1997**, 11, 1040-1043.

Ternan M. and Kriz J. F., "Effects of H/C Ratio and Molecular Weight on Microcarbon Residue of Vacuum Resid Sub-Fractions", *Petroleum Science and Technology*, **1998**, 16 (1&2), 167-178.

Ternan M. and Kriz J. F., "+525°C Pitch Content Versus Microcarbon Residue: A Correlation for Charaterizing Reaction Products Obtained by Hydrocracking Bitumens, Heavy Oils, and Petroleum Residua" *AOSTRA Journal of Research*, **1990**, 6, 65-70.

Thiel J. and Gray M.R., "NMR Spectroscopic Characteristics of Alberta Bitumens", *AOSTRA Journal of Research*, **1988**, 4, 63-73.

Trasobares S.; Callejas M.A.; Benito A.M.; Martinez M.T.; Severin D. and Brouwer L., "Kinetics of Conradson Carbon Residue Conversion in the Catalytic Hydroprocessing of a Maya Residue", *Ind Eng. Chem. Res.*, **1998**, 37, 11-17.

Thakur D.S. and Thomas M. G., "Catalyst Deactivation in Heavy Hydrocarbon and Sythetic Crude Processing: A Review" *Applied Catalysis*, **1985**, 15, 197-225.

Wang S, "Deposition of fine particles in hydrotreaters", PhD. Thesis, University of Alberta, **2000.**

Wiehe, I.A., "The Enhanced Microcarbon Tester and Other Ideal Laboratory Cokers", *Symposium on Residuum/Asphaltene/Coke/Solids Characterisation in Petroleum Processing*, American Chemical Society, **2000**, August 20-24

Wiehe I.A. and Liang K.S., "Asphaltenes, resins and other petroleum macromolecules", *Fluid Phase Equilibria*, **1996**, 117, 201.

Wiehe I. A., "The Pendant-Core Building block Model of Petroleum Residua", *Energy & Fuels*, **1994**, 8, 536-544.

Wiehe I. A., "A Phase-Separation Kinetics Model for Coke Formation", *Ind. Eng. Chem. Res.*, **1993**, 32, 2447-2454.

Wiehe I. A., "A Solvent-Resid Phase Diagram for Tracking Resid Conversion", *Ind. Eng. Chem. Res.*, **1992**, 31, 530-536.

Williams H.R. and Meyers C.J., "Manual of Oil and Gas Terms", Matthew Bender, New York, **1964.**

Yen T.F., "Present Status of the Structure of Petroleum Heavy Ends and its Significance to Various Technical Applications", *Symposium on advances in analysis of petroleum and its products presented before the division of petroleum chemistry*, American Chemical Society, **1972,** Aug.27-Sept.1972.

Yen T. F; Erdman G. and Pollack S.S., "Investigation of the Structure of Petroleum Asphaltenes by X-Ray Diffraction" *Analytical Chemistry*. **1961,** 33, 11, 1587-1594.

Young D.C. and Galya L.G., "Determination of Paraffinic, Naphthenic and Aromatic Carbon in Petroleum Derived Materials by Carbon-13 NMR Spectroscopy", *Liquid Fuels Technology*, **1984**, 2, 3, 307-326.

Zhao S.; Kotlyar L.S.; Woods J.R. Sparks B.D. and Chung K.H., "Effect of Thermal and Hydro-Catalytic Treatment on the Molecular Chemistry of Narrow Fractions of Athabasca Bitumen Pitch", *Energy & Fuels*, **2001**, 15, 1, 113-119.

# Appendix 1 Definitions of refining and upgrading terms

API gravity: A density scale that allows representation of the small changes in density on a larger scale.

$$^{o}API = (141.5/\text{Specific Gravity @}15.6^{o}C) - 131.5$$

Aromaticity: The ratio of the aromatic carbon to the total carbon is defined as aromaticity.

Atmospheric Equivalent Boiling Points: The boiling points of non-volatile residue materials under atmospheric pressure; these are estimated from the actual boiling points at reduced pressures.

Conradson Carbon: It is a standardised test (ASTM D-189) to determine amount of carbon residue left behind after pyrolysis of a hydrocarbon. It has now been replaced by the MCR test (see pg 31).

Conradson Decarbonizing Efficiency: The difference between the weights of Conradson carbon in the coker feedstock and in the liquid product streams divided by the weight of Conradson carbon in the coker feedstock is defined as Conradson Decarbonizing Efficiency.

Heteroatoms: Usually refers to sulphur, nitrogen and oxygen compounds present in petroleum. The definition may or may not include metals.

Proved Reserves: The amount of crude oil that can be recovered by present day technology.

Residue: The material left behind after distillation to remove the volatile material from the crude oil/bitumen fraction. For bitumen upgrading, this usually implies material with a cut point over 524°C.

## Appendix 2 $CS_2$ insoluble vs toluene insoluble coke

Coking experiments were performed in the quartz tube reactors at similar conditions using vacuum residue feed. The amount of coke was determined as toluene insoluble or $CS_2$ insoluble. The coke yields listed in Table A 1 show that the yield of coke whether determined as toluene insoluble or $CS_2$ insoluble was comparable, within the margin of error.

**Table A 1 Coke yields**

| $CS_2$ insoluble, wt.% | Toluene insoluble, wt.% |
|---|---|
| 27.7 | 28.5 |
| 26.4 | 27.0 |

## Appendix 3 Micro scale distillation at reduced pressure

The micro scale distillation technique was first validated using bitumen samples. Distillation was performed on a sample of Athabasca bitumen using 50 ml, 15 ml and 10 ml flasks to test the repeatability of the experimental cut points over a range of flasks. The temperature was increased rapidly to 100°C and then ramped up at a rate of 5°C/min to 325°C. The temperature was held at 325°C for one minute before the heater was switched off. The temperature was allowed to drop below 150°C before the vacuum pump was switched off and the apparatus dissembled. The total recovery was approximately 100% for all samples of bitumen used.

The weight % of bitumen distilled for different flasks with different amounts of feed is shown in Table A 2. Since the residue fraction showed evidence of residual amounts of solvent ($CS_2$) in the sample, the distillate curve and the bitumen curves were used to generate the residue curves by means of a mass balance. The results are shown in Figure A 1 and they clearly show that the results were repeatable over the range of the flasks. Figure A 2 shows data from several repeat runs performed at 320°C to check repeatability of the distillation with respect to weight % of bitumen distilled.

**Table A 2 Amount distilled for varying flask sizes**

| Flask size, mL | Feed amount, g | % Residue | % Recovery |
|---|---|---|---|
| 50 | 30.268 | 70.3 | 99.5 |
| 15 | 4.069 | 72.7 | 99.7 |
| 10 | 1.36 | 70.1 | 100.1 |

**Figure A 1 Simdist curves for varying flask sizes**

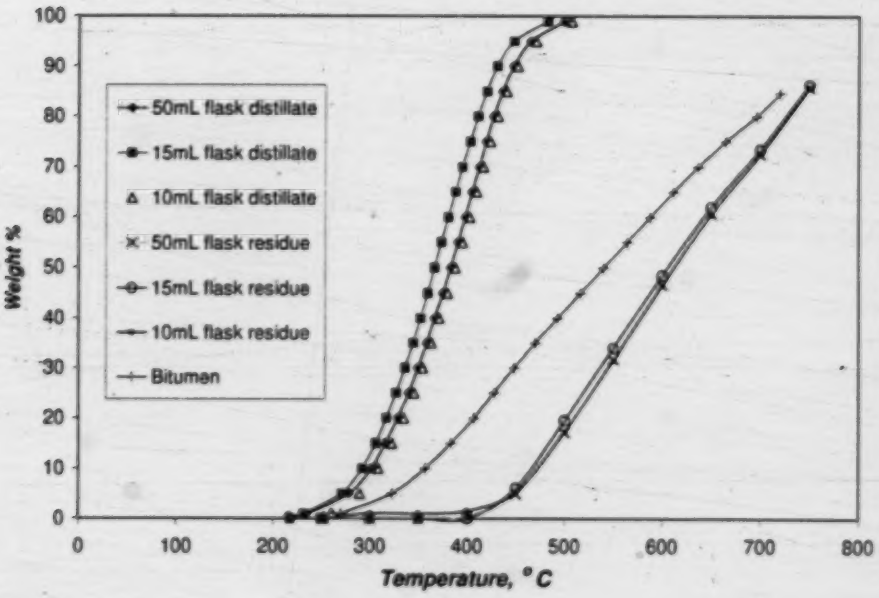

**Figure A 2 Residue remaining on repeat experiments (320°C)**

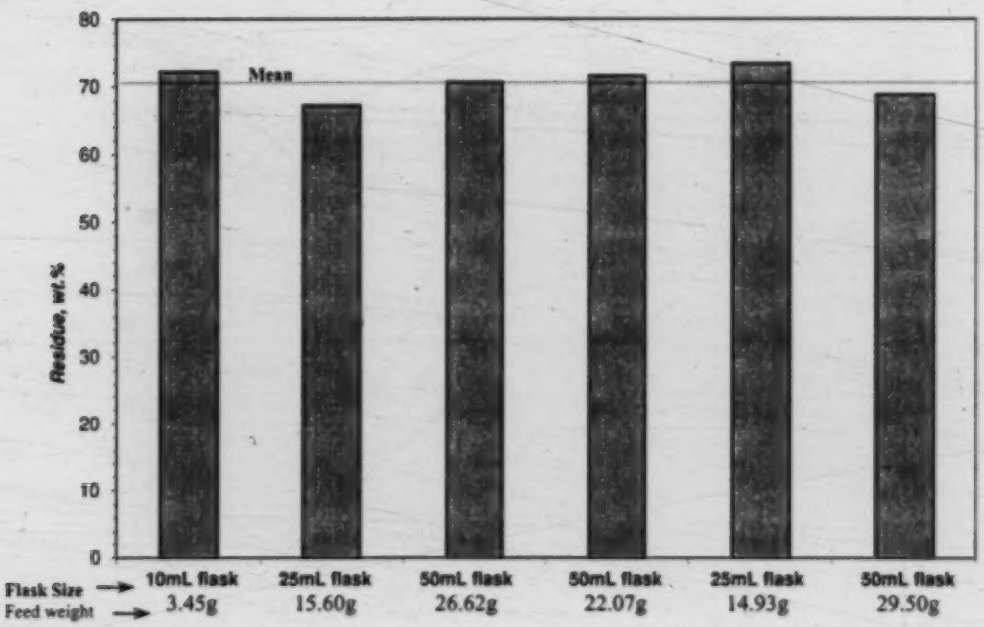

# Appendix 4 Simulated distillation by gas chromatography

The simulated distillation gas chromatography results for the residue and distillate fractions are shown in Figure A 3. The distillate curves abruptly stopped at 80% recovery. This peculiar feature could not be explained although it was suspected that it could be the result of storage time and resultant fouling problems. Generally for GC distillation methods 100% recovery of the samples is assumed (ASTM D2887). The boiling curves obtained from the liquid samples in this study were also assumed to have given 100% recovery and the simdist curves shown in this thesis have been normalised (Figure A 4). Note that the vacuum distillation technique was first tested using bitumen samples. It was found to be repeatable and gave consistent cut points.

**Figure A 3 Original simdist curves for the liquid fractions**

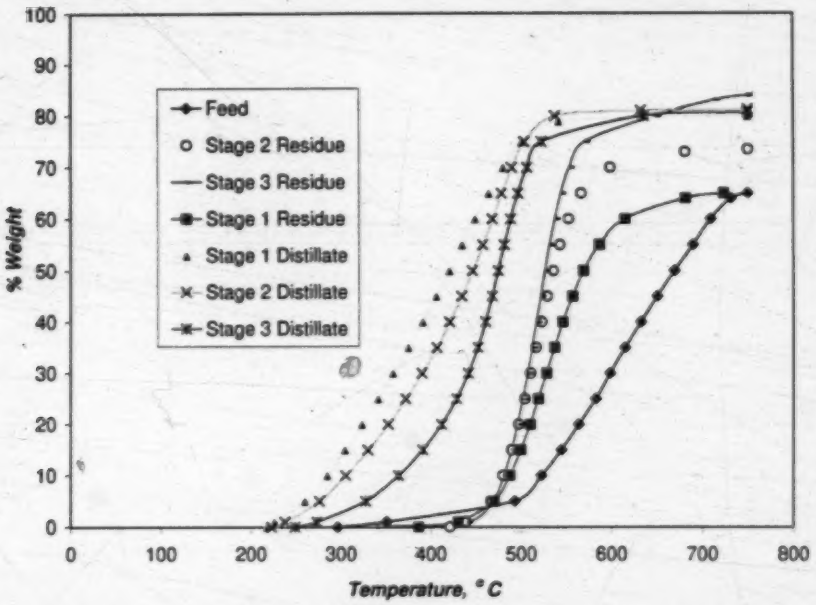


**Figure A 4 Normalised simdist curves for the liquid fractions**

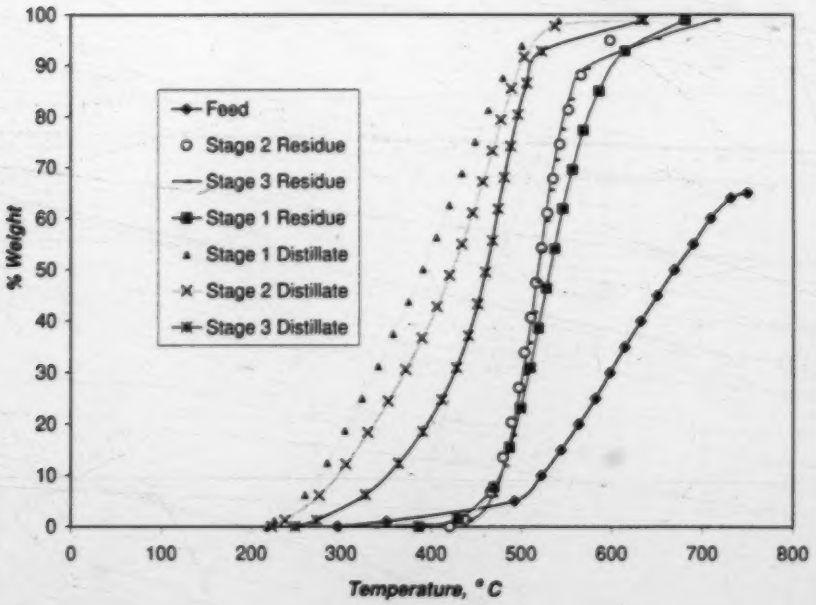

# Appendix 5 High Performance Liquid Chromatography

The ELSD data for the HPLC fractions did not give acceptable mass balance closures (Table A 3). As can be seen the mass balance closures for the two sets of repeat experiments range from 76 to 98% and from 79 to 103%. The range of the variations for most of the groups across the stages was much smaller than this 20% variation in mass balance closures. Obviously data from this analysis was suspect and could not be used for any definite analysis. The solvent, the flowrates and the columns used for HPLC are shown in Table A 4.

**Table A 3 ELSD data for the distillate fractions**

| | | % Saturates | %Mono | %Di | %Tri | %Poly | %Polar | %Asph. | %Mass Balance |
|---|---|---|---|---|---|---|---|---|---|
| Set 1 | Stage 1 | 18.4 | 10.7 | 14.0 | 9.0 | 8.7 | 10.0 | 5.2 | 76.0 |
| | Stage 2 | 17.8 | 9.5 | 13.8 | 14.8 | 16.1 | 9.8 | 6.2 | 87.9 |
| | Stage 3 | 12.0 | 6.3 | 8.9 | 19.0 | 32.4 | 12.3 | 7.0 | 97.9 |
| Set 2 | Stage 1 | 21.3 | 12.2 | 14.1 | 8.8 | 8.5 | 8.9 | 5.2 | 79.0 |
| | Stage 2 | 20.1 | 11.4 | 13.7 | 14.4 | 15.1 | 8.9 | 6.2 | 89.9 |
| | Stage 3 | 19.0 | 12.6 | 8.7 | 18.4 | 30.4 | 11.3 | 7.0 | 107.4 |

**Table A 4 Solvents used and their respective flowrates**

| Time, min | Column | Solvent in hexane | % IPA in solvent | Flow rate, mL/min |
|---|---|---|---|---|
| 0-4.5 | Both | Hexane | | 1.5 |
| 4.5-10.0 | PAC | Hexane | | 1.5 |
| 10.0-12.5 | RingSep | Hexane | | 1.5 |
| 12.5-13.5 | RingSep | 5% Methylene chloride | | 1.5 |
| 13.5-16.5 | RingSep | 2% Methylene chloride | | 1.5 |
| 16.5-17.5 | RingSep | 25% Methylene chloride | | 1.5 |
| 17.5-23.5 | RingSep | 20% Methylene chloride | | 1.5 |
| 23.5-27.5 | RingSep | 90% Methylene chloride | | 1.5 |
| 27.5-35.5 | RingSep | 90% Methylene chloride | 10% | 1.5 |
| 35.5-36.0 | RingSep | 75% Methylene chloride | 25% | 1.5 |
| 36.0-39.5 | RingSep | 100% Methylene chloride | | 2.0 |
| 39.5-40.0 | Both | 100% Methylene chloride | | 2.0 |
| 40.0-46.0 | Both | Hexane | | 2.0 |
| 46.0-48.0 | PAC | Hexane | | 2.0 |
| 48.0-50.0 | RingSep | Hexane | | 2.0 |
| 50.0-75.0 | Both | Hexane | | 1.5 |

# Appendix 6 Mass balance for the quartz tube reactor

To check the overall mass balances obtained from the quartz tube reactor the yield of gas was determined by running a representative reaction and collecting the gas in a gas sampling bag. Since the nitrogen flow rate was measured the yield of the other gases was simply obtained by calibration. Note that oxygen and $CO_2$ were ignored in the calculation of yield of gas. The mean liquid and coke yields were determined from all the repeat experiments. As shown in Figure A 5 good balance closures were obtained for all three stages.

**Figure A 5 Mass balance for quartz tube reactor**

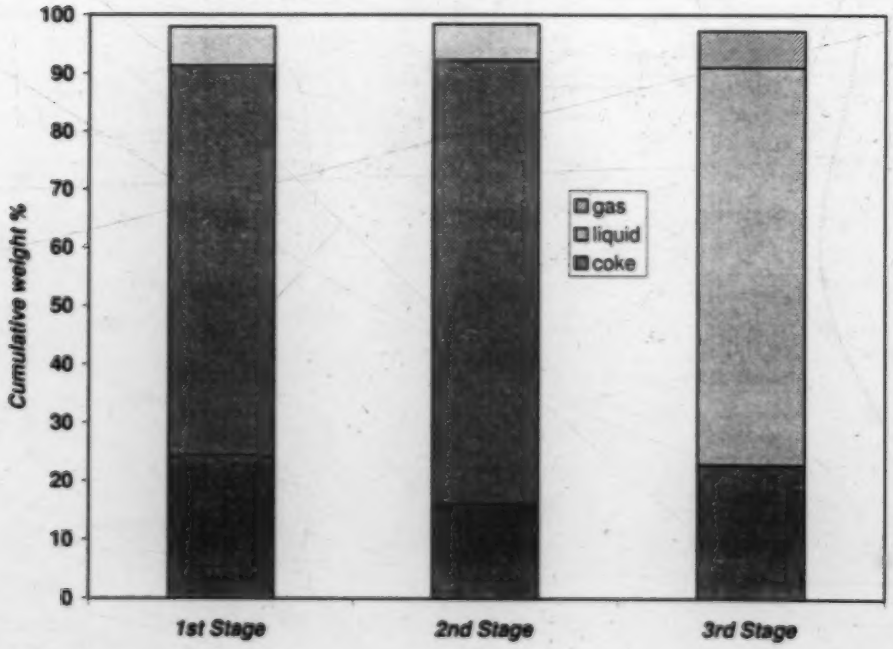

# Appendix 7 Thermal cracking experiments on the 3"reactor products

Coking experiments were performed on material obtained from the Syncrude 3" diameter pilot coker. The 3" coker is a fluidised bed reactor that was operated at atmospheric pressure and a temperature of 530°C. The feed used for the 3" reactor was either Athabasca bitumen or Athabasca vacuum residue. The liquid product from this reactor was separated and distilled to obtain a residue 524°C+ material. The residue was reacted in a ½" quartz tube reactor and the coke yields thus obtained are shown in Figure A 6. The % MCR is also plotted in the same figure. Although the coke yields for the residue product produced from the vacuum residue feed to the 3" coker and the fresh vacuum residue were comparable within the margin of error, the MCR content for the same feeds showed a significant decrease. The drop in % MCR was consistent with what was observed in case of repeated coking in the 1" quartz tube reactor.

**Figure A 6 MCR and coke yields for 3" reactor products**

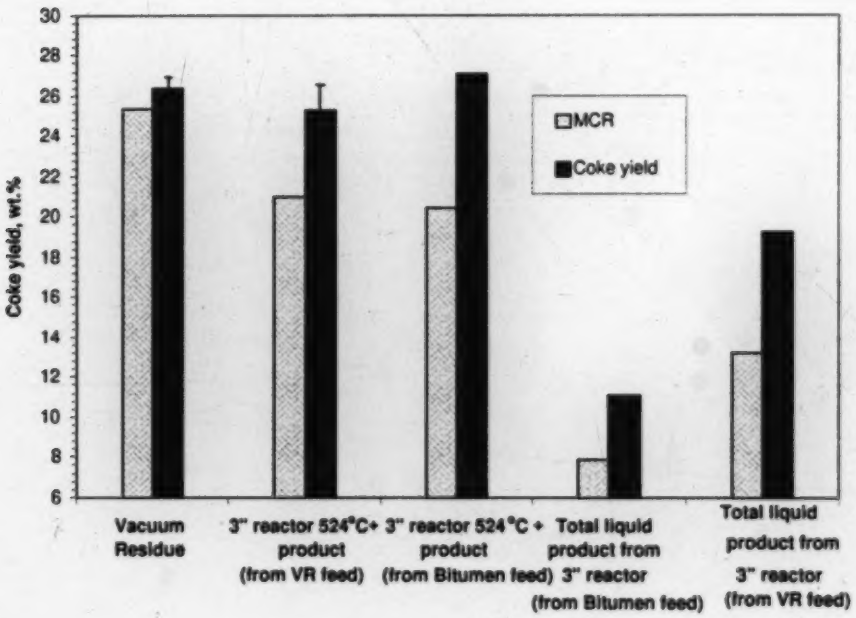

# Appendix 8 Rotameter Calibration

The nitrogen flow rates were measured by a rotameter. The rotameter used was first calibrated with the help of a wet test meter. The calibration chart thus obtained is shown in Figure A 7.

**Figure A 7 Calibration chart for flowmeter**